Technical Memorandum

Delta Risk Management Strategy (DRMS) Phase 1

Topical Area

Levee Vulnerability

Draft 2

Prepared by:
URS Corporation/Jack R. Benjamin & Associates, Inc.

Prepared for:
Department of Water Resources

June 15, 2007

URS

June 15, 2007

Mr. Ralph R. Svetich, P.E.
Delta Risk Management Strategy Project Manager
Department of Water Resources
Division of Flood Management
Delta-Suisun Marsh Office
901 P Street, Suite 313A
Post Office Box 942836
Sacramento, CA 94236-0001

Subject: Delta Risk Management Strategy
Phase 1 Draft 2 Draft Technical Memorandum – Levee Vulnerability

Dear Mr. Svetich:

Please find herewith a copy of the subject technical memorandum. Members of the Steering Committee's Technical Advisory Committee and agency staff have reviewed the draft technical memorandum, and this second draft addresses their comments.

This document was prepared by the Levee Vulnerability Team listed in the Acknowledgements (Section 1.3). Internal peer review was provided in accordance with URS' quality assurance program, as outlined in the (DRMS) project management plan.

Sincerely,

URS Corporation

Said Salah-Mars, Ph.D., P.E.
URS Engineering Division Manager
DRMS Project Manager
1333 Broadway Ave, Suite 800
Oakland, CA 94612
Ph. 510-874-3051
Fax: 510-874-3268

Jack R. Benjamin & Associates, Inc.

Martin W. McCann, Jr., Ph.D.
President JBA
DRMS Technical Manager
530 Oak Grove Ave., Suite 202
Menlo Park, CA 94025
Ph. 650-473-9955

Preamble

The Delta Risk Management Strategy (DRMS) project was authorized by DWR to perform a risk analysis of the Delta and Suisun Marsh (Phase 1) and to develop a set of improvement strategies to manage those risks (Phase 2) in response to Assembly Bill 1200 (Laird, Chaptered, September 2005). The Technical Memorandum (TM), is one of 12 TMs (2 topics are presented in one TM: hydrodynamics and water management) prepared for topical areas for Phase 1 of the DRMS project. The topical areas covered in the Phase 1 Risk Analysis include:

1. Geomorphology of the Delta and Suisun Marsh
2. Subsidence of the Delta and Suisun Marsh
3. Seismic Hazards of the Delta and Suisun Marsh
4. Global Warming Effects in the Delta and Suisun Marsh
5. Flood Hazard of the Delta and Suisun Marsh
6. Wind Wave Action of the Delta and Suisun Marsh
7. Levee Vulnerability of the Delta and Suisun Marsh
8. Emergency Response and Repair of the Delta and Suisun Marsh Levees
9. Hydrodynamics of the Delta and Suisun Marsh
10. Water Management and Operation of the Delta and Suisun Marsh
11. Ecological Impacts of the Delta and Suisun Marsh
12. Impact to Infrastructure of the Delta and Suisun Marsh
13. Economic Impacts of the Delta and Suisun Marsh

Note that the Hydrodynamics and Water Quality topical area was combined with the Water Management and Operations topical area because they needed to be considered together in developing the model of levee breach water impacts for the risk analysis. The resulting team is the Water Analysis Module (WAM) Team and this TM is the Water Analysis Module TM.

The work product described in these TMs will be used to develop the integrated risk analysis of the Delta and Suisun Marsh. The results of the integrated risk analysis will be presented in a technical report referred to as:

14. Risk Analysis – Report

The first draft of this report was made available to the DRMS Steering Committee in April 2007.

Assembly Bill 1200 amends Section 139.2 of the Water Code, to read, “The department shall evaluate the potential impacts on water supplies derived from the Sacramento-San Joaquin Delta based on 50-, 100-, and 200-year projections for each of the following possible impacts on the delta:

1. Subsidence.
2. Earthquakes.
3. Floods.
4. Changes in precipitation, temperature, and ocean levels.
5. A combination of the impacts specified in paragraphs (1) to (4) inclusive.”

In addition, Section 139.4 was amended to read: (a) The Department and the Department of Fish and Game shall determine the principal options for the delta. (b) The Department shall evaluate and comparatively rate each option determined in subdivision (a) for its ability to do the following:

1. Prevent the disruption of water supplies derived from the Sacramento-San Joaquin Delta.
2. Improve the quality of drinking water supplies derived from the delta.
3. Reduce the amount of salts contained in delta water and delivered to, and often retained in, our agricultural areas.
4. Maintain Delta water quality for Delta users.
5. Assist in preserving Delta lands.
6. Protect water rights of the "area of origin" and protect the environments of the Sacramento- San Joaquin river systems.
7. Protect highways, utility facilities, and other infrastructure located within the delta.
8. Preserve, protect, and improve Delta levees.…"

In meeting the requirements of AB 1200, the DRMS project is divided into two parts. Phase 1 involves the development and implementation of a risk analysis to evaluate the impacts to the Delta of various stressing events. In Phase 2 of the project, risk reduction and risk management strategies for long-term management of the Delta will be developed.

Definitions and Assumptions

During the Phase 1 study, the DRMS project team developed various predictive models of future stressing events and their consequences. These events and their consequences have been estimated using engineering and scientific tools readily available or based on a broad and current consensus among practitioners. Such events include the likely occurrence of future earthquakes of varying magnitude in the region, future rates of subsidence given continued farming practices, the likely magnitude and frequency of storm events, the potential effects of global warming (sea level rise, climate change, and temperature change) and their effects on the environment. Using the current state of knowledge, estimates of the likelihood of these events occurring can be made for the 50-, 100-, and 200-year projections with some confidence.

While estimating the likelihood of stressing events can generally be done using current technologies, estimating the consequences of these stressing events at future times is somewhat more difficult. Obviously, over the next 50, 100, and 200 years, the Delta will undergo changes that will affect what impact the stressing events will have. To assess those consequences, some assumptions about the future "look" of the Delta must be established.

To address the challenge of predicting impacts under changing conditions, DRMS adopted the approach of evaluating impacts absent changes in the Delta as a baseline.

This approach is referred to as the "business-as-usual" (BAU) scenario. Defining a business-as-usual Delta is required, since one of the objectives of this work is to estimate whether 'business-as-usual' is sustainable for the foreseeable future. Obviously changes from this baseline condition can occur; however, as a basis of comparison for risks and risk reduction measures, the BAU scenario serves as a consistent standard rather than as a "prediction of the future" and relies on existing agreements, policies, and practices to the extent possible.

In some cases, there are instances where procedures and policies may not exist to define standard emergency response procedure during a major (unprecedented) stressing event in the Delta or restoration guidelines after such a major event. In these cases, prioritization of action will be based on: (1) existing and expected future response resources, and (2) highest value recovery/restoration given available resources.

This study relies solely on available data. Because of the limited time to complete this work, no investigation or research were to be conducted to supplement the state of knowledge.

Perspective

The analysis results presented in this technical memorandum do not represent the full estimate of risk for the topic presented herein. The subject and results are expressed whenever possible in probabilistic terms to characterize the uncertainties and the random nature of the parameters that control the subject under consideration. The results are the expression of either the probable outcome of the hazards (earthquake, floods, climate change, subsidence, wind waves, and sunny day failures) or the conditional probability of the subject outcome (levee failures, emergency response, water management, hydrodynamic response of the Delta and Suisun Marsh, ecosystem response, and economic impacts) given the stressing events.

A full characterization of risk is presented in the Risk Analysis Report. In that report, the integration of the probable initiating events, the conditional probable response of the Delta levee system, and the expected probable consequences are integrated in the risk analysis module to develop a complete assessment of risk to the Delta and Suisun Marsh.

Consequently, the subject areas of the technical memoranda should be viewed as pieces contributing to the total risk, and their outcomes represent the input to the risk analysis module.

Table of Contents

Tables

Figures

1.0 Introduction

The scope of this technical memorandum (TM) addresses the levee vulnerability analysis for various stress events. These events include normal ("sunny day") conditions, floods, and seismic events, and the effects of climate change and subsidence on these events. This TM describes the methodology for analyzing the vulnerability of the Delta and Suisun Marsh levees under these stress events, the inputs required to perform the analysis, and presentation and interpretation of results.

1.1 Background

The Delta has approximately 1,100 miles of levees, many of significant height (up to 25 feet), which continuously impound sloughs and river waters and protect agriculture and urban areas within islands and tracts. The islands' floor in the central and western Delta is below sea level by several feet as a result of subsidence from farming of organic and peaty soils. The Suisun Marsh has over 220 miles of exterior levee that protect over 50,000 acres of managed wetland habitats, Delta water quality, and Suisun public and private infrastructure. These levees are primarily privately maintained and considerably smaller in height and width than those levees in the Delta. Due to the Suisun Marsh's geographic location in the estuary, the channel water salinities are higher and more seasonally variable than those of the Delta. Historical land use in the Suisun Marsh has resulted in less significant subsidence in comparison to land in the Delta.

There have been 166 Delta failures leading to island inundations since 1900. No reports could be found to indicate that seismic shaking has ever induced significant damage. However, the lack of historic damage should not be used to conclude that Delta levees are not vulnerable to earthquake shaking. The present day Delta levees have never been significantly tested under moderate to high seismic shaking since the levees have been at their current size (CALFED 2000).

The objective of the levee vulnerability analysis was to evaluate the probability of failure of levee reaches for each stressing event, considering all modes of failures that may occur during the event. A fragility curve expresses the conditional probability of levee failure in a particular mode given a stressing event, such as seismic loading.

1.2 Report Organization

After this introductory section, the TM is organized into the following sections and appendices:

- Section 2 presents the methodology for probabilistic evaluation of levee failures
- Section 3 provides an overview of historical failure data and analysis
- Section 4 discusses the data review process, data analysis, and development of GIS maps
- Section 5 discusses the results of seepage analyses
- Section 6 discusses the results of seismic analyses

- Section 7 presents the summary and conclusion of this study
- Section 8 presents the selected references

1.3 Acknowledgements

The following individuals and agencies have contributed to the preparation of this technical memorandum or have provided insightful and valuable reviews and comments. Their contribution is a greatly appreciated.

The levee vulnerability team was composed of the following members:

Said Salah-Mars, Ph.D. P.E., DRMS Project Manager and Topical Team Leader (URS)
Ram B. Kulkarni, Ph.D., Senior Risk Analyst (URS)
Kanax Kanagalingam, Ph.D., Geotechnical and Earthquake Engineer (URS)
Segaran Logeswaran, MS, P.E., Geotechnical and Earthquake Engineer (URS)
Arulnathan Rajendram, Ph.D., P.E., G.E., Geotechnical Engineer (URS)
Sathish Murugaiah, M.S., Geotechnical and Earthquake Engineer (URS)
Scott E. Shewbridge, Ph.D., G.E., Senior Geotechnical and Earthquake Engineer (URS)
Martin W. McCann, Ph.D., DRMS Technical Manager and Risk Analyst (JBA)
Michael Forrest, M.S., P.E., G.E., Senior Civil-Geotechnical Engineer (URS)
Lelio H. Mejia, Ph.D., P.E., G.E., Senior Geotechnical and Earthquake Engineer (URS)
Faiz Makdisi, Ph.D., P.E., G.E, Principal Geotechnical-Earthquake Engineer (Geomatrix)
Kevin Tillis, P.E., G.E., Principal Geotechnical Engineer (Hultgren & Tillis)
Ed Hultgren P.E., G.E., Principal Geotechnical Engineer (Hultgren & Tillis)
Professor Greg Baecher, Ph.D., (University of Maryland)

The Technical Advisory Committee (TAC) members provided valuable guidance, insightful suggestions, and discussions throughout this study. Members of the TAC included:

Les Harder, Ph.D., G.E. Deputy Director, DWR
Prof. Ray Seed, Ph.D., P.E., TAC Chair (UCB)
Ralph Svetich, Project Manager, DWR
David Mraz, Contract Manager, DWR
Michael Driller, (DWR)
Michael Ramsbotthom, (USACE)
Lynn O'Leary, (USACE)
Gilbert Cosio, (MBK)

Firms and agencies that contributed valuable data included:

DWR
U.S. Army Corps of Engineers
Hultgren & Tillis Engineers
MBK Engineers
Kleinfelder
Geomatrix
University of California, Davis (Professor Ross Boulanger and Tadahiro Kishida)

2.0 Probabilistic Evaluation

2.1 Overall Approach

The probabilistic evaluation of levee fragility will involve an assessment of the conditional probability of damage state of each levee reach given the loading associated with a stressing event defined by the hazard teams. These results will be used in the risk quantification module to define multiple realizations (events and failure modes) of the spatial distribution of damaged levees reaches. Two distinct damage states will be defined for a given levee reach: (1) a breach; and (2) damage without a breach. The probability of a breach will be assessed directly for each failure mode. The probability of damage without a breach will be calculated by applying an adjustment factor to the breach probability.

The probability of a levee breach will be evaluated for the following stressing events and the corresponding failure modes:

Stressing Event	**Failure Mode**
Flood	Under-seepage
	Through-seepage
	Overtopping (considering flood stage plus wind set-up and wave action)
Earthquake	Seismic deformation (followed by slumping & overtopping, seepage, or piping though cracks)
Wind/Waves	Erosion (water- or land-side)
Normal conditions	Through- or under-seepage, slope instability, erosion, rodents activities

Figure 2-1 shows a schematic representation of the technical approach that will be used to evaluate levee breach probabilities in different failure modes. (Note: figures are located at the end of the text.) Levee response to the loading from a stressing event will be analyzed using a suitable geotechnical model, and the aleatory uncertainty in the estimated levee response will be assessed. The probability of levee breach will be estimated as a function of levee response. In addition, the epistemic uncertainty in the estimated probability of breach (i.e., estimated probability of breach at different confidence levels) will be assessed. The results of these analyses are combined to estimate the probability of levee breach as a function of the loading from the stressing event and the epistemic uncertainty in the estimated probability of breach.

The specific steps involved in implementing this approach are as follows:

1. Identify suitable geotechnical analysis models to assess levee response to the loading from a given stressing event. Suitable models were identified for the failure modes of seismic deformation due to an earthquake (section 6.0), under-seepage (section 5.0) overtopping due to a flood event (Section 5.0), and erosion due to wind/waves (Wind Wave TM, 2007 and Emergency Response TM, 2007). For the remaining failure modes under normal (“sunny day”) conditions, no feasible predictive model of geotechnical analysis could be identified. For these latter failure modes, an empirical model for estimating the frequency of occurrence of levee breaches was estimated

based on the record of historical levee breaches in the Delta (Section 3.0). This empirical breach rate was assumed to be applicable for all levees in the study area with a spatially uniform rate of occurrence.

2. For each selected geotechnical analysis model, identify important input parameters. Define categories for each input parameter that vary spatially. Use combinations of the categories for different input parameters to define vulnerability classes for each failure mode. Vulnerability classes are defined as those levee reaches expected to yield the same response under a given stressing event. Each levee reach will be assigned to one and only one vulnerability class.
3. Estimate levee response to different loading levels of a stressing event for different combinations of model input parameters and representative levee cross sections.
4. Using the results of Step 3, develop a multiple regression equation to estimate levee response as a function of loading level and model parameters.
5. Based on statistical analysis of available data and published information, develop probability distributions for the input variables that exhibit random spatial variability.
6. For each vulnerability class and each combination of loading level, use Monte Carlo simulation to generate values of the input random variables. For each set of values of the input variables, calculate levee response using the regression equation developed in Step 4.
7. Using input from a panel of geotechnical experts, develop a relationship between probability of levee breach and levee response. Use the range of the expert elicitation inputs to define a median curve and upper and lower confidence bounds around the median value curve. These curves quantify the epistemic uncertainty in the estimated breach probability.
8. For each value levee response calculated in Step 6, assess the probability of breach for each of the curves developed in Step 7. Fit an empirical equation to estimate the median probability of breach as a function of loading level for each vulnerability class. Use the alternative curves (expert input range) developed in Step 7 to assess confidence bounds on the breach probability.
9. Use the empirical equation and confidence bounds on the breach probability developed in Step 8 to estimate the breach probability for each selected loading level within the expected range of loading at different confidence levels. Repeat this analysis for each vulnerability class. All levee reaches within a given vulnerability class will be assigned the same probability of breach.

The following sections provide details of implementing this approach for the various failure modes under each stressing event.

2.2 Probability of Breach due to a Flood Event

2.2.1 Under-Seepage Failure Mode

For the under-seepage failure mode, levee response was analyzed in terms of exit gradient. The loading from a flood was expressed in terms of the water-surface elevation

in the channel. The geotechnical model used to calculate exit gradient is described in Section 5.2.

The following factors are used to define levee vulnerability classes in the under-seepage failure mode:

- Peat thickness
- Presence of sediment layer
- Presence of drainage ditch
- Slough width
- Average island ground surface elevation
- Peat permeability

For the calculation of exit gradient, the differential head was defined to be the distance between the water surface elevation in the channel and the average island ground surface elevation.

Table 2-1 shows the format in which the results of levee fragility analysis in under-seepage will be summarized. For each vulnerability class, the table will show the probability of breach at various confidence levels for given water surface elevations.

2.2.2 Through-Seepage Failure Mode

As discussed in Section 5.0, an empirical breach rate was estimated based on the frequency of historical failures that could be attributed to through-seepage. The estimated breach rate of 0.00048/year/levee-mile will be applied to all levees in the study area.

2.2.3 Overtopping

Water surface elevations (WSE) will be estimated based on the flood stage plus wind set-up and wave action. The estimated WSE could exhibit random (aleatory) variability, which will be characterized in terms of a coefficient of variation. Based on observations of wave heights during floods, a coefficient of variation of 25% was assumed for the WSE. The probability of a breach was then calculated as the probability that WSE would exceed the available freeboard.

2.3 Probability of Breach due to Seismic Deformation

Levee response to an earthquake was analyzed in terms of the vertical displacement of the levee crest. Such displacement would cause slumping of the levee crest and could also cause cracking. The slumping would reduce the available freeboard above the estimated water surface elevation. If the freeboard is inadequate, the levee section could breach due to overtopping. The levee could also breach because of piping through the cracks. Based on input of a group of experts, the probability of a breach is assessed as a function of the amount of vertical displacement and available post-earthquake freeboard.

The loading on a levee section from an earthquake is characterized in terms of the earthquake magnitude and peak ground acceleration (PGA) at the site of the levee

section. The geotechnical models used to calculate vertical displacement are described in Section 6.

The factors used to define the levee vulnerability classes under seismic loading/deformation are presented in Section 6.2.

Table 2-2 shows the format in which the results of the levee seismic fragility analysis will be summarized. For each vulnerability class, the table will show the probability of breach at various confidence levels for given combinations of earthquake magnitude and PGA.

2.4 Probability of Breach due to Wind/Waves

High winds and associated waves could also occur without a flood event and could cause levee breaches due to erosion or overtopping. The effect of wind and waves during flood and non-flood events are presented in the Wind Wave Technical memorandum and the erosion potential of levee interiors resulting from the wind wave are presented in Emergency Response Technical Memorandum. The probability of wind-wave induce erosion failure during non-flood conditions failure are included in the failure rate for normal ("sunny day") conditions in Section 3.3.

2.5 Probability of Breach under Normal Conditions

An empirical rate was estimated for breaches that occur during non-flood conditions and without a seismic event. The frequency of historical breaches that occurred in the Sacramento Delta region is discussed in Section 3.0. Based on this data, a breach rate of 5.74×10^{-4} /year/levee mile was estimated for a breach during normal conditions. This rate will be applied to all levees within the study area with a uniform probability of occurrence.

Table 2-1
Format for Summarizing Results of Levee Fragility Analysis in Under-Seepage

		Probability of Breach for Given Water Surface Elevation (WSE)										
Underseepage Vulnerability Class	Confidence Level based on Epistemic Uncertainty	WSE1	WSE2	.	.	.						
1	1%											
	2%											
	3%											
	.											
	.											
	.											
	.											
	100%											
2	1%											
	2%											
	3%											
	.											
	.											
	.											
	.											
	100%											

Table 2-2
Format for Summarizing Results of Levee Fragility Analysis in Seismic Deformation

				Probability of Breach for Given Ground Motion Level							
Seismic Vulnerability Class	Earthquake Magnitude	Post-Earthquake Water Surface Elevation	Confidence Level based on Epistemic Uncertainty	a1	a2	a3	.	.	.		
1	7	e.g., MHHW	1%								
			2%								
			3%								
			.								
			.								
			.								
			100%								
	7.5		1%								
			2%								
			3%								
			.								
			.								
			.								
			.								
			.								
			.								
			100%								

3.0 Delta and Suisun Marsh Levee Historic Failures

3.1 Historic Delta and Suisun Marsh Islands Flooding

Since 1900, 166 islands flooded as a result of levee breaches in the Delta and Suisun Marsh. However, records on Suisun Marsh levee failures are incomplete. Table 3-1 (located at the end of Section 3) summarizes the number of islands/tracts flooded and their corresponding years. Figure 3-1 illustrates the number of times islands or tracts flooded since 1900. Figure 3-2 identifies the locations (when available) of the levee breaches that resulted in Islands/tracts flooding. Most the breach locations have been mapped except for few flood events whose corresponding levee breach locations were not available.

A plot of island cumulative flooding trend is presented in Figure 3-3. This plot should be viewed in the context of the historic changes the levee system has undergone in the last century. For instance, the levees were only few feet tall at the turn of the century compared to 20 feet tall levees today. Furthermore, island/tracts were reclaimed at different periods. The levee maintenance and subvention practices also changed and improved over the past few decades. At the turn of the century, the levees were not engineered. The construction of the levees then consisted mainly of dredging and piling slough side material indiscriminately of it origin or engineering properties. The levees were smaller in size and more prone to overtopping, and not maintained to today's standards. In recent years the levees have been built up to contain larger floods and were upgraded/maintained to meet some engineering standards (free-board, and attend to maintain stability). Part of the recent changes included: a) levee raise to meet higher flood protection level, b) levee raise to compensate for foundation consolidation and settlement, c) levee raise to mitigate for the continued subsidence (peat and organic marsh deposits) as a result of farming practices, and d) improved/increased maintenance to mitigate/contain the higher stresses on the levee system due to higher hydrostatic heads. Figure 3-3 should be considered as just a historic evolution of the levee system performance. During the period since 1900, the average annual frequency of island flooding corresponds to about **157 percent** or **1.57** expected flooded islands per year including all events **except for earthquakes**.

The higher maintenance standards and subvention programs in the recent years do not indicate a strong improvement trend in the performance of the levee system as seen in the trend lines of Figure 3-3. The trend of levee failure seems to indicate a slight improvement (1.32 average annual island flooding) for the period from 1951 to 2006 compared to 1.86 average annual island flooding for the period from 1900 to 1950. It is interesting to note that if the 11 flooded islands in 1950 are included in the last period (1950-2006), the trends for the two historic periods, 1900-1949 and 1950-2006, will be similar with 1.54 and 1.59 annual failure frequencies, respectively.

The historic and recent levee failure trends indicate that taller levees are subjected to higher and sustained stresses, requiring a higher maintenance to merely keep up with the adverse changes the flood control system is experiencing through time.

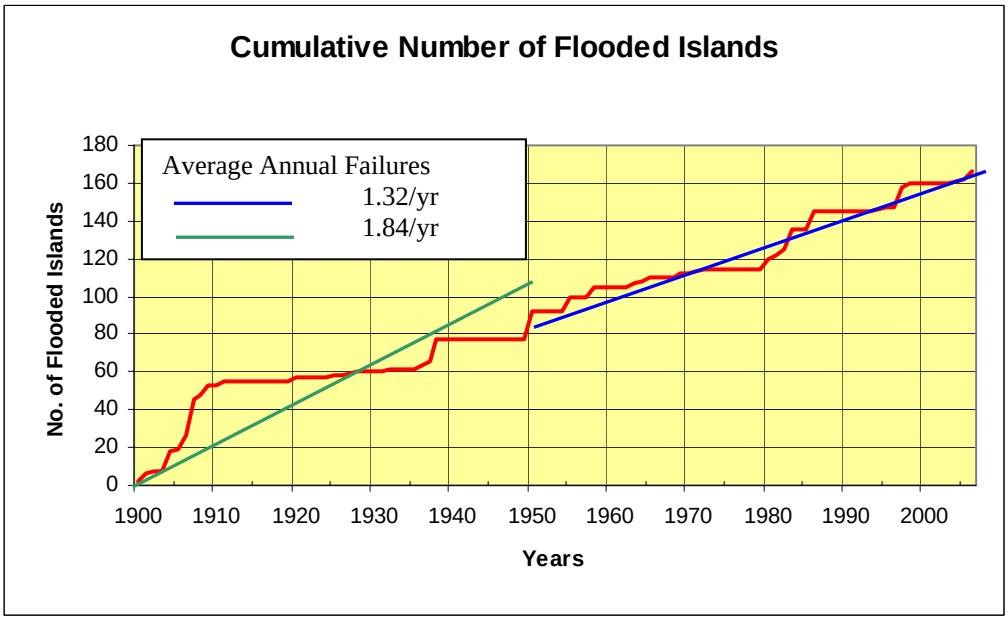

Figure 3-3 Cumulative Number of Flooded Islands Since 1900

A further analysis of levee failures and island flooding history related to: recent years events, storm related failures, and "sunny weather" failures, are presented in the following paragraphs.

3.2 Analysis of Storm Related Failures Since 1950

During the past 56 years (1950 excluded), there were 74 reported levee failures resulting in island/tract flooding. The annual frequency of island flooding is about **132 percent**, or **1.32.** Excluding the summer events, there were 68 failures corresponding to an annual frequency of failures of about **121 percent** due to storm related failures. The storm-related failure modes considered in this set of data includes: under-seepage, through-seepage, overtopping, or stability failure due to high hydrostatic head on the levees. These failure modes would include any pre-existing conditions related to rodent activities, on-going internal erosion or weaknesses in the levee and foundation.

Figure 3-4 shows the cumulative number of levee breaches resulting in island flooding since 1950. The "sunny weather" island flooding events are excluded from these data. The data cut-off at 1950 was intentionally selected to remove the older historic events during which the levee configurations were dissimilar to the current levee conditions. These recent years represent a better data set to use for comparison with the results of the predictive levee analysis numerical models presented in Sections 2.0 and 3.0 of this Technical Memorandum. One should recognize that since 1950, the levee geometry and crest elevation kept changing through time.

A further examination of the failure trends (Figure 3-4) indicate an average annual frequency of failures of **1.62** for the period between 1981 and 2006 compared to **0.87** for the period between 1951 and 1980. These trends clearly indicate that during the recent 26

years, the Delta and Suisun Marsh have experienced a higher number of flooded islands and tracts than the period between 1951 and 1980 (30 years) despite the increasing maintenance efforts and subvention programs, as shown in Figure 3-4.

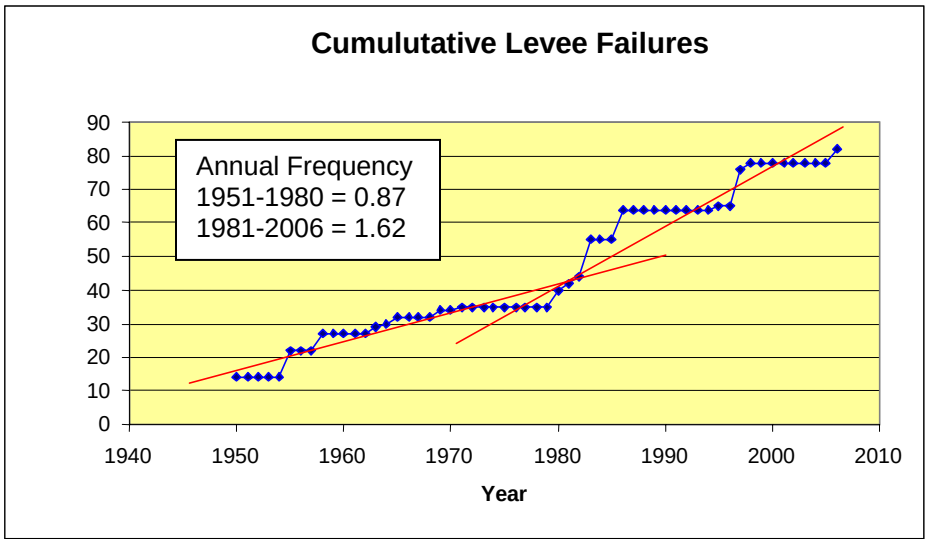

Figure 3-4 Cumulative Plot of Island Flooding Since 1950

To better understand the higher occurrence of island flooding events in the last 26 years, a flow hydrograph (since 1955, available records) is presented in Figure 3-5.

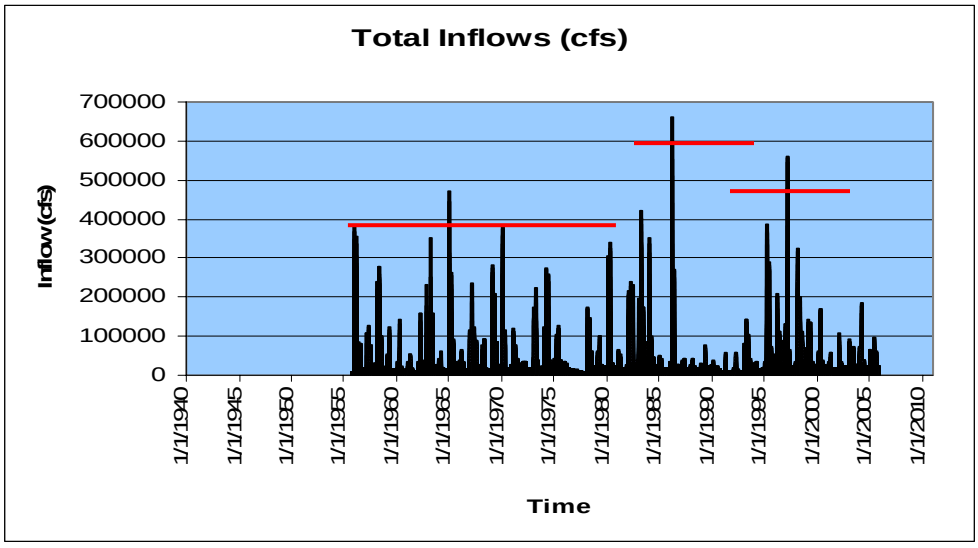

Figure 3-5 Total Delta Inflows (cfs) Since 1955

The total in-flow hydrograph shows that the storms events recorded since 1980 are more potent and characterized by higher magnitudes then the storms recorded in the 25 years prior to 1980. Furthermore, the higher magnitude storm events, since 1980, correlate with

higher number of flooded islands/tracts. These particular events include the 1980 (5 islands flooded), 1983 (11 islands flooded), 1986 (9 islands flooded), 1997 (11 islands flooded). The higher frequency of island flooding in the last 26 years seems to have a strong correlation with the larger storms events compared to the 1851-1980 period of storm records.

During the 1983 flood, 11 islands/tracts flooded. Shima Tract, Prospect Island, and VanSickle Island breached at two locations. Mildred Island and Little Franks Tract were not reclaimed after flooding. During the 1986 flood, 9 islands/tracts flooded. Tyler and Deadhorse Islands and McCormack-Williamson Tract breached at two locations each. During the 1997 flood, 11 islands/tracts flooded. Multiple levee breaches occurred along the Cosumnes River and along the levees north and east of Glanville Tract. Similarly, multiple levee breaches occurred to the south along the levees adjoining Pescadero, Paradise Junction, Stewart Tract, McMullin Ranch, and River Junction.

Figures 3-6 through 3-13 obtained from the USACE 1999 post flood assessment report illustrate the flooded areas during the 1983, 1986, 1995 and 1997 flood events in the Delta.

3.3 Analysis of Sunny-Weather Island Failures

Historic data were used to estimate the rate of levee breaches during non-flood and non-seismic conditions “sunny day failures”. The frequency of historical failures that occurred in the Delta and Suisun Marsh were determined from the 6 recorded sunny day failures in Delta and the 2 sunny day breaches in Suisun Marsh. Assuming 911 miles of Delta levees within the MHHW boundary, a failure rate of 1.18x10-4 /year/levee mile or 0.107 failures/year was estimated. Assuming 75 miles of Suisun Marsh exterior levees within the MHHW boundary, a failure rate of 4.76 x10-4 /year/levee mile or 0.036 failures/year was estimated. Each failure rate will be applied to all levees for its area within the MHHW boundary, assuming a uniform probability of occurrence.

The methodology uses the historical sunny day levee failures that have occurred in the Delta to estimate future failure rate. In the last 56 years, there were 8 levee failures that occurred during summer that resulted in island flooding. Sunny day, or summer time, is defined as the period between June and October. Data prior to 1950 were not used because the information is sparse and lacks the necessary details, and also the levee configuration is not comparable to today’s levees. The information associated with the summer island flooding is summarized in Table 3-2. The water levels in the nearby sloughs were obtained from gage station historic records operated and maintained by the California CDEC. Levee crest elevations were obtained from the IFSAR data in the GIS files provided by DWR. The descriptions of the failure modes are not complete and very anecdotal. No post-failure investigation reports providing detailed descriptions of the causes of levee failures were available. The information provided in Table 3-2 is conjectural and relates to few available data and communication with DWR personnel and reclamation district’s engineers. It seems like well engineered levees may be less vulnerable to failure than older non-engineered levees. However, there isn’t enough data to determine failure rates by levee classes.

Figure 3-14 shows the levee crest elevations versus the water stage (NAVD-88) for the eight levee breaches at the time of failure; Figure 3-2 shows the approximate locations of the breaches. A close examination of the data indicates that failures occurred during an unusually high tide conditions. At Simmons-Wheeler, the water stage rose above the crest of the levee at Suisun Marsh and may have caused failure of the levees by overtopping. Other reports also indicate the levee failure at Simmons-Wheeler may have been caused by rapid drawdown during the period of receding stage. These summer time failure events may be the result of the combination of high tide and pre-existing internal levee and foundation weaknesses (i.e., burrowing animals, internal cumulative erosion of the levee and foundation), and other human interventions (dredging at the toe of the levee). The unusual high tide could be the result of offshore storm surges arriving in the Delta, astronomic conditions resulting in higher gravitational pull from the concurrent alignment of the sun and the moon, or a combination of the two. Higher tides caused by astronomic gravitational pull occur twice a year. Post-failure reports indicate the failure of Brannan Andrus Island may have been caused by excavation activities at the land side toes of the levee. At MacDonald Island, the levee may have been breached as a result of dredging on the water side toe (information not confirmed).

Whether the failures occurred during a high tide condition or not, rodent activities and pre-existing weaknesses in the levees and foundation seem to have contributed considerably to the levee failures. It is believed by most practicing engineers, scientists, and maintenance personnel in the Delta and Suisun Marsh that rodents are prolific in the Delta and use the levees for borrowing and hence causing undo weaknesses by creating a maze of internal and interconnected galleries. Under-seepage is a process that tends to work through time by removing fines from the foundation material during episodes of high river stage. The cumulative deterioration through the years, can lead to foundation that would ultimately fail by uncontrollable internal erosion leading to slumping and cracking of the levee.

Four out of the eight levee failures occurred during unusual high tide. Because of the incomplete information on the exact causes of the sunny day levee failures, the recurrence model of sunny day failures assumes that the probability of levee failure represents all the above failure modes and that occurrences are uniformly distributed throughout the Delta and Suisun Marsh.

Table 3-2 Sunny Weather Failures

Island/Tract	Year	Month	Day	Failure Mode	Water Level (NAVD-88)	Levee Crest (NAVD-88)
Webb Tract	1950	June	2	High Tide, Stability	6.1	10.8
Brannan-Andrus Is.	1972	June	22	Excavation at LS Toe	6.2	10.8
Lower Jones Tract	1980	Sept.	26	Seepage & Rodents Activities	6	11
McDonald Island	1982	August	23	Seepage from Dredging at WS?	5.48	11.5
Little Mandeville	1994	August	2	High Tide, abandoned	6.1	11.5
Upper Jones Tract	2004	June	3	High Tide, Underseepage & Rodent Activity	6.85	11
Simmons-Wheeler	2005	July	20	High Tide, breached occurred between two water control structures. Beaver activities suspected	7.51	7.3
Sunrise Duck Club	1999	July	NA	High tide and possible beaver activities	NA	5 to 6

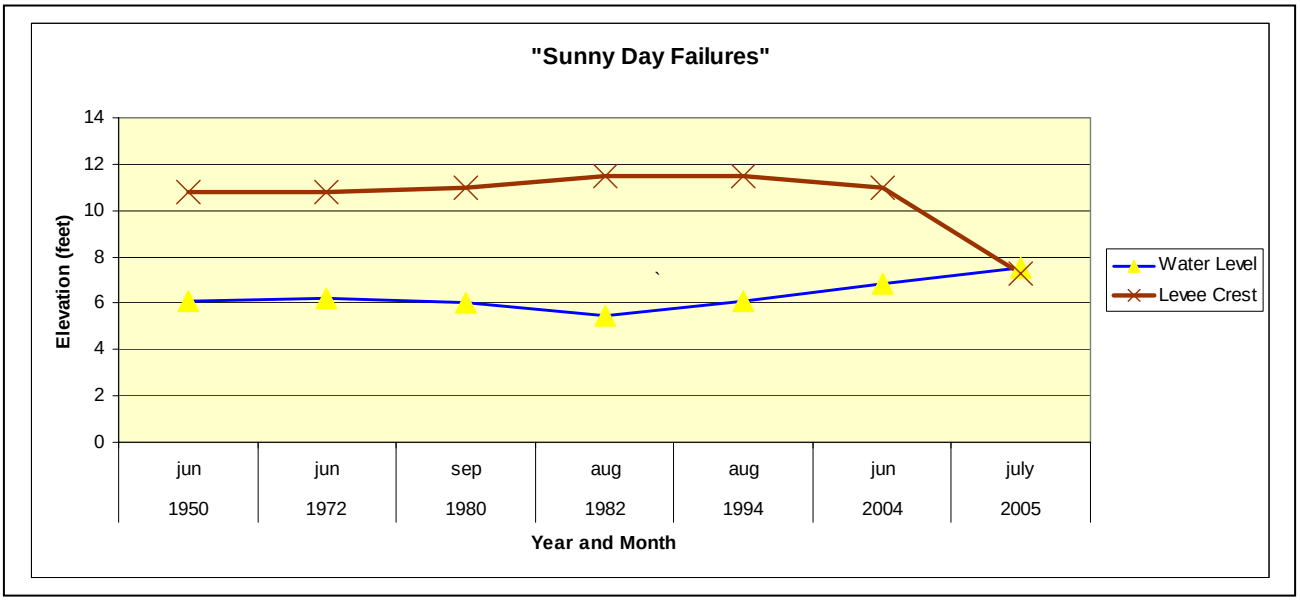

Figure 3-14 Water Stage versus Crest Elevation at Breach Locations

3.4 Observation of Levee Breaches and Scour Holes

Levee breaches in the Delta leave large scars (scour holes) in the interior of the islands or tracts, visible for many years after their occurrence. Some of these visible scars date back to 1938, if not filled in and subsequently farmed.

3.4.1 Observation of Scour Holes from Aerial Photographs

Table 3-3 summarizes the dimensions of scour holes still visible from the air. These data represent post-repair dimensions of the scour holes left in the ground and consist of scour hole lengths and widths. The aerial photographs presented in this section were obtained from Google and Yahoo satellite imagery (see Google and Yahoo URL site references). The depths of the scour holes (when available) were obtained post-failure mapping studies or information in the DWR GIS files. For the older events, the scour hole dimensions listed below may not reflect the full dimensions at the time of the event, as farming and backfilling around the edges of the scour holes are common. Aerial photographs of scour holes still visible from the air are shown in Figure 3-15 through 3-34a. The aerial photograph of the more recent event (June 3, 2004 Upper Jones Tract) shows a fresher scar on the interior of the island as illustrated in Figure 3-15. Generally the width of the scour holes are larger than the levee breach width as the released water from the levee breach fans out towards the interior of the levee. High velocity flows from the levee breach tend to tear and erode the island interior floor. Generally the size of the hole becomes larger as thicker peat is present at the location of the breach. It has been observed that large chunks of peat floated up during island flooding, as shown in Figures 3-16 and 3-17 during the 2004 Upper Jones Tract failure.

The scaled dimensions of the scour holes from the aerial photographs are summarized in Table 3-3. The data seems to indicate that on average, the length of the scour holes is about **2000 feet**, the width is about **500 feet** and the depth is about **35 feet**. The highest depth recorded was 77 feet at Mildred Island after the 1983 failure (Table 3-4).

Table 3-3 Mapping of Scour Holes From Aerial Photographs

Island/Tract	Date	Length (ft)	Width (ft)	Depth (ft)
Upper Jones	6/3/2006	1680	432	35
Venice Island	11/30/1982	2210	613	24
Venice Island	12/3/1950	997	235	40
Venice Island	1938	1056	176	NA
Ryer Island	Feb. 1986	1745	633	NA
Webb Tract	01/18/1980	4168	1018	45
Webb Tract	6/2/1950	3936	926	31
Tyler Island	02/19/1986	2087	368	NA
Bradford Island	12/03/1983	2945	736	35
Holland Tract	1/18/1980	1842	417	40
Empire Tract	12/26/1955	2534	950	
MacCormack-Williamson	Jan. 1997	902	258	NA
Quimby Island	12/26/1955	1560	360	22
Sherman Island	1/20/1969	1320	475	22
Assumed Average		**2000**	**500**	

3.4.2 Observation of Remnant Levees at Unreclaimed Islands

Few islands flooded in the Delta were not reclaimed after flooding. Such Islands include: Franks Tract (abandoned in 1938), Little Franks Tract (abandoned in 1983), Mildred Island (abandoned in 1983), Little Mandeville (abandoned in 1994), and Rhode Island (abandoned in 1971) as shown in Table 3-4. A review of the remnant levees after last flooding, indicate that the remaining levees tend to erode and slough off around the crest area, but generally keep most of their mass. Visual observations of these remnant levees is documented below from aerial photographs 3-42 through 3-46 obtained from Google and Yahoo web site satellite photographs (see URL site reference for: Google & Yahoo).

Table 3-4 Remnant Levees and Breach Widths at Unreclaimed Islands

Island/Tract	Scour Depth	Breach Date	Current Breach Width	Remarks
Mildred Island	77	1/27/1983	502	23 years after flooding
Little Mandeville	10	8/2/1994	270	12 years after flooding
Rhode Island	NA	1971	196	35 years after flooding
Franks Tract	34-42	1938	520	68 years after Flooding
Little Franks Tract	15-23	1983	100	23 years after flooding

Island remnant levees survive for a long time. Twenty three years after Mildred Island flooded, except for the breach area, the entire levee is still visible from the air as shown in Figures 3-34b through 3-34c. Similar observations can be made for Little Franks Tract (Figure 3-35), Little Mandeville (Figures 3-36a and 3-36b), and Rhode Islands (Figure 3-37a and 3-37b), flooded 23, 12, and 35 years ago, respectively. These observations indicate, that the remaining levees do not undergo extensive erosion damage. The levee crests erode until they find a stable slope under the cyclic tide action. At that point they re-vegetate, and the roots help develop a more stable levee surface and crest. Out of the abandoned islands, Franks Tract has lost the most of its remnant levees. Figures 3-38a and 3-38b show about 65% of Franks Tract levee remnants are still visible from the air, 68 years after it was abandoned.

These observations holds also true for the width of the levee breaches. Levee breaches are still visible from aerial photographs for Mildred, Little Franks Tract, Little Mandeville and Rhode Islands, as shown in Figures 3-34c, 3-38b, 3-36b, and 3-37b, respectively. The levee breach widths shown in Table 3-4 were measured from scalable aerial photographs. Despite the fact that the breaches occurred 12 to 35 years ago, the levee breach widths observed from the aerial photographs, are still within few tens of feet from first occurrence as compared in Tables 3-4 and 3-5. These comparisons indicate that levee breaches did not grow uncontrollably with time. It should be noted though, that it is not known which levee breaches had been capped and which had not. Table 3-5 was obtained from DWR GIS group (Mr. Joel Dudas). Additional data noted were obtained from available post-failure topographic survey of the scour holes. The **average breach width** based on these data is about **438 feet**.

Table 3-5 Levee Breach Width Following Island Flooding

Island/Tract	Breach Date	Levee Breach Width (feet)	Remarks
Bouldin Island	1909	355	
Bradford Island	1983	450	
Empire Tract	1955	860	
Franks Tract	1936	520	
Franks Tract	1938	390	
Holland Tract	1980	250	
Lower Jones	1980	275	
Little Franks Tract, WL	1981	40	
Little Franks Tract, WR	1982	60	
Little Franks Tract, S	1983	174	
Little Mandeville	1986/1994	263	
Mandeville	1938	930	
McCormack-Williamson	1997	871	
MacDonald Island (1)	1982	250, 600	Conflicting Data
Mildred Island	1983	473	
Mildred Island	1969	330	
New Hope	1986	170	
Quimby Island	1955	260	
Sherman Island	1969	260	
Sherman Island	1904	1150	
Staten Island	1907	311	
Tylor Island (1)	1986	300	
Upper Jones (1)	2004	432	
Venice Island	1982	500	
Webb Tract	1950	690	
Webb Tract	1980	825	
Average		**438**	

Table 3-1 Historic Islands/Tracts Flooded Since 1900

	Location		Years	No. Of Failures
1	Bacon	Island	1938	1
2	Big Break	Island	1927	1
3	Bishop	Tract	1904	1
4	Brack	Tract	1904	1
5	Byron	Tract	1907	1
6	Coney	Island	1907	1
7	Donlon	Island	1937	1
8	Edgerly	Island	1983	1
9	Grand	Island	1955	1
10	Holland	Tract	1980	1
11	Honker Bay Club	Island	2006	1
12	Little Holland	Tract	1963	1
13	Lower Roberts	Island	1906	1
14	Mandeville	Island	1938	1
15	Mc Donald	Island	1982	1
16	Medford	Island	1936	1
17	Palm	Tract	1907	1
18	Rd 1007	Tract	1925	1
19	Shima	Tract	1983	1
20	Union	Island	1906	1
21	Upper Jones	Tract	2004	1
22	Upper Roberts	Tract	1950	1
23	Walthall	Tract	1997	1
24	Wetherbee	Lake	1997	1
25	Bradford	Island	1950-1983	2
26	Cliftoncourt	Tract	1901-1907	2
27	Empire	Tract	1950-1955	2
28	Fabian	Tract	1901-1906	2
29	Fay	Island	1983-2006	2
30	Glanville	Island	1986-1997	2
31	Grizzly	Island	1983-1998	2
32	Ida	Island	1950-1955	2
33	Mcmullin Ranch	Tract	1997-1950	2
34	Middle Roberts	Island	1920-1938	2
35	Rhode	Island	1938-1971	2
36	Sargent Barnhart	Tract	1904-1907	2
37	Simmons Wheeler	Island	2005-2006	2
36	Staten	Island	1904-1907	2
37	Terminous	Tract	1907-1958	2
38	Victoria	Island	1901-1907	2
39	Webb	Tract	1950-1980	2
40	Little Mandeville	Island	1980-1986-1994	3
41	Ryer	Island	1904-1907-1986	3
42	Franks	Tract	1907-1936-1938	3

	Location		Years	No. Of Failures
43	Little Franks	Tract	1981-1982-1983	3
44	Lower Jones	Tract	1906-1907-1980-2004*	3
45	Mildred	Island	1965-1969-1983	3
46	Mossdale Rd17	Tract	1901-1911-1950	3
47	Paradise	Junction	1920-1950-1997	3
48	Pescadero	Tract	1938-1950-1997	3
49	River Junction	Junction	1958-1983-1997	3
50	Stewart	Tract	1938-1950-1997	3
51	Twitchell	Island	1906-1907-1908	3
52	Tyler	Island	1904-1907-1986	3
53	Van Sickle	Island	1983-1998-2006	3
54	Bethel	Island	1907-1908-1909-1911	4
55	Bouldin	Island	1904-1907-1908-1909	4
56	Jersey	Island	1900-1904-1907-1909	4
57	Quimby	Island	1936-1938-1950-1955	4
58	Shin Kee	Tract	1938-1958-1965-1986	4
59	Brannan-Andrus	Island	1902-1904-1907-1909-1972	5
60	Sherman	Island	1904-1906-1909-1937-1969	5
61	Dead Horse	Island	1950-1955-1958-1980-1986-1997	6
62	McCormack-Williamson	Tract	1938-1950-1955-1958-1964-1986-1997	7
63	New Hope	Tract	1900-1904-1907-1928-1950-1955-1986	7
64	Prospect	Island	1963-1980-1981-1982-1983-1986-1995-1997	8
65	Venice	Island	1904-1906-1907-1909-1932-1938-1950-1982	8
	Number Of Flooded Islands/Tracts			**166**

4.0 Data Review and Development of GIS Maps

4.1 Introduction

The purpose of the data review work discussed herein was to compile and review pertinent existing geotechnical data, identify the general characteristics of the main soil units underlying the Delta and Suisun Marsh levees, and summarize the data for use in subsequent tasks of the DRMS study.

The first step in the data review was to collect previous reports of geotechnical investigations in the study area for data that may be pertinent to the DRMS project. In addition, the DRMS team collected available reports on problem areas, general maintenance practices, and information on past failures. Based on the available boring logs, test data, geophysical records, and other information, an electronic database was developed. The electronic database was then used to develop a Geographic Information System, G.I.S.-based Delta levee catalogue that provides data regarding the spatial and temporal variation in the levee and foundation conditions. This catalogue can then be used to select levee vulnerability classes (discussed in detail in Section 5.0) using factors

that differentiate the performance of the levees when subjected to the same stressing event.

4.2 Data Collection

The members of levee vulnerability team prepared a list of names of agencies and reclamation districts likely to have undertaken projects in the study area that appeared to meet the study's need. The list also included data needed for the risk analysis. A sample list is presented below:

List of agencies/ firms:

- Department of Water Resources
- Several Reclamation districts
- KSN engineers
- MBK engineers
- Kleinfelder
- U.S. Army corps of engineers
- Hultgren-Tillis Engineers

List of data needed:

- Levee geometry: crest elevation, side slopes, crest width, height
- Thickness of peat/organic soil layer
- Thickness, type, penetration resistance, and density of levee fill
- Thickness, type, penetration resistance, and density of levee foundation
- Strength parameters of peat/organic and other soils
- Dynamic properties of peat/organic and other soils
- Extent and size of riprap
- Maintenance practices
- Problem areas
- Past failure data
- Groundwater and tidal data
- Any other useful data

The first step in actual data collection was to request data packages from each agency/firm. The data packages were to consist of the following: geotechnical investigation reports, construction documents, reports on problem areas, data on levee geometries, and any other easily obtained documents considered of interest.

DWR provided large volume of electronic data which included scanned levee cross sections, crown elevations, and borings logs for several islands, bathymetric (only few

islands), riprap (only for few islands), and others. The dataset from other agencies/firms were used to supplement the dataset received from DWR. In addition, data from some of URS projects such as Delta Wetlands (Bacon Island, Webb Tract, Bouldin Island, and Holland Tract), In-delta storage (Bacon Island, Webb Tract), and Delta Coves (Bethel Island) were also retrieved and added to the collected dataset. Table 4-1 (all Section 4 tables are at the end of the section) lists borings collected for this study along with information regarding date of investigation, provider of data, and other relevant data.

In general, the collected data included logs of test pits and exploratory borings, geophysical data, cone penetration test, information on historical failures and problem areas, scanned levee cross sections, limited data on bathymetric and Light Detection and Ranging (LIDAR) survey results, and limited information on riprap and other features in the study area.

4.3 Development and Processing of Database

4.3.1 Compilation of Boring Data

The majority of the collected data were in the form of logs of soil borings that were drilled in the Delta and Suisun Marsh areas. These borings were drilled as part of several investigation studies conducted in the study area, some of these investigations are: the Salinity Control Barrier Investigation (1956-1958), the Peripheral Canal Investigation (1960-1968), The Geological Investigation Relocated Montezuma Slough (1985), the South Delta Facilities-Old River (1995-1997), the South Delta Water Management Facilities (2005). A complete list of the projects is presented in Table 4-1.

A total of more than 5,000 soil borings were collected from various agencies. The database consisted of borings drilled on the crest, landside, and waterside of the levee. The boring data was spatially displayed on a GIS. base map (Figure 4-1). The base map for this work consisted of boundaries of Delta and Suisun Marsh islands and water bodies. Location data for borings were found to be in the form of: 1) latitude and longitude, or 2) scalable from plan sheets. The boring location map was used to identify data gaps and to select borings for digitizing. Figure 4-1 shows the following:

- In general, most of the past investigations covered the central Delta.
- Some of the islands within the central Delta have reasonably spaced borings all around their perimeter levees (e.g., Sherman Island, Webb Tract, Mandeville Island, and Medford Island)
- Some of islands have good coverage of borings on one side and few or no borings on other side (e.g., Victoria Island, Jersey Island, Holland Tract, Bacon Island, Palm-Orwood Tract, and Venice Island)
- Some of the eastern boundary islands have only interior borings (e.g., Bishop Tract, Shin Kee Tract, and Rio Bianco Tract)
- There are no borings or only very few borings available for some of the southern Delta islands (e.g., Roberts island, Union island, Fabian Tract, Jones Tract, Victoria Island, Veale Tract, and Byron Tract)

- There are no borings or only very few borings available for some of the northern Delta area (e.g., west Sacramento in particular along the Sacramento water ship channel, Netherlands, and Hastings Tract)
- In general, there are only few borings available for the Suisun Marsh area.

The database will be continuously updated as the data become available. For each island or tract, a screening process was employed to minimize the number of borings to be digitized. If reasonable numbers of borings are available around the perimeter levee for a given island or tract, then interior borings of that island/tract were not digitized. However, if there were only few borings/no borings available around the perimeter levee for a given island or tract, then both interior and levee borings of that island/tract were digitized. Total of 2,129 borings were reviewed, interpreted, and entered into a geo-database. Some of the key statistics on these digitized borings are as follows:

- Levee borings (included borings drilled on the crest and slopes) – 953
- Other borings (most of these borings were drilled on the landside) – 1176
- Deepest boring elevation: -311.5 ft (NGVD 29)
- Number of borings with bottom elevation less than –100 ft (NGVD 29): 62
- Number of borings with bottom elevation between –50 ft and –100 ft (NGVD 29): 320
- Average maximum depth of explorations: El –37 ft (NGVD 29)

The interpretation of borings was focused on gathering thickness, type, and sequence of different geological units. The geologic units of interest are organic/peat, levee fill, and levee foundation materials. In addition, blowcount and laboratory data were also entered into the database. The database was developed using the Microsoft Excel program. Every exploratory boring was assigned a unique name that relates to the island/tract name and original boring name from data source. To ensure the quality of the database, a systematic quality assurance/ quality control process was used for this project.

4.3.2 Compilation of Other Data

4.3.2.1 Problem Areas and Historic Failure Data

Data on problem areas were collected: (1) through interviewing reclamation district engineers, DWR personnel, and others who have the knowledge of the Delta and Suisun Marsh areas; and (2) from investigation/repair reports. The collected data were entered directly into a G.I.S. database and to produce locations of problem areas map. Some of reported causes of problems are associated with levee instability, under-seepage, through seepage, boils, cracks, landslide, and slumping. Similarly, data on historic failure were collected by many ways such as reports, Internet, news articles, and interviewing reclamation district engineers, DWR personnel, and others. The interpretation of the data is presented in detail in Section 3.0.

4.3.2.2 Data Related to Levee Geometry

The collected levee geometry database consisted of scanned transverse and longitudinal sections of levees, bathymetric survey, IFSAR, and LIDAR. A limited number of scanned sections were digitized to develop typical values for slopes, width, and height of levees to be used in engineering analyses. The bathymetric survey were used for developing profiles on the slough side for some of the analysis cross sections. In addition, these data are currently being used to develop elevation contours for the slough side. The IFSAR and LIDAR survey results were used to develop surface and crown elevation maps (discussed in Section 4. 5). Note that, LIDAR survey results are available only for few islands in the Delta and Suisun Marsh but DWR is currently working with a consultant to perform LIDAR survey for the entire study area. Our current database will be updated when these data become available.

4.4 Vertical Datum

The Department of Water Resources has been operating a network of water level (tide) stations in the Delta since the early 1950's. All of these stations were established using the National Geodetic Vertical Datum 29 (NGVD29) standard, which was the accepted datum at the time. In the 1970's the National Geodetic Survey (NGS) started using satellites to establish a new datum that would be based on elevation at one base monument. The NGS, in cooperation with professionals in Canada and Mexico, established the North American Vertical Datum (NAVD) 88 standard in the late 1980s. The NAVD88 datum is now the standard datum used by the surveying community. All major data collection agencies that operate in the Delta, including DWR, have converted over to NAVD88 datum. The actual difference between NGVD29 and NAVD88 is between 2 to 3 feet depending on location in the Delta. The datum for this project is taken as NAVD88.

4.5 Analysis of Data

4.5.1 Generation of GIS Maps

The geo-database was integrated into the G.I.S. system for creating and displaying several maps such as the peat/organic soil thickness map. Following are some of the GIS maps created for this project:

- **Peat/organic thickness (Figure 4-2)**: The top and bottom elevations of the peat/organic layer were entered into the database for computing the thickness. Since the geo-database consisted of crest, landside, and waterside borings, it was necessary to define a reference datum for computing the thickness. The thickness of peat/organic layer was taken as the difference between the elevation near the landside toe and bottom elevation of peat/organic layer. The thickness maps were generated using the Kriging interpolation technique. Kriging is essentially a weighted moving average technique for estimation whereby the selection of weights is made such that the estimation variance is minimized. This gives the most likely value that the parameter will have at a given location (at a specific point, area, or volume) together with the range within which it is likely to lie, determined using the kriging error variance of estimation. In practice, the effectiveness of kriging depends upon the

appropriate selection of the model variogram parameters and how representative the observation points are of the phenomenon.

- **Type of levee material (Figure 4-3)**: For each crest boring, the type of levee materials was entered into the database. The levee materials were grouped into two categories, sand, or no sand. The prime purpose for generating this map was to facilitate the assessment of liquefaction potential of levees. In general, levee sand is loose to medium and if saturated has the potential for liquefaction.
- **Blowcount and Cyclic resistance ratio (CRR) distributions for foundation sand (Figure 4-4 and Figures 6-9 through 6-11)**: For each boring that encountered foundation sand, the blowcounts were entered into the geo-database. Figure 4-4 shows the corrected blowcount distribution for foundation sandy materials throughout the study area. Figures 6-9 through 11 show CRR distribution for foundation sandy materials for M 7.5, 6.5, and 5.5, respectively. The procedure for estimating the CRR for the study area is presented in Section 6.0
- **Problem areas (Figure 4-5)**: The past and the ongoing problems in the Delta were mapped based on information gathered from several individuals. Some of the problems reported are: under-seepage, through seepage, levee cracking, slumping, settlement, and others.
- **Failure Areas (Figure 3-2):** This map shows approximate historic failure locations. The year and locations were collected from various sources.
- **Surface elevation (Figure 4-6)**: Both IFSAR and LIDAR data were used to create a surface elevation map (elevation near the landside toe). The following are the major steps for the creation of this map:
  - Calculated a surface extract from a digital elevation model (combined IFSAR and LIDAR digital elevation models) by removing all locations where the percent slope values are greater than 0.01 and less than or equal to 4. This defines flat areas (slope less than or equal to 4), and excludes water (slope greater than 0.01).
  - Derived a surface from step 1 by taking the mean values of these flat areas over a 1000 ft circular radius.
  - Filtered the resulting surface of step 2 by removing all locations where the elevation ranges within 1000 ft within the surface of step 1 is less than 7 ft.
  - Converted the result of step 3 into points.
  - Created a TIN surface (Triangulated Irregular Network) from the points in step 4 to visually inspect for topographic smoothness.
  - Removed points that were anomalously high or low in elevation value.
  - Repeated steps 5 and 6 until a surface is created that expresses a smooth ground-surface elevation model with no elevation values from engineered structures.
  - The final surface was created by smoothing the result of step 7 over a radius of 3000 ft., and removing any values less than or equal to 20 ft.

- **Crest elevation (Figure 4-7)**: The draft version of the crown elevation map comprises layers displayed in the following order:
  - LIDAR digital topographic surfaces for the Yolo bypass (Merrick & Company, August, 2006) and north delta areas (Airborne One, 11/2003)
  - A USACE topographic surface comprising an area north from along the Sacramento Deep Ship Channel, Brannan-Andrus Island, Sherman Island to Van Sickle Island and Chipps Island
  - Surveyed levee crown elevation points, and lastly,
  - An IFSAR topographic surface (2002).

The data was extracted from these layers within polygons of 100-foot levee line reaches with widths of 100 feet on each side. The maximum value of the topographic surface within the polygon, and the survey point nearest to or within the polygon was used as the crown elevation.

4.5.2 Assumption and Limitation

- Locating borings based on scanned images/ scalable plan sheets relies not only on the accuracy of the base map, but also the accuracy in locating the scanned images on the map. Therefore, these locations are less accurate than using quality latitude and longitude data.
- Data gaps necessitated the use of interpolation for displaying spatial variation of conditions in the study area. The accuracy of interpolation depends on the quality and quantity of sampled data points.
- Most of borings and surveyed cross sections were made more than 25 years ago and may not have used most current techniques.
- Organic thickness map: Due to the large variability in the depositional environment, the map represents only a very general indication of the thickness of organic soils that may be present at a particular location.
- The DWR is currently undertaking a project to complete the LIDAR survey of the entire study area. It was necessary to create the elevation maps based on available LIDAR and IFSAR data to facilitate the analysis for the DRMS project. Therefore, these maps should be considered as drafts and would be updated once the LIDAR survey of the entire study area has been completed.

4.5.3 Levee Geometries

The large-scale sustained agricultural development in the Delta first required levee building to prevent flooding. The levee surrounded marshland tracts then had to be drained. Between 1860 and 1880, workers using had tools reclaimed about 140 square miles of Delta for agriculture. Levees and drainage system were largely completed by 1930, and the Delta had taken on its current appearance, with most of its 1,100 square mile area reclaimed for agricultural use (Thompson, 1957). Reclamation and agriculture have led to subsidence of the land surface on the developed islands in the central and western Delta (Subsidence TM #). Islands that were originally near sea level are now

well below sea level, and large areas of many islands are now more than 15 feet below sea level. As subsidence progresses, the levees must be regularly maintained and periodically raised and strengthened to support the increasing stresses on the levees that result when the islands subside (Figure 4-8). Table 4-2 presents levee geometry attributes for some of the islands in the Delta. Figure 4-9 shows typical cross sections for four islands in the Delta. A summary of geometry attributes is provided below:

- Landside slopes: 1.5H:1V to 5.5H:1V
- Water side slope: 1.1H:1V to 4.5H:1V
- Crest Width: 11 to 38 ft
- Levee Height with respect to landside toe: 7 to 26 ft
- Bottom elevation of the slough: -10 to -35 ft (Datum: NAVD88)

The Suisun Marsh levees are primarily maintained as wetlands and thus have resulted in less significant subsidence in comparison to land in the Sacramento-San Joaquin Delta. In general, these levees are considerably smaller in height and width than those levees in the legal boundary of the Delta. Table 4-3 presents the typical geometry attributes for levees in the Suisun Marsh. Figure 4-10 shows a typical cross section of Suisun Marsh levee.

The main Delta channels have been widened, dredged, and straightened to allow for passage of ships. Dredging of the Sacramento River Deep Water Ship Channel (SRDWSC) makes it navigable for ocean-going ships as far inland as Sacramento. Cache Slough is also dredged as it forms part of the SRDWSC. Along the San Joaquin River, the dredged Stockton Deep Water Ship Channel (SDWSC) makes the lower reach of the river navigable for ocean shipping as far inland as Stockton. At Stockton, there is an abrupt change in channel geometry from a deep channel downstream to a shallow river channel upstream.

4.5.4 Geomorphology, Geology, and Subsurface Conditions

4.5.4.1 Geomorphology

This section presents a brief discussion of the Delta geomorphology (more detailed discussion can be found in geomorphology TM). The historic Delta evolved at the inland margin of the transgressive San Francisco Bay-estuary as two overlapping geomorphic units. The Sacramento Delta to the north comprised about 30% of the total area and was influenced by the interaction of rising sea level and river floods, creating an inland of channels, natural levees, and marsh plains. During large river flood events, silts and sands were deposited adjacent to the river channel, forming natural levees above the marsh plain. In contrast, the larger south-centrally-located San Joaquin Delta, with its relatively small flood flows and low sediment supply, formed as an extensive unleveed freshwater tidal marsh dominated by tidal flows and organic (peat) accretion (Atwater and Belknap, 1980). Because of the less well-defined levees, sediments were deposited more uniformly across the floodplain during high water, creating an extensive tule marsh with many small branching distributary channels. Due to the differential amounts of inorganic sediment supply, the peat of the south-central Delta (San Joaquin River system) grades northwards

into peaty mud and mud towards the natural levees and flood basins of the Sacramento River system (Atwater and Belknap, 1980).

4.5.4.2 Geology

The Delta is a northwest trending structural basin separating the primarily granitic rock of the Sierra Nevada from the primarily Franciscan formation rock of the California Coastal Range (CWDD, 1981). The basin is filled with approximately 5 to 10 km of sedimentary deposits, including peat and peaty alluvium, that were deposited by streams originating in the Sierra Nevada, Coast Ranges, and South Cascade Range that enter San Francisco Bay (Figure 4-11). The Delta received thick accumulations of sediments from the Sierra Nevada to the east and the Coast Range to the west during the Cretaceous and Tertiary periods. The Delta has experienced several cycles of deposition, non-deposition, and erosion that resulted in the accumulation of thick poorly consolidated to unconsolidated sediments overlying the Cretaceous and Tertiary formations since late Quaternary time.

Shelmon and Begg, 1975 believe that the peats and the organic soils in the Delta began to form about 11,000 years ago during one of the sea level rises. The sea level rise created tule marshes that covered most of the Delta. Peat formed from repeated burial of the tules and other vegetation growing in the marshes.

As the Suisun Marsh formed, plant detritus slowly accumulated, compressing the saturated underlying base material. Mineral sediments were added to the organic material by tidal action and during floods. Generally, mineral deposition decreased with distance from the sloughs and channels (Miller and others 1975). Suisun Marsh soils are termed “hydric” because they formed under natural tidal marsh conditions of almost constant saturation. The soils adjacent to the sloughs are mineral soils with less than 15% organic matter, and although classed as “poorly drained,” they are better drained than the more organic soils in the marsh. Suisun soils occur farthest from the sloughs, at the lowest elevations and have over 50% organic matter content. Another common soil in the Suisun Marsh is the Valdez series, which formed on alluvial fans and contain very low amounts of organic material. Valdez series soils are found primarily on Grizzly Island (Miller and others 1975).

4.5.4.3 Subsurface Conditions

In general upper portion of the Delta levee embankments are comprised of mixtures of dredged organic and inorganic sandy, silty, or clayey soils that have been placed on either natural peat or natural sand and silt levees. The review of several thousands of borings revealed that the variability in the foundation materials for Delta levees are great, even between islands that are in close proximity to each other. This heterogeneity is due to a history of continuous channel migration and river meandering within the Delta.

Several available transverse cross sections and their associated geology were reviewed to better understand the composition of Delta and Suisun Marsh levees and foundation materials. The locations of the reviewed cross sections are shown in Figure 4-12 and the sections themselves are presented in Appendix A. These sections were chosen based on availability and quality of information to show the variability that exists in the Delta. The general subsurface conditions revealed in these sections are presented below:

Delta Area

- South levee in Sherman Island: The levee materials consist of dredged loose to medium sand and silt. Beneath the levee is a thick layer of peat/organic layer. This peat/organic layer is typically 35 feet thick in the fields away from the levee but has been consolidated under the weight of the levee. Underlying the peat/organic is an approximately 25 feet thick layer of silty clay, under which is a dense sand stratum.
- North levee in Webb Tract: The levee materials consist of dredged peat, silty/clayey sand and silt. Beneath the levee is a 25 to 30 feet thick layer of peat/organic layer. Underlying the peat/organic is an approximately 40 feet thick layer of loose to dense silty sand, under which is a silty clay stratum.
- West levee in Bacon Island: The levee materials consist of predominantly silty/sandy clay. Beneath the levee is about 20 feet thick layer of peat/organic layer. Underlying the peat/organic is loose to dense silty sand.
- South levee (Grant Line Canal) in Union Island: The levee materials consist of predominantly silty clay. Beneath the levee is about 5 feet thick layer of peat/organic layer. Underlying the peat/organic is an approximately 50 feet thick layer of stiff clay, under which is a silty/clayey sand stratum.
- West levee in Grand Island: No borings were drilled through the levee at this location. The silty sand/silty clay layer is exposed at the surface in most of the interior of the island except near the landside toe of the levee where approximately 10 feet thick layer of organic silt layer was detected. Underlying the top layer is an approximately 50 feet thick layer of loose to dense silty sand, under which is a silty clay/silt/silty sand stratum.
- West levee in Terminous Tract: The levee materials consist of silty clay, silt and silty sand. Beneath the levee is about 20 feet thick layer of peat/organic layer. Underlying the peat/organic is loose to dense silty sand/sand.
- East Levee in Netherlands Island: The levee materials consist of mainly loose to medium sand with some clay layers. No peat/organic layer was detected at this location.

Suisun Marsh Areas

The Suisun Marsh is bordered by upland soils that are non-hydric and contain very little organic material. The Suisun Marsh was originally formed by the deposition of silt particles from floodwaters of Suisun Slough, Montezuma Slough, and the Sacramento-San Joaquin river network. The cross sections presented in appendix indicate that the top foundation layer in Suisun Marsh area is mainly peat and organic soils, generally called as young bay mud, which is underlain by sand aquifer.

Figure 4-2 is an organic/peat isopach map of the Delta and Suisun Marsh and shows the approximate thickness of organic soils in the study area. Figure 4-13 and 4-14 show the variation in thickness of organic soils south to north (S-N) and west to east (W-E), respectively. No organic soils present beyond Fabian Tract on the south and Ryer Island on the north. In general, S-N line shows that the thickness of organic soils ranges between about 1 foot and 28 feet. The thickness of organic soils in the Suisun Marsh

areas is relatively higher than that of the Delta. The W-E line shows that the thickness of organic soils ranges from about more than 50 feet to about a foot. The thickness of organic soils in the eastern most levees is approximately zero to 5 feet.

4.6 Groundwater Conditions

Water levels in the low-lying Delta islands are maintained 2 to 5 ft below land surface by an extensive network of drainage ditches, and accumulated agricultural drainage is pumped through or over the levees into stream channels. The groundwater level beneath the levees is generally near sea level. Based on some of the monitoring well data collected, it was found that the groundwater levels varied with tidal fluctuations in nearby sloughs and rivers and also with the seasons. It was also found that the groundwater variations over a year could be fitted either with a straight line or with a simple harmonic (sine function) curve.

4.7 Tidal Conditions

The DWR has been operating a network of water level (tide) stations in the Delta since the early 1950's. All of these stations were established using the NGVD29. DWR operates 35 stations in the Delta that are set up to telemeter data to the California Data Exchange Center (CDEC). These stations are identified in the Flood hazard TM #.

Most of the Delta is influenced by tide and tidal currents and is varied by seasonal river runoff. During the winter and early spring months, Delta waters may rise due to flood control releases from upstream dams. August is consistently one of the low Delta inflow months. During low Delta inflows, the stages at most stations are primarily a function of tide and not flow, particularly in the central and western part of the Delta.

A review of some of the gages indicates that water levels vary greatly during each tidal cycle, from less than a foot on the San Joaquin River near Interstate 5 to more than 5 feet near Pittsburg. The tidal variations within the Delta are as follows:

- Northern Delta: between Elevation 5.0 and 7.0 ft
- Central/Eastern Delta: between Elevation 1.2 and 5.0 ft
- Southern Delta: between Elevation 3.0 and 4.5 ft
- Western Delta: between Elevation 0.3 and 5.5 ft

Table 4-1 List of Reviewed Data Sources

Data Source	Data	Project Name	Year Drilled	Number of Available Borings	Number of Digitized Borings	Site Name	Levee/Free Field Boring	Performed by	Comments
DWR Package 1	2001	Brack Tract District 2033	2001	3	3	Brack Tract	Levee	Lowney Associates	
	1987	Brannan Levee Projects	1987	1	1	Brannan Island	Free Field	Raney Geotechnical	
				4	4		Levee		
	1990		1990	4	4		Levee		
	1987		1987	5	5		Free Field		Test pits
	1990		1990	6	2		Free Field		Used VC-1 and VC-2
	1989		1989	10	10		Levee	Wahler Associates	
	1989	Canal Levee	1989	11	11	Canal Levee	Levee	Raney Geotechnical	
				1	1		Free Field		
	1991		1991	16	16		Levee		
				4	4		Free Field		
	2000	Decker MBK	2000	15	15	Decker Island	Levee	Hultgreen-Tillis Engineers	
	1992	Delta Rock Barriers	1992	1	1	Delta Rock Barriers	Free Field	DWR	
	2003	DWR Dixon Property	2003	9	0	DWR Dixon Property	NA	Hultgreen-Tillis Engineers	1 boring, 8 Test pits, Not used since shallow borings
	1976	East Central Delta Canal	1976	1	1	East Central Delta Canal	Levee	DWR	
				9	9		Free Field		
	1976	Isleton Canal	1976	4	4	Isleton Canal	Free Field		
	2000	McW Hablevee Borrow	2000	9	0	McCormack Williamson Tract	NA	Hultgreen-Tillis Engineers	Not used since shallow test pits
	1992	N Delta Seepage Monitoring	1992	8	8	North Delta	Levee	DWR	
				63	63		Free Field		
	1960s	Delta Facilities	1960s	60	58	Peripheral Canal	Levee		Originally, 111 used 89
				40	31		Free Field		
	1968		1968	22	0		Free Field		Shallow, not used
	1992	Phase 1 Study	1992	15	0	New Hope Tract	Free Field	Charles Van Alstine	Not used since along same levee reach as ones below
				5	5		Free Field	Roger Foot Associates	
				7	7		Levee		
	1966	Delta Facilities	1966	10	10		Free Field	DWR	
				10	10		Levee		
DWR Package 2				25	25	Sherman	Levee	Roger Foot Associates	
				33	33		Free Field		
	1990	Twitchell Levee Repair	1990	3	3	Twitchell	Levee		
				1	1		Free Field		

Table 4-1 List of Reviewed Data Sources

Data Source	Data	Project Name	Year Drilled	Number of Available Borings	Number of Digitized Borings	Site Name	Levee/Free Field Boring	Performed by	Comments
DWR Package 3	1956	Salinity Control Barriers	1956	13	13	Bouldin Island	Levee	DWR	
				4	4		Free Field		
				1	0	Terminous Tract			
				2	0				
				14	14	Bouldin Island	Levee		
				7	7		Free Field		
				27	0	Staten Island	Levee		
				14	0		Free Field		
				25	0	Terminous Tract	Levee		Report does not contain 24, 25, 26
				2	0		Free Field		Report does not contain 24, 25, 27
Kleinfelder Package 1	1977	Project Number S-2268-1	1977	4	4	Brannan Andrus Island	Levee	Kleinfelder	
	1990	Isleton River Park	1990	9	0	Andrus Island	Free Field	Kleinfelder	Not used since elevation not known
	1968	Byron Tract Levees-Stability Investigation	1968	13	13	Byron Tract	Levee	Not Given	
	1974	Byron Tract Levee Study	1974	7	0		Levee	Kleinfelder	No map. Not used
	1990	Discovery Bay Elementary School Expansion	1990	9	1		Free Field	Kleinfelder	Used only 1
	1973	Storage Bin Additions, Byron Sand Plant	1973	2	0			Kleinfelder	Not used
	1995	Wet Surge Tank, Unimin Corporation	1995	3	1		Free Field	Kleinfelder	Ignore 2 , 3
	1979	Discovery Bay Relocatable Classroom Building	1979	9	1		Free Field	Kleinfelder	Ignore all except B-4
	1984	Discovery Bay, Contra Costa County	1984	6	1		Free Field	Kleinfelder	Ignore all except B-1
	1978	Wedron-Silica Plant	1978	2	1		Free Field	Kleinfelder	Ignore B-2
	1976	Byron Tract Levee Stability	1976	4	4		Levee	Kleinfelder	
				1	1		Free Field		
	2005	Proposed Subdivision Borroughs Property, Oakley, CA	2005	7	0	Hotchkiss Tract	Free Field		Not used, since elevation data is not given
	1997	Proposed Bernard Road Bridge, Delta Point Development	1997	2	0		Free Field	Kleinfelder	Not used, since elevation data is not given
	1999	Cypress Lakes and Country Club	1999	33	0		Free Field	Kleinfelder	Borings too congested, not entered
				26	0		Free Field		Borings too congested, not entered
	1992		1992	3	3		Levee		

Table 4-1 List of Reviewed Data Sources

Data Source	Data	Project Name	Year Drilled	Number of Available Borings	Number of Digitized Borings	Site Name	Levee/Free Field Boring	Performed by	Comments
Kleinfelder Package 1 (cont'd.)				25	25		Free Field		
	1988	Bethel Island Area Project	1988	16	12	Bethel Island	Free Field	Kleinfelder	Not used 4 Test Pits
				1	1		Levee	Kleinfelder	
	2002	Cypress Grove Levee, Oakley, CA	2002	14	0	Oakley	Free Field	Kleinfelder	Not used, no elevation data
	2004	Proposed Residential Subdivision, Cypress Grove Development, Oakley, CA	2004	12	0			Kleinfelder	Not used, no elevation data
	2000	Proposed 60-Acre Subdivision, East Cypress Road, Oakley, CA	2000	4	0			Kleinfelder	Not used, no elevation data
	2001	Proposed Residential Development, Cypress Road, Oakley, CA	2001	8	0			Kleinfelder	Not used, no elevation data
Kleinfelder Package 2	2002	PG&E Pipeline 57 C, San Joaquin County, CA	2002	4	4	Jones Tract	Free Field	Kleinfelder	
	2005	Line 57 Reliability Project, Mc Donald, Lower Jones, Bacon and Palm Tract, San Joaquin County, CA	2005	2	0	Palm Tract	Free Field	Kleinfelder	Not used
	1980	Levee Study, McDonald Island, San Joaquin County, CA	1980	3	3	McDonald Island	Levee	Kleinfelder	
				1	1		Free Field	Kleinfelder	
	1980	Piezometer Installation, Along Zuckerman Road, Parallel to Empire Cut, McDonald Island	1980	3	0		Levee	Kleinfelder	No Site Map. Not used.
	1984	McDonald Island	1984	3	3		Levee	Dames and Moore	
	1981	Summary of Field Explorations, Proposed Grain Storage Silos, Zuckerman-Mandeville Ranch, McDonald Island, Near Holt, CA	1981	4	0		Free Field	Kleinfelder	No Site Map. Not used.
	1989	Proposed Packing and Storage Shed	1989	5	0		Free Field	Kleinfelder	Not used.
	1984	McDonald Island Levee Stability	1984	4	0		Free Field		No Site Map. Not used.
	1998	PG&E Gas Compressor Pads, McDonald Island, San Joaquin County, CA	1998	2	2		Free Field		Ground elevation assumed 0 feet.

Table 4-1 List of Reviewed Data Sources

Data Source	Data	Project Name	Year Drilled	Number of Available Borings	Number of Digitized Borings	Site Name	Levee/Free Field Boring	Performed by	Comments
Kleinfelder Package 2 (cont'd.)	2005	Line 57 Reliability Project, McDonald, Lower Jones, Bacon and Palm Tract, San Joaquin County, CA	2005	1	0				Not used
	2002	PG&E Pipeline 57 C, San Joaquin County, CA	2002	1	1	Orwood Tract	Free Field		
	2003	Proposed Plant Expansion, White Slough Water Pollution Control Facility, Lodi, CA	2003	7	2	Rio Blanco Tract	Levee		Used B-1 and B-3.
	2006	Port of Stockton Levee Evaluation, Stockton, CA	2006	6	1	Rough and Ready Island	Levee	Kleinfelder	Used 1 only, B-32
	1984	Proposed Fire Protection Pipeline, Naval Communications Station, Stockton, CA	1984	25	3		Free Field	Kleinfelder	Used only three, 3, 12, 22
	1986	Northern California Distribution Center	1986	13	1		Free Field	Kleinfelder	Used only one, B-7
	2001	Proposed Boat and Storage Facility, Stockton, CA	1992	6	1		Levee	Kleinfelder	Used only one, B-4
	1986	Proposed warehouse and Dock Facility	1986	9	0		Free Field	Kleinfelder	Not used
	1997	Service Processing center	1997	30	3		Levee	Kleinfelder	
					6		Free Field	Kleinfelder	
	1998	INS Facility	1998	15	0		Free Field	Kleinfelder	Not used
		Wharf Evaluation	2003	7	2		Levee	Kleinfelder	
	1998	Unit 27 Levee Seepage Analysis, Brookside Development, Stockton, CA	1998	3	3	Sargent Barnhart Tract	Free Field	Kleinfelder	
	1988	Brookside Project	1988	14	14		Levee	Kleinfelder	
	1990	Levee Analysis, Calaveras River/Brookside Development, Stockton, CA	1990	6	6		Levee	Kleinfelder	
	1978	Brookside Development	1978	39	13		12 Free Field, 1 Levee	Kleinfelder	
	1978	S-2026-30	1978	14	0		NA	Kleinfelder	No Map, not used
Kleinfelder Package 3	1989	Proposed Spanos Land Development, Stockton, CA	1989	8	0	Shima Tract	Free Field	Kleinfelder	Not used
	2004	Levee Study, Shima Tract, Stockton, CA	2004	15	15		Levee	Kleinfelder	Did not use B-21
				6	5		Free Field		
	1999	Farmworld, Manthey Road, Lathrop, CA	1999	18	0	Stewart Tract	Free Field	Kleinfelder	Not used
	2000	Farmworld, San Joaquin County, CA	2000	6	0		Free Field	Kleinfelder	Not used
	1996	Storage Maintenance Facility, Mossdale Boats, Lathrop, CA	1996	3	0		Free Field	Kleinfelder	Not used
	1999	Monitoring Wells, Lothrop, CA	1999	12	0		Free Field	Kleinfelder	Not used
	1996/1997	Proposed Gold Rush Development, Stewart Tract, San Joaquin Tract, CA	1996	57	57		Levee	Kleinfelder	
	2005	River Islands, Phase I, Lathrop, CA	2004	81	0	River Islands	Free Field	Engeo/Kleinfelder	Not used
	2003		2003	3	0				
	2004-05		2004-05	5	0				

Table 4-1 List of Reviewed Data Sources

Data Source	Data	Project Name	Year Drilled	Number of Available Borings	Number of Digitized Borings	Site Name	Levee/Free Field Boring	Performed by	Comments
Kleinfelder Package 3 (cont'd.)	2002		2002	1	0				
	2003		2003	3	0				
	1995	Effluent Disposal Field Data	1995	9	0			Neil Anderson and Asso./Kleinfelder	Not used
	1984	Tyler Island Levee, Station 440+00, Sacramento County, CA	1983	11	11	Tyler Island	Levee	Kleinfelder	
	1985			4	4		Free Field		
	1988	Additions to Union Island Dehydration Station/Howard Road	1988	4	4	Union Island	Free Field		Used only 1, B-4
	1974	Proposed Dehydration Station, Howard Road, Union Island, San Joaquin County, CA	1974	3	0		Free Field		Not used
	2002	PG&E Pipeline 57 C, San Joaquin County, CA	2002	1	1	Woodward Island	Free Field		
Hultgren-Tillis Package 1	1981	Evaluation of levees at aqueduct crossings for EBMUD, Middle River Crossing	1981	2	2	Middle River Crossing, Jones Tract	Levee	ConverseWardDavisDixon	
	1980	Evaluation of levees at aqueduct crossings for EBMUD, Old River Crossing	1980	6	6	Old River Crossing, Ordwood Tract	Levee		
			1980	1	1		Free Field		
	1979	Engineering Studies for East Bay Mud-Woodward Island	1979	13	13	Woodward Island	Levee		
				3	3		Free Field		
	1980	Supplementary Engineering Studies for East Bay MUD-Woodward Island	1980	17	17		Levee		
				18	18		Free Field		
	2001	Interim South Delta Program-Old River Seepage Monitoring Program	1997-99	1	1	Byron Tract	Levee	DWR	
				13	13		Free Field		
	1997	Interim South Delta Program-Old River Seepage Monitoring Program	1997	19	19	Victoria island	Free Field		
				3	3	Union Island	Free Field		
				4	4	Woodward Island	Free Field		
				3	3	Byron Tract	Free Field		
				3	3	Victoria Island	Free Field		
	2004	Byron Tract Pump Station	2004	1	1	Byron Tract	Levee		
				2	2		Free Field		
	Not Given	Byron Tract, Delta Lands Levee	Not Given	13	0		Levee		
	1995	South Delta Facilities-Old River Barrier	1995	4	4	Fabian Tract	Levee		
				5	5		Free Field		
		South Delta Facilities-Middle River Barrier		6	6	Union Island	Levee		
				1	1		Free Field		
	1969	Relocation of Old River and Middle River Bridges	1969	5	5	Victoria Island	Free Field		

Table 4-1 List of Reviewed Data Sources

Data Source	Data	Project Name	Year Drilled	Number of Available Borings	Number of Digitized Borings	Site Name	Levee/Free Field Boring	Performed by	Comments
Hultgren-Tillis Package 2	2000	Seepage Monitoring Study	2000	6	6	Roberts Island	Levee	DWR	
	1994	Delta Seismic Stability Study, Deep Hole Drilling Program	1994	2	2	Bacon Island	Levee	DWR	
				1	1		Free Field		
	1990	Levee Status Mokelumne River	1990	7	0	Brannan-Andrus Island	Free Field	Roger Foot Associates	
	1998-2000	Montezuma Wetlands	1998-2000	18	18	Montezuma Wetlands	Free Field	Levine Fricke	
				1	1		Levee		
	2003	Triple Decker Project, Van Sickle Island, Solano County, CA	2003	7	7	Van Sickle Island	Levee	Hultgren-Tillis Engineers	
	2004		2004	2	2		Free Field		
DWR	1958	Salinty Control Barrier Investigation	1956-1957	6	6	Andrus Island	Free Field	DWR	
			1956-1957	16	16		Levee		
			1957	42	42	Bacon Island	Free Field		
			1958	11	0	Bouldin Island	Free Field		
				27	0		Levee		
	1957		1957	1	1	Bradford Island	Levee		
				23	23		Free Field		
				1	1	Byron Tract	Levee		
				35	35		Free Field		
				9	9	Canal Ranch Tract	Free Field		
				12	12	Brack Track	Free Field		
				6	6	Clifton Court Tract	Levee		
				26	26		Free Field		
	1956		1956	25	25	Empire Tract	Free Field		
	1958		1958	15	15	Bethel Tract	Free Field		
				8	8	Franks Tract	Free Field		
				4	4	Little Franks Tract	Levee		
				4	4		Free Field		
				9	9	Grand Island	Levee		
				2	2		Free Field		
	1957		1957	31	31	Holland Tract	Free Field		
				40	40	Jersey Island	Free Field		
				35	0	Little Venice Island	Free Field		
				4	0		Levee		
				63	60	Mandeville Island	Free Field		
	1958			34	34	McDonald Tract	Free Field		
				3	3	Mildred Island	Free Field		
				33	33	Medford Island	Free Field		
			1958	12	12	Merritt Island	Levee		
				1	1		Free Field		

Table 4-1 List of Reviewed Data Sources

Data Source	Data	Project Name	Year Drilled	Number of Available Borings	Number of Digitized Borings	Site Name	Levee/Free Field Boring	Performed by	Comments
DWR (cont'd.)	1957		1957	5	5	McCormick Williamson Tract	Levee		
				4	4		Free Field		
				2	2	New Hope Tract	Levee		
				10	10		Free Field		
				26	26	Palm Tract	Free Field		
	1958		1958	13	13	Pierson Tract	Levee		
				4	4	Pierson Tract	Free Field		
				17	17	Quimby Island	Free Field		
	1957		1957	19	19	Rindge Tract	Levee		
				18	18		Free Field		
	1958		1958	5	5	Roberts Island	Levee		
				17	17		Free Field		
				3	3		Free Field		
				18	17	Sacramento River	Levee		
				91	91	Sherman Island	Levee		
				9	9		Free Field		
DWR	1957	Salinty Control Barrier Investigation	1957	27	27	Staten Island	Levee	DWR	
	1956		1956	14	14		Free Field		
				9	9	Sutter Island	Levee		
				4	4	Steamboat Slough	Levee		
				2	2		Free Field		
				4	4	Paradise Dam	Levee		
			1958	25	25	Terminous Tract	Levee		
				2	2		Free Field		
	1955		1955	28	28	Twitchell Island	Levee		
				8	8		Free Field		
	1958		1956	4	4	Union Island	Free Field		
				9	9		Levee		
			1958	8	8	Coney Island	Free Field		
				2	2		Levee		
				3	3	Coney Island - Paradise Cut	Levee		
				1	1	Coney Island - Sugar Cut	Levee		
	1956		1956	35	35	Venice Island	Free Field		
				4	4		Levee		
	1958		1958			Victoria Island			
	1957		1957-1958	55	55	Webb Tract	Free Field		
	1958		1957	11	11	Sargent-Barnhart Tract	Levee		
				5	5		Free Field		
				8	8	Wright-Elmwood Tract	Free Field		

Table 4-1 List of Reviewed Data Sources

Data Source	Data	Project Name	Year Drilled	Number of Available Borings	Number of Digitized Borings	Site Name	Levee/Free Field Boring	Performed by	Comments
				4	4		Levee		
			1958	11	11	Woodward Island	Free Field		
DWR	1967	Ground Water Investigation Intake	1967	6	0	Clifton Court Forebay	Free Field		
	1995	South Delta Facilities	1994	3	3	Grant Line Canal Barrier Site No.2	Free Field	DWR	
	1985	Geological Investigation Relocated Montezuma Slough	1983	14	14	Suisun Marsh	Levee		
				13	13	Suisun Marsh	Free Field		
	2001	Geology report	1994-1995	9	1	South Delta Facilities Permanent Old River Barrier Site	Free Field		
Anderson & Associates	1991	Geo Investigation-Restaurant & Fuel Tank		4	4	King Island Resort	Free Field		
DWR	1994	Geological Foundation Investigation	1993	2	2	South Delta Grant Line Canal Barrier	Levee		
				3	3		Free Field		
	2001	Geology report	1994	5	0	South Delta Facilities Permanent Middle River Barrier Site			
USACE	1993	Geotechnical Evaluation of Levees-Data Report	1993	124	124	Sacramento River-Right Bank Levee	Levee	MBK	
				10	10		Free Field		
					0	Liquefaction potential of Sacramento-San Joaquin Delta			
		Trenches & Borings to 9 feet			0	Prospect Island			
Roger Foott Associates	1991	Field Investigation & Lab Testing	1991	0	0	Mokelumne River on New Hope tract			
Charles Van Alstine				25	0				
DWR	1994	South Delta Facilities	1994		0	Old River Dredging			
Hultgren & Tillis Engineers	2003	Geotechnical Data Report-Triple Decker Project	2003	9	0	Van Sickle Island, Solano County			
United Permit Company	1992	Geotech Report	1992	2	2	Honker Cut	Free Field		
Wahler Associates	1989	Levee Investigation	1989	4	4	Left bank white Slough - King Island	Levee		
Wahler Associates				1	1		Free Field		
DWR	2006	South Delta Water Management Facilities	2005	3	3	Old River	Levee	DWR	
DWR				2	2		Free Field		
DWR	2004	South Delta Facilities Permanent Barrier-Old River	2002	2	2		Levee		
DWR				3	3		Free Field		
Lowney Associates	2004	Piezometer Installation Report	2004	2	2	McDonald Island	Levee	Lowney Associates	
Lowney Associates				2	2		Free Field		
	2005	South Delta Facilities Permanent Barrier-Middle River	2005	6	4	Mid River	Levee	DWR	
	2005		2002	2	2		Free Field		
Wahler Associates	1987	Levee Investigation, Reclamation District's 537 and 900 and Maintenance Areas 4 and 9	1987	26	26			Wahler Associates	

Table 4-1 List of Reviewed Data Sources

Data Source	Data	Project Name	Year Drilled	Number of Available Borings	Number of Digitized Borings	Site Name	Levee/Free Field Boring	Performed by	Comments
Kleinfelder	2005	Line 57 Reliability Project, San Joaquin County, CA	2005	4	3	Bacon Island	Free Field	Kleinfelder	
Kleinfelder	2003		2003	4	4	Lower Jones Tract	Free Field		
Kleinfelder	1997	Geotechnical Investigation, Venice Island	1997	3	3	Venice Island	Levee		
Kleinfelder				1	1		Free Field		
DWR	1993	Franks Tract SRA Wave Wall	1993	5	5	Franks Tract	Free Field	DWR	
DWR		Levee Investigation, Eight Mile Road to King Island Café, San Joaquin County, CA		4	4	King Island	Levee		
DWR				2	2		Free Field		
DWR	1979	Geology and Construction Materials Data	1979	12	12	Suisun Marsh	Levee	DWR	
DWR				5	5		Free Field		
DWR	2001	Morrow Island Distribution System, Proposed Intake Structure	2000	2	2		Levee		
DWR	1981	Geology and Construction Materials Data, Grizzly Island Distribution System	1981	17	17		Levee		
DWR				3	3		Free Field		
DWR	1993	Suisun Marsh Facilities, temporary Rock Barrier Sites in Goodyear and Chadbourne Sloughs	1993	1	1		Levee		
DWR				5	5		Free Field		
DWR	2000	Geotechnical Services, Report in Support of the Supplemental EIR/EIS	2000	2	2	Bacon Island	Levee		
DWR				6	6		Free Field		
DWR				3	3	Webb Tract	Levee		
DWR				5	5		Free Field		
Kleinfelder	1997	Geotechnical report for Seepage Concerns	1997	7	7	Bradford Island	Levee		
Kleinfelder				2	2		Free Field		
			Total	**2851**	**2090**				

Table 4-2 Delta Levee Geometry Attributes

Island/Tract	Landside Slope (H:V)	Waterside Slope (H:V)	Levee Height* (ft)	Crest Width (ft)
Bacon Island	3:1 to 4:1	2.5:1 to 3.5:1	17 to 18	26 to 28
Byron Tract	3:1 to 5:1	1.5:1 to 3:1	17 to 22	11 to 27
Holland Tract	1.5:1 to 4:1	1.5:1 to 2.5:1	10 to 18	17 to 35
Pierson District	3.5:1 to 5.5:1	3:1 to 4.5:1	9 to 26	18 to 41
Rindge Tract	2:1 to 5:1	1:1 to 2.5:1	12 to 32	16 to 38
Sherman Island	3:1 to 5:1	2:1	7 to 22	12 to 40
Terminous Tract	1.5:1 to 3.5:1	1.5:1 to 2.5:1	13 to 21	11 to 29
Webb Tract	3.5:1 to 5:1	2:1 to 3:1	16 to 20	17 to 30

* With respect to the landside toe of the levee

Table 4-3 Suisun Marsh Levee Geometry Attributes

Island/Tract	Landside Slope (H:V)	Waterside Slope (H:V)	Levee Height* (ft)	Crest Width (ft)
Suisun Marsh	1.5:1 to 3:1	0.5:1 to 2.5:1	6 to 8	7 to 26

* With respect to the landside toe of the levee

5.0 Levee Vulnerability to Flood

5.1 Introduction

Over the last 150 years or so, levees of the Delta were built progressively, mostly by individual farmers or reclamation groups, using light equipment, local uncompacted sediments and organics, and with little to no foundation preparation. Failures were expected and were often responded to by simply rebuilding to the pre-failure condition, often with only minor or no improvements. As islands subsided, the levees were simply enlarged, often just past the point of marginal stability. The foundations of these levees are comprised of a complex mélange of river sediments and organic materials, with overlapping and interfingered zones of widely varying compositions and consistencies. Materials range from coarse-grained sediments, including gravels and loose, clean sands, to soft, fine-grained materials, such as silts, clays and organics, including fibrous peat. Combined with subsiding interiors and high flood levels, both the levees and their foundations are vulnerable to seepage and seepage-induced failures.

This section addresses methods used to assess seepage-induced risks for the levees and their foundations. Current practice is to separate levee seepage into two general categories: under-seepage and through-seepage. Under-seepage refers to water flowing under the levee in the underlying foundation materials, often emanating from the bottom of the landside slope and ground surface extending landward from the landside toe of the levee. Through seepage refers water flowing through the levee prism directly, often emanating from the landside slope of the levee. Both conditions can lead to failures by several mechanisms, including excessive water pressures causing foundation heave and slope instabilities, and immediate and progressive internal erosion, often referred to as piping.

Excessive under-seepage is often accompanied by the formation of sand boils. Boils often look like miniature volcanoes, ejecting water and sediments, usually due to high under seepage pressures. These boils can lead to progressive internal erosion, undermining and levee failure. Boils have been widely observed in all of the historic floods and are believed to have caused significant failures in 1986 and 1997.

Excessive through-seepage often leads to levee landside slope stability problems. At almost all locations, Delta levees are comprised of either dredged, clean, highly permeable river sands, or interbedded layers of organic and mineral soils with contrasting permeabilities. During high water conditions, because of their high permeability and layering, these materials will allow large volumes of water to flow through the levee, at rates high enough to cause internal erosion and slope instability. Often, water is seen exiting the landside slope of the levee, above the landside toe. As this increases, slumping of the levee slopes is often seen progressing from surficial slumps to complete rotation and/or translation of the levee prism and eventual breach of the levee.

Under- and through-seepage are both manifestations of essentially the same mechanism; seepage induced water pressures are high enough to internally erode materials and/or cause soil instabilities. Each can progress to complete failure of the levee. Combined with knowledge about the levee and foundation materials and their variability, both under- and

through-seepage can be evaluated qualitatively and/or quantitatively using standard principles of soils and hydraulic engineering.

For this study, conventional seepage computation methods, combined with engineering judgment and observations were used to assess the relative vulnerability of various typical configurations of levee and foundation materials representative of conditions throughout the Delta. These analyses were performed using standard computational methods, using actual measured and estimated geometric configurations and material properties. To develop the initial models, laboratory test data from past geotechnical studies conducted were compiled and used to assess material seepage properties to conduct the initial analyses. Because it is common for laboratory and field geotechnical behavior to vary, the results of these models were then compared to observed behavior of two actual levees during recent flood events, helping to calibrate the laboratory-derived parameters to actual field behavior. Then, computations and sensitivity analyses were conducted on a series of levee configurations representative of the range of conditions of levees throughout the Delta. The results of these analyses were then used to formulate "fragility curves," which relates expected seepage gradients to water levels for the range of levee configurations addressed in this study.

This study is being done at a regional scale, so it is possible that the modeled conditions and associated fragility curves at any particular site will not be an exact model of the exact conditions or performance at any particular location. However, the Levee Vulnerability Team members believe that the relative computed assessment of seepage pressures and failure potential at most locations will be reasonably representative of the relative actual failure potentials of real levees (i.e., sites computed to have relatively poor conditions will have actual performance that is worse than the comparison sites considered to have relatively good conditions). By combining a representative relative assessment of vulnerability with a historic-based calibration of the seepage models, the team believes these tools will provide a consistent and reasonable assessment of levee vulnerability throughout the Delta. These tools can then be used to assess anticipated relative future performance, considering various changing factors, including island ground surface subsidence, climate change, and future flood and seismic impacts

In the following sections, analysis methods, calibration evaluations, and parametric assessments will be described for both under-seepage and through-seepage, leading to the development of seepage fragility curves to be used in the risk model.

5.2 Failure Modes

Three main modes of failures through-seepage, under-seepage, and overtopping were considered to estimate the risk associated with flooding for this project. The erosion and slope-instability were not considered as one of the main modes of failures but they were considered as fraction of total mode of failures. For example, the through-seepage emanating from landside slope of the levee could lead to slope instability.

Our review of past failures included review of reports and interviewing local and state employees. For most of the past failures, information regarding mode of failure, time and date of failure, water level in the slough are either not available at all or very limited. Therefore, the allocation of number of failures to different mode of failure was based on

engineering judgment and experience of Vulnerability team members. There are no supporting documents available to verify our assumption regarding the mode of failure. The Vulnerability team believes 80 percent of the past failures can be attributed to seepage-induced failures. The team also believes that both through and under seepage-induced failures occurred in equal numbers. The remaining 20% of past failures can be attributed to overtopping.

5.3 Under-Seepage

5.3.1 Analysis Method

Seepage analyses were conducted using steady-state analysis procedures of the finite element program Seep/W (Geo-Slope International Ltd., 2004). Models in this program were developed using two-dimensional, planar and isoparametric and higher-order finite elements models. The program can model multiple soil types, each having different anisotropic hydraulic conductivity characteristics to model the behavior of essentially all soil-types encountered in the Delta.

Boundary conditions in the steady-state analyses were modeled as a variety of conditions, including constant head, no-flow, constant flow or variable, based in-situ conditions expected for each model. Infinite elements can also be included in the model section to model and infinite half-space at the edge of the model.

Water levels in the low-lying Delta islands are maintained 2 to 5 ft below land surface by an extensive network of drainage ditches, and accumulated agricultural drainage is pumped through or over the levees into stream channels. Therefore, it is reasonable to assume that steady-state seepage conditions exist in the tidal Delta and Suisun Marsh for the purpose of calibrating models and developing fragility curves. In the northern Delta and in the Delta fringes, flood waters may rise and then drop fast enough that full steady state conditions may not always develop in every area, especially if the foundation materials are of low permeability. In these locations, steady-state analyses may slightly overestimate seepage conditions, but because of the low permeability, these areas will likely not be vulnerable to significant under-seepage problems. Conversely, based on observations from past floods, most, if not all of the levees that have under-seepage problems are founded on materials that are relatively permeable, where steady-state seepage analyses are appropriate. Therefore, steady-state seepage models were used in these areas too.

5.3.2 Seepage Model Development and Basis

1. Levee geometry: As described previously, several thousands of levee cross sections were reviewed and ranges and typical values for levee slopes, crest widths, and heights were compiled. All cross-sections were developed using NAVD 88 as the vertical datum. From this compilation, configurations of typical levees were selected for analysis.
2. Water levels: A range of river, slough and bay water levels were used in the seepage models to represent the range of possible water levels, from low tide to different flood stages. To model the impact of internal drainage and storm water removal systems within the basins protected by the levees (discussed above),

water levels on the landside of the levees was assumed to be maintained at 2 to 3 feet below the ground surface.

3. Drainage ditches: Seepage gradients and pressures can be significantly affected by the thickness of low permeability layers, located at the landside toe of a levee. These layers are often referred to as blankets and their effective thickness can be reduced by any removal of material, such as a drainage ditch. Because agriculture requires water levels to be below the ground surface, fields are often surrounded by drainage ditches, and often abut levees. While development of a comprehensive catalogue of agricultural ditches throughout the Delta was beyond the scope of this study, since ditches can significantly affect estimated seepage impacts, models for levees with and without adjacent drainage ditches were developed and evaluated.
4. Slough/river channel sediments: Sediment erosion, transport and depositional processes generally cause scouring and movement of materials during high flows and deposition during low flows. As discussed in the Geomorphology Technical Memorandum, the Delta can be divided into two generalized geomorphic provinces. In the northern portion of the Delta, where the river channel has higher gradients, higher flows and higher velocities, much of the sediment transported and deposited is coarse-grained and relatively permeable. In the other portions of the Delta, especially those subject to tidal influences, river channel gradients and velocities are lower, leading to the transport and deposition of predominantly finer-grained, lower permeability materials. These low permeability materials can accumulate at the base of the river channel, often to great depths and can act as a seepage reduction barrier. Some members of the Levee Vulnerability Team report that there is some anecdotal historical evidence that dredging of these "slough sediments" has led to increased seepage in the islands adjacent to recently dredged channels. While development of a comprehensive catalogue of the location and thickness of fine grained slough sediments is beyond the scope of this study, since these sediments can significantly affect estimated seepage impacts, models for levees with and without fine-grained slough materials in the adjacent waterway were developed and evaluated.
5. Permeability values: Parameters to describe and model the behavior of the various soils including permeability and anisotropy, were derived from previous laboratory test results, published correlations, and the Levee Vulnerability Teams' experience. As described above, these laboratory- and experience-derived values were then calibrated using actual levee performance during flood events. This will be discussed in further detail in subsequent sections.
6. Thickness of peat/organic soil: A significant factor affecting actual and modeled seepage conditions is the thickness of the peat and organic marsh deposits under and adjacent to a levee. It was one of the significant factors affecting the results of the under-seepage analyses, and used to catalogue fragility curves and define the vulnerability classes.

5.3.3 Review and Discussion of Material Permeability Characterization

Despite the large number of levees built on and with peat materials in contrast to mineral soils, there are relatively few detailed historic studies and measurements of permeability of Delta peat/organic materials. As discussed previously, as a part of the Levee Vulnerability Teams' compilation of information on conditions throughout the Delta, numerous government, municipal and private organizations were solicited for information, including permeability data. As expected, relatively few studies involved laboratory testing of the permeability of these organic soils. Tables 5-1 and 5-2 (all Section 5 tables are located at the end of the section) present a summary of reported vertical and horizontal permeability values of organic and sandy soils, respectively (HLA 1989, 1991, 1992). The permeability data were obtained from laboratory tests and field pump tests. For each data set, the table also provides details of soil type, type of test, sample location, and other sampling details.

The reported permeability data for free-field peat/organic soils listed in Table 5-1 indicates that both horizontal and vertical laboratory-measured values of permeability are approximately equal and on the order of 10^{-6} cm/s. However, based on project team's experience on flood fights and levee repairs, these permeability values were considered too low. During high water levels, seepage is observed occurring at higher rates and water pressures measured are different than would be expected if the material were this impermeable in both the horizontal and vertical direction. Consistent with its depositional history, the team believes that the horizontal permeability (k_h) of peat/organic soils will generally be higher than the vertical permeability (k_v), especially if the peat is in a "free-field" condition, away from the consolidating loads of a constructed levee. Therefore, for the initial evaluations, the Levee Vulnerability Team recommended using an anisotropy (k_h/ k_v) of 10, with a k_h of $1x10^{-4}$ and a k_v of $1x10^{-5}$ cm/s, for "free-field" peat/organic soil.

As expected, due to the consolidating impact of the weight of a constructed levee, peat/organic materials lying beneath the levee showed lower permeability than the free field peat (Table 5-1). Therefore, for the initial analyses, the levee vulnerability evaluation team recommended using horizontal and vertical permeability values of $1x10^{-5}$ and $1x10^{-6}$ cm/s, respectively. This is one order of magnitude lower than the permeability of free field peat/organic soils.

There is vastly more data, empirical and theoretical correlations and field performance data available for assessing the permeability of sandy soils (designated as SP/SM materials in the unified Soils classification system, ASTM-D2487). Table 5-2 contains results from both laboratory and field pump tests from materials evaluated during past Delta studies. These values are consistent with measurements and correlations developed for these types of soils in other locations, including correlations from the US Army Corps of Engineers (EM-1110-2-1910, USACE, 1986/1993), Terzaghi and Peck (1967), Freeze and Cherry (1979) and Cedergren (1979). For the initial analyses, the Levee Vulnerability Team recommended using values of horizontal permeability equal to 1x10-3 cm/s and a kh/kv ratio of 4 for these sandy materials.

As described above, low permeability silt sediments deposited on slough bottoms can significantly reduce the infiltration rate of water into underlying levee foundation

materials, leading to beneficial reductions of seepage rates and water pressures below the levee. This phenomenon is often referred to as "entrance head losses." To model this condition, the Levee Vulnerability Team recommended using an isotropic permeability of 1x10-5 cm/s with a kh/kv ratio of 1 for these fine-grained slough sediments.

5.3.4 Finite Element Model Details: Mesh Development and Boundary Conditions

Mesh Development – Actual site data was used to develop idealized cross-sections for each location and then the SEEP/W mesh generation program finite element mesh was used to develop the seepage models.

Boundary Conditions – The following boundary conditions were used in all of the seepage models:

- To avoid boundary effects and more accurately model conditions at the levee itself, the landside lateral boundary (left side of the models) was set approximately 1000 ft from the crest of the levee.
- On the river/slough side (right side of the models), to accurately portray seepage conditions below the water, the analysis sections were extended to the middle of the river and a no-flow boundary condition at the vertical face of the elements below the mud-line was set as an axis of symmetry.
- Fixed total head boundary condition was used to model the contact between the water and the riverbank and levee.
- Fixed constant head boundary conditions were used to model drainage ditch water levels, set to 2 ft below the top of the ditch.
- Fixed head boundary conditions were used to model far-field groundwater levels at the left boundary of the models. On the far-field left boundary, the water level was assumed to be at 2 ft below the ground surface.
- Other portions of the levee, and ground surface were modeled using review nodes. Internally, the SEEP/W program assigns to all review nodes a flux-type boundary condition. After the heads are computed for all nodes, the head at the review node is modified if any have a computed head greater than the elevation of the node. Use of these nodes allow the water table to rise above or fall below the nodes, which leads to a more accurate assessment of the location of the phreatic surface and allows seepage to emanate from the model at a free-seepage face.

5.3.5 Model Analysis Process, Results Format and Hand Calculation Confirmations

After the seepage models are setup and material properties (i.e., permeability values) are assigned, the seepage analyses were performed for steady state conditions for different water levels in the slough/river. The results from these analyses were then used to evaluate average gradients, exit gradients, steady state phreatic surface location, the total head distribution throughout the model, and flow paths. Special attention was given to computed gradients at several important locations, including the landside levee toe for cases without drainage ditches and directly below and away from the drainage ditch for cases with a ditch.

To confirm the validity of the finite element model results, calculated exit gradients from SEEP/W were compared to average gradients calculated using the "blanket theory," an empirically-based hand calculation method developed by the US Army Corps of Engineers (USACE 1956 and USACE, 1999). Blanket theory uses performance data and measured seepage conditions from numerous sites in the Mississippi Valley, combined with a theoretically-based model, to develop predictions for under-seepage flow conditions, pressures and failure potential as a function of site conditions and flood level rise above the levee landside toe. The sites evaluated in those studies and used to develop the blanket theory are characterized as having a relatively thin layer of relatively low permeability soil (i.e., the blanket) overlying a more permeable material directly connected to the river. This condition is the same as conditions throughout the Delta and California Central Valley and blanket theory has therefore been widely used by private consultants and the US Army Corps of Engineers to evaluate seepage conditions and cross-check the results of finite element seepage models in this area.

5.3.6 Initial Seepage Analyses

As part of the model and parameter verification process and especially to better assess the impacts of various material characteristics on computed seepage conditions, several initial seepage analyses were performed using information from sites where data is readily available.

Several of the sections were derived from information contained in the 1956-1958 DWR Salinity Control Barrier study (DWR, 1958) including sections on Bradford Island, Sherman Island, and Terminous Tract. The cross sections and boring log "stick" profiles indicating subsurface material types from these sites are presented in the Appendix A. Not all of these sites had information regarding subsurface materials on the slough side. For these locations the peat/organic layer present on the landside was assumed to extend into the slough.

Sections for locations on Bouldin Island, Byron Tract, and Union Island were also developed using data obtained from the USACE (1987), the Mark Group (1992), and DWR (1994), respectively.

Table 5-3 presents values of horizontal permeability and anisotropy ratios used in the initial analyses. The aleatoric uncertainties associated with subsurface material properties, in particular permeability values of the blanket layer (often comprised of peat or organic materials in the Central Delta) and underlying sandy soil strata, were evaluated by conducting analyses using mean estimated and mean plus and minus one standard deviation values.

Because of the similarity in results from these initial analyses, and for the sake of brevity, only the process and results from analysis of the Terminous Tract are presented herein. These results are considered by the authors of this memorandum to be representative of results from all of the initial analyses. The following is a summary of the process and results of this analysis:

1. Based on the cross section with boring logs information from the DWR (1958), and presented in Appendix A, an idealized soil profile was developed. In some

locations, additional information from adjacent deep borings was used to supplement the interpretation.

2. Because subsidence of peat/organic soil has been an ongoing process in the Delta, the cross sectional data obtained from the 1956 study is likely not still sufficiently representative of current ground surface conditions, though it is likely representative of the elevation at the bottom of the peat/organic layer. Therefore, the topography of the cross section was corrected using recently surveyed IFSAR topography data (DWR survey provided with the GIS data base). To better evaluate current slope profiles below the slough water levels, bathymetry data available from the DWR GIS database was used.
3. For the model cases with slough sediments, a 2-foot thick silt sediment layer at the bottom of the slough/river was incorporated in the seepage model.
4. Based on the above data and interpretation, an analysis cross section was developed (Figure 5-1).
5. Using the above cross section, a finite element model was then developed using SEEP/W. Often, it was difficult to confirm whether drainage ditches abutting the levee were present or had been filled in after problems were identified during the 1986 and 1997 flood. Therefore, models were developed for both "with" and "without" ditch conditions (Figure 5-2 and 5-3).
6. These models were then used for analyses assuming three different slough water elevations: 0, +4, and +7 feet NAVD88, representing low tide, high tide, and flood water level conditions (Figures 5-4 through 5-9).

5.3.7 Review of Initial Seepage Analysis Results

Figures 5-4 through 5-6 show the total head distribution and vertical gradient contours for the "with ditch" condition at the three slough water elevations (0, +4, and +7 feet, respectively). Figures 5-7 through 5-9 show the total head distribution and vertical gradient contours for the "without ditch" condition at the three slough water elevations (0, +4, and +7 feet, respectively). Review of these figures indicates that as slough water levels rise, head and gradients increase. For the "with ditch" condition, gradients at Point A, located directly below the ditch, are significantly higher than at Point B, located approximately 100 feet from the toe of the levee (Figures 5-4 through 5-6). In contrast, for the "without ditch" models, the vertical gradients near the landside toe and at Point B are approximately the same (Figures 5-7 through 5-9). These results show that the presence of a ditch adjacent to a levee may have a significant impact on seepage conditions.

To assess the impact of material property variations (i.e., aleatory uncertainty), the "with ditch" model was also analyzed for the following additional cases:

1. mean minus one standard deviation value of permeability for the blanket layer (peat/organics),
2. mean plus one standard deviation value of permeability for the blanket layer (peat/organics),

3. mean minus one standard deviation value of permeability for the underlying higher permeability (SP/SM) foundation layer,
4. mean plus one standard deviation value of permeability for the underlying higher permeability (SP/SM) foundation layer, and
5. no slough sediment layer.

The results of these analyses are summarized in Table 5-4 and are presented in Figures 5-10 through 5-13. For comparison purposes, Table 5-4 also summarizes results from analyses conducted for the "with ditch" and slough sediments case for the initial mean values of permeability, using estimated values of permeability for peat and organic or fine-grained blanket soils.

Review of Table 5-4 and Figure 5-10 indicates that the blanket (peat) permeability has a direct and highly significant impact on computed gradients. Computed gradients increased by about 50% for a one standard deviation increase in permeability and decreased by about 50% for a one standard deviation decrease in permeability. Therefore, for the range and distribution of blanket permeabilities believed to exist throughout the Delta, blanket permeability is a significant factor affecting calculated under-seepage gradients and the Levee Vulnerability Team recommended that it be included in as a factor for developing under-seepage fragility curves in the risk model.

Review of Table 5-4 and Figure 5-11 indicates that for the case of low permeability sand and in the model with sediments, sand permeability has a less obvious impact on computed gradients. Computed gradients decreased by about 50% for a one standard deviation increase in permeability and also decreased less than 10% for a one standard deviation decrease in permeability. In this situation, the sand layer is effectively "capped" on both the water entry and water exit surfaces by the lower permeability slough sediment and blanket layers. Therefore, in the seepage models, these two interface permeability contrasts cause two counter-acting impacts, yielding a more complex relationship and skewed distribution around the mean. Because of the strong contrast between the permeability of the blanket and the sand aquifer the variation of the permeability of the sand was found to be of a second-order effect, and was not further considered in the development of the fragility curves.

Review of Table 5-4 and Figure 5-12 indicates that the presence of slough sediments has a potentially important impact on computed gradients. Computed gradients increased by about 25% for the case without slough sediments over the case with slough sediments. Unfortunately, confirmation of the presence of slough sediments at each location throughout the Delta is beyond the scope of this study and therefore cannot be used as an independent variable during the development of the risk model. Therefore, based on these results, while slough sediment presence was found to be a potentially important factor and should be included when developing under-seepage fragility curves in the risk model, it must be modeled as part of the uncertainty regarding conditions at any site. Based on anecdotal evidence, members of the Levee Vulnerability Team believe that slough sediments are more likely to exist in smaller channels and backwaters and less likely to exist in large, main flow and dredged channels. This may serve as a basis for considering an identifiable skew in the slough sediments distribution in the Monte Carlo simulations.

Further assessment of the extent and thickness of slough sediments throughout the Delta is recommended.

Review of Table 5-4 and Figure 5-13 indicates that the presence of a ditch has a potentially important impact on computed gradients near the ditch and little impact on computed gradients away from the ditch. Computed gradients increased by more than 100% near the levee when a ditch is present, but increases by less than 5% about 100 feet away from the levee when a ditch is present. Similar to the situation with slough sediments, unfortunately, confirmation of the presence of ditches at each location throughout the Delta is beyond the scope of this study and it cannot be used as an independent variable during the development of the risk model. Therefore, since it is a potentially important factor, it should be included as a factor for developing under-seepage fragility curves in the risk model, but must be modeled as part of the uncertainty regarding conditions at any site. The Levee Vulnerability Team members opined that anecdotal evidence indicates that the presence of ditches might be less random than the presence of slough sediments and a skewing of the distribution indicating a higher likelihood of their presence in the Monte Carlo simulation should be considered in this study.

Overall, review of theses initial analyses indicates that for the conditions modeled, computed gradients are expected to be less than those necessary to cause under-seepage problems. For the worst case modeled (mean minus one standard deviation blanket permeability, "with ditch" and slough water at +7 feet), the maximum computed vertical gradient is approximately one, which would probably be near the point of the initiation of under-seepage problems. This is generally consistent with observed behavior throughout the Delta, where levees are believed to be in "just stable" conditions during high water events.

5.3.8 Observation of Seepage Problem Areas

As previously discussed, since 1950, there have been about 74 levee failures resulting in island flooding (Figure 3-4). The Levee Vulnerability Team asked its members to help identify those sites where known under-seepage problems that could be used as a location to evaluate the seepage models against in-situ conditions. A compilation of eyewitness or documented reports of seepage problems in the Delta were recorded on a map, as shown Figure 4-6. Generally these observations represent a good empirical data to gage the model results against (verification of fatal flows).

After discussion and review of conditions, the under-seepage problem observed during 1997 flooding at East-levee in Grand Island and the under-seepage reported at Woodward Island after Upper Jones Tract Failure in June 2004 are presented below.

Grand Island – To develop a model for conditions at the site, topography data was derived from the IFSAR and bathymetry datasets (provided in the DWR GIS data) and no ditch exist adjacent to the levee at the problem area (Cosio, 2007). Subsurface data obtained from nearby borings (stick logs) as shown in Figure 5-14, were used to develop a representative cross-section for analysis. A cross section representing the geometry and subsurface conditions during the 1997 flood was developed as shown in Figure 5-15.

To evaluate water levels during the 1997 flood, recorded flood elevation data was obtained from the DWR monitoring station on the Sacramento River at Walnut Grove (B91650). This is the closest station to the site, and is located approximately 2 miles upstream (Figure 5-16). This distance is short enough that a water level distance correction is considered insignificant to the results of this seepage calibration. Based on this data, a water elevation of +16 feet was used in the seepage model in addition, since the seepage problem was observed during a flooding event, when the flow velocity in the slough would be higher, it was decided that slough sediment was not likely to be present.

Figure 5-17 presents the finite element model and boundary conditions at that site. Analyses were performed for a blanket anisotropy of 10, 100, and 1000 whose results are presented on Figures 5-18, 5-19, and 5-20, respectively. Computed gradients near the landside toe and away from the toe (Point B) are also summarized on Table 5-5. The results for anisotropy ratio of 10 indicate that the computed gradients in the vicinity of the toe would be insufficient to initiate an under-seepage problem at this location during the 1997 flood. Exit gradients do not go in excess of 0.5 until the anisotropy, k_h/ k_v, exceeds 100, yielding and effective vertical permeability of $1x10^{-6}$. The vertical gradient appears to be less sensitive to the increased anisotropy beyond 100.

Woodward Island – The properties from the above analysis (anisotropy of 100) were used at the observed seeps and boils site located at the South-East corner of Woodward Island. During the June 3, 2004 breach of Upper Jones Tract, the slough water was at elevation +6 feet (NAVD88). One of two boring logs at the south-east corner shows the presence of an upper soft organic clay layer with more than 30% organic content overlaying a thick sand deposit. The levee landside toe was at elevation – 7.5 feet (NAVD88). The results of the analysis, assuming no slough silt, showed that exit gradient for these conditions was estimated to be around 2.0, clearly confirming the observed sand boils. It is believed that during the Jones Tract failure, the breach induced large flow velocities that caused extensive scouring of the channel, which removed any recent silt deposit and exposed the sand layer.

Based on the initial evaluations, the above results, and discussion with the Levee Vulnerability Team an agreement was reached on the use of the material properties summarized in Table 5-6. These values were to represent conditions throughout the Delta and Suisun Marsh.

5.3.9 Delta Under-seepage Fragility Curve Models, Analyses and Results

To develop fragility curves representative of conditions throughout the Delta, seepage models with the range of subsurface conditions throughout the Delta were developed. Based on the previously discussed review of cross-section data (as discussed in Section 4.0), an average levee geometry was selected and had the following characteristics:

- Landside slopes: 1.5H:1V to 5.5H:1V
- Water side slope: 1.1H:1V to 4.5H:1V
- Crest Width: 11 to 38 ft

- Levee Height with respect to landside toe: 7 to 26 ft
- Bottom elevation of the slough: -10 to -35 ft (Datum: NAVD88)

As shown on the peat/organics map (Figure 4-2), the thickness of a landside blanket layer varies through out the Delta. Therefore, a series of models with a layer of lower permeability blanket materials varying in thickness from 5 to 35 feet were developed. For each of these models, "with ditch" and "without ditch" models were considered. Figure 5-21 shows a typical cross section for a "with ditch" model and a 25 feet thick low permeability blanket. Figure 5-22 shows a typical cross section for a "without ditch" model and a 25 feet thick low permeability blanket.

Several other factors were considered in these models. Based on a polling of the Levee Vulnerability Team members, anecdotal evidence, field experience, and limited available slough boring data, it was decided that blanket layer, often comprised of peat/organic soils would be terminated below the waterside toe of the slope. Based on a review of available data and from past modeling experience, the bottom elevation of foundation sands was set at -80 ft. To model the landside downward slope of the ground surface away from most Delta levees, a slope of about 500H:1V was used. If the section was modeled with drainage ditch, the ditch was modeled as being 5-feet deep and located approximately 100 ft away from levee centerline. Based on a review of the available bathymetry data, the average slough dimensions were modeled as having an average width of 600 feet and average bottom elevation of -25 feet. For the cases modeling the presence of slough bottom sediments, a 2 ft thick lower permeability fine-grained soils was included in the models.

Figures 5-23 and 5-24 present typical models used to estimate seepage conditions as a function of flood water levels and to develop fragility curves. Typical results from these models are presented in Figures 5-25 through 5-28, showing only the "with ditch", with slough sediments, and slough water at elevation +4 feet, for peat/organic deposits thickness of 5 feet, 15 feet, 25 feet, and 35 feet, respectively.

Figures 5-29a and 5-29b present the computed vertical gradients (below the ditch and 100 feet away from the ditch, respectively) versus water level (from +0 feet to levee crest elevation) for a levee founded on a 5-foot thick blanket layer with a ditch. Maximum vertical gradients are found below the ditch, which also cuts all the way through the peat layer. This is a special case for this series of models. In this situation, the ditch completely pierces the blanket layer and acts as a drain to the underlying sandy layer. While seepage flow rates into the ditch may be high, the pressures in the sand layer are greatly reduced, lowering the gradients to subcritical levels (i.e., <~0.24).

In contrast, for the model with a 5 feet thick blanket layer and without a ditch (Figures 5-30a and 5-30b), the gradients at the toe (Figure 5-30a) and away from the toe (Figure 5-30b) show a substantial increase in the calculated vertical gradients, 1.2 to 2.4 and 1.0 to 2.0, respectively. For this condition, the exit gradients are mostly above 1.0 indicating a state of active failure. Separate fragility curves for both "with ditch" and "without ditch" have been produced for the mean and standard deviations.

Figures 5-31a and 5-31b and Figures 5-32a and 5-32b present the computed vertical gradients for 15 feet thick blanket layer as a function of river/slough water levels for

"with" and "without" ditch, respectively. Review of these results indicates that the vertical gradient under the ditch increase to values ranging from 0.8 to 1.6 as a function of higher water levels (Figure 5-31a) effectively representing the average gradient through a 10-foot thick blanket. On the other hand, the vertical gradients calculated for the case without the ditch, are smaller and range from 0.4 to 0.9 near the toe (Figure 5-32a) and 0.3 to 0.8 away the toe (Figure 5-32b).

The same calculations were conducted for blanket thicknesses of 25 and 35 feet, as shown in Figures 5-33 through Figure 5-36. Generally, the results indicate that the vertical gradients are below 0.8 for the case with the ditches and below 0.6 for the cases without the ditches. Therefore, blankets with 25 feet or more in thickness show a lesser potential for under-seepage failures. It is noted also that the 84-th percentile of the vertical gradients are constrained to value very close to the mean. Beyond a certain contrast between the sand and the blanket permeability coefficients, the vertical gradients become insensitive to the further reduction of the peat/organic permeability.

5.3.10 Under-seepage Analyses and Results for Suisun Marsh

Review of available information indicates that the levees in Suisun marsh area have special characteristics that should be accounted for slightly differently than those in the main Delta. Most significantly, these levees are smaller and typically hold back lower flood levels. Therefore, separate models were developed to evaluate the relationships between flood levels and computed gradients.

Appendix A contains cross-sectional and subsurface information on levees located in the Suisun Marsh area. Based on a review of available data, for the purpose of the development of fragility curves, this location is believed to be reasonably representative of conditions of levees throughout the Suisun Marsh. Figure 5-37 presents the idealized cross section used to model Suisun Marsh conditions.

Similar to the process for the main Delta, a model based on this section was developed and evaluated for a series of different possible conditions and water levels. Figure 5-38 presents a typical model of Suisun Marsh levees. Figure 5-39 presents the calculated values of head and gradient using this model and a water surface elevation of +4 feet.

As with the Delta levees, sensitivity of the model to changing conditions was again evaluated. Figure 5-40 shows the relationship between computed vertical gradient as a function of blanket thickness and water level. All cases were run without ditch and 2-foot thick slough sediment. Review of this figure indicates that the calculated gradients for Suisun Marsh are much smaller than those calculated for the main Delta. For example, the calculated vertical gradients for the 5-foot thick blanket range from 0.4 to 1.1 for Suisun Marsh compared to 1.2 to 2.4 for the main Delta. The main reason for the difference with the main Delta is the higher surface elevation of the interior island floors. Under-seepage at Suisun Marsh appears to be of a lesser concern compared to the main Delta.

5.3.11 Sensitivity Analysis

Sensitivity analyses were carried out using the models for typical cross section for Delta with 15 feet blanket thickness. Figure 5-41 presents computed vertical gradients as a

function of underlying foundation sand thickness and slough bottoms with and without slough sediments. Review of this figure indicates that sand layer thickness has some impact on the computed gradients. Figure 5-42 shows the results of analyses relating vertical gradient to the thickness of slough sediments for models with and without ditches. Review of this figure indicates that both the presence of a ditch and the thickness of the slough sediments have an impact on computed vertical gradients. Figure 5-43 presents the results of analyses relating vertical gradient to the bottom elevation of the slough for models with and without ditches. Review of this figure indicates that presence of a ditch is important, but depth of the adjacent slough bottom may not be significant for the range of slough depths expected for this study. Figure 5-44 presents the results of analyses relating vertical gradient to slough width. Review of this figure indicates that for slough widths less than 500 feet, width has an impact on computed gradients, but above 500 feet it does not.

5.3.12 Vulnerability Class

The system of levees in the Delta study area was divided into vulnerability classes using factors that differentiate the performance of the levees when subjected to the same flood event. These vulnerability classes and the under-seepage analysis results described above were used as the input in the risk model.

The factors considered in defining levee vulnerability classes were:

- Thickness of peat and organics (0, 0.1-5 ft, 5.1-10 ft, 10.1-15 ft, 15.1-30 ft, and >30 ft)
- Slough width (narrow (<500 ft), not narrow (>500 ft))
- Presence of slough sediment (presence, not presence) and
- Presence of toe drainage ditch (presence, not presence)

The main variables in defining under-seepage vulnerability classes were thickness of peat and organics, and slough width. The vulnerability classes for Delta and Suisun Marsh were developed considering all possible combinations of these main variables. The variations in the permeability of peat, the variations in peat and organic layer thickness, presence of slough sediment, and presence of drainage ditch were treated as random input variables, where applicable (see Table 5-7). For example, vulnerability class 1 has presence of slough sediment and presence of drainage ditch as random input variables; other potential random variables are not applicable because the vulnerability class has no effect of peat. Conversely, vulnerability class 3 has presence of slough sediment, presence of drainage ditch, thickness of peat and organics, and permeability of peat as random input variables. Table 5-7 lists the vulnerability classes considered for under-seepage analyses for Delta and Suisun Marsh area along with the random input variables for each vulnerability class. The probability distribution of variations in peat and organic layer thickness within a vulnerability class was defined based on a statistical analysis of available data. Randomness in presence of slough sediment and presence of toe drainage ditch were individually assumed to have 50% chance of occurrence.

5.3.13 Fragility Curves - Probability of Failure Versus Under-Seepage Gradient

The final step in the development of a fragility curve is to relate the predicted vertical gradient to a probability of failure. To complete this last step, expert elicitation methods were used.

Members of the Levee Vulnerability Team and the DRMS Technical Advisory Committee were given summary presentations regarding the above data compilations, model development, model results and final developed relationships between computed gradients as a function of water levels and blanket permeability. In addition, this group of experts was asked to make the following assumptions:

1. The intend behind the development of this relationship is to characterize the likelihood that erosion and piping will progress to the point of full "failure" (breaching).
2. High water persists for one to several days (or so) with tides causing some fluctuation, but the principal source of high water risk is high flood levels.
3. In some cases, but not all cases, pre-existing partial erosion degradation may already be present from previous events.

With the model results and above assumptions as a uniform basis for evaluation, this group of experts was then asked to independently develop estimates of the probability of failure as a function of vertical gradient. Each separately submitted a spreadsheet showing their estimated probability of failure as a function of vertical gradient. They were then asked to estimate the probability of failure for the same situation, but that human intervention was initiated at an appropriate level at that location. These curves were compiled and statistically analyzed.

Figure 5-45 presents a summary of the results of this exercise, assuming no human intervention. As shown, the mean value of the probability of failure is less than 50% for computed vertical gradients of less than 0.8. Probabilities of failure are expected to be greater than 80% when the vertical gradient is greater than about 1.1. This value is in general agreement with values suggested by the US Army Corps of Engineers (USACE, 1999).

Figure 5-46 presents a summary of the results of this exercise, assuming human intervention. Comparison of Figure 5-45 with Figure 5-46 indicates that the expert panel believes that human intervention, unimpeded by resource constraints, can significantly reduce the probability of failure for a levee, as indicated by the significant shift of the mean value curves to the right on the graphs.

The vertical gradient versus water level curves are combined with the probability of failure versus gradient curves (Figures 5-45 or 5-46) to produce the probability of failure versus water level (flood stage) for the entire Delta and Suisun Marsh for each vulnerability class as illustrated in Figure 5-47. The Levee Vulnerability Team believes these curves represent a reasonable numerical model to assess flood induced under-seepage fragility of levees in both the Delta and Suisun Marsh. The resulting curves represented by Figure 5-47 will be used as input in the risk model.

5.4 Through-Seepage

The majority of the Delta and Suisun Marsh levees have some pervious materials within the embankments and can therefore transmit water. It is believed that developing a failure model for predicting through seepage induced failures considering the record of past failures is much more reliable than performing a series of seepage model analyses. The accuracy and usefulness of the failure model can be improved by checking against a record of actual recorded events and adjust if necessary.

Based on the information collected regarding past failures, there has been a total of 74 levee failures over the last 56 years, assuming that 40% of these failures are related to through seepage, the annual average probability of through-seepage failure is approximately 0.53 or 53 percent.

5.5 Overtopping

The overtopping failure occurs when the flood water level rises above the crest of a levee. The main factors required for assessment of the probability of overtopping are levee crest elevation and the probability of flood water levels exceeding this elevation. Note that, in some locations some amount of overflow can occur without complete failure of the levee. The human intervention can also result in preventing the overtopping failure by raising the crests with sandbags during high water periods. Computations of the probability of overtopping failure will be conducted by directly evaluating the probability of a particular flood level occurring that is excess of the measured crown elevations of levees. Therefore, a fragility curve is not required to evaluate this situation in the risk model. The flood levels for current days and future days (50 years, 100 years, and 200 years from now) are currently being completed by the Flood Hazard Team. The flood frequency and stage values from the Flood Hazard Team and the levee crest elevations GIS maps will be used in the risk model to assess probability of current and future years overtopping.

5.6 Erosion

The mode of failure associated with stream flow erosion and wind-wave induced erosion is addressed in the “Wind Wave Technical Memorandum” and the “Emergency Response Technical Memorandum”.

Table 5-1 Reported Permeability Data for Organic Soils

(Source: HLA 1989, 1992)

Soil Type	k_h (cm/s)	k_v(cm/s)	Type of test	Location	Sampling detail
Black peat (PT) with fat clay	2.4×10^{-7}	-	Lab test	Levee, Bacon Island	1988, Sample depth = 22 ft
Black peat (PT) with fat clay	7.2×10^{-7}	-	Lab test	Levee, Web Tract	1988, Sample depth = 25 ft
Black Peat (PT)	4.7×10^{-6}	1.3×10^{-6}	Falling head lab test	Wilkerson Dam-Test fill, Bouldin Island	1989, Sample depth = 9 ft
Black Peat (PT)	5.5×10^{-6}	7.6×10^{-8}	Falling head lab test	Wilkerson Dam-Test fill, Bouldin Island	1989, Sample depth = 9 ft
Black Silty Peat (PT)	1.5×10^{-6}	2.1×10^{-6}	Falling head lab test	Wilkerson Dam-Bouldin Island	1989, Sample depth = 4 ft
Black Silty Peat (PT)	-	7.5×10^{-7}	Falling head lab test	Wilkerson Dam-Bouldin Island	1989, Sample depth = 5 ft
Black Silty Peat (PT)	1.9×10^{-6}	9.7×10^{-7}	Falling head lab test	Wilkerson Dam-Bouldin Island	1989, Sample depth = 11 ft
Black Silty Peat (PT)	2.6×10^{-6}	1.8×10^{-7}	Falling head lab test	Wilkerson Dam-Bouldin Island	1989, Sample depth = 10 ft
Black Silty Peat (PT)	8.8×10^{-7}	1.5×10^{-6}	Falling head lab test	Wilkerson Dam-Bouldin Island	1989, Sample depth = 5 ft
Brown elastic silt w/ peat (MH)	1.2×10^{-6}	3.2×10^{-7}	Falling head lab test	Wilkerson Dam-Bouldin Island	1989, Sample depth = 8 ft
Black organic silt (OH) contains peat		5.7×10^{-7}	Falling head lab test	Wilkerson Dam-Bouldin Island	1989, Sample depth = 15 ft

Table 5-2 Reported Permeability Data for Sandy Soils and Silt

(Source: HLA 1989, 1991, 1992)

Soil Type	k_h (cm/s)	k_v(cm/s)	Type of test	Location	Sampling detail
Gray Silty sand (SM), fine to medium grained	2.2×10^{-5}	-	Lab test	Levee, Bacon Island	1988, Sample depth = 40 ft
Gray Silty sand (SM), fine to medium grained	3.3×10^{-4}	-	Lab test	Levee, Web Tract	1988, Sample depth = 45 ft
Brown silty sand (SM)	3.9×10^{-4}	-	Constant head lab test	Barrow pit, Bouldin Island	1991, Natural sample
Brown silty sand (SM)	1.2×10^{-4}	-	Constant head lab test	Barrow pit, Bouldin Island	1991, Natural sample
Brown poorly graded sand (SP)	6.9×10^{-4}	-	Constant head lab test	Barrow pit, Bouldin Island	1991, Washed sample
Brown poorly graded sand (SP)	8.6×10^{-4}	-	Constant head lab test	Barrow pit, Bouldin Island	1991, Washed sample
Brown silty graded sand (SP)	3.9×10^{-3}	-	Falling head lab test	Barrow pit, Bouldin Island	1991, Natural sample
Brown sand (SP)	6.4×10^{-3}	-	Falling head lab test	Barrow pit, Bouldin Island	1991, Washed sample
Brown silty sand (SM)	6.8×10^{-5}	-	Falling head lab test	Barrow pit, Bouldin Island	1991, Natural sample
Brown silty sand (SM)	1.1×10^{-5}	-	Falling head lab test	Barrow pit, Bouldin Island	1991, Natural sample
Brown poorly graded sand (SP)	5.6×10^{-4}	-	Constant head lab test	Barrow pit, Bouldin Island	1991, washed sample
Brown poorly graded sand (SP)	4.6×10^{-4}	-	Constant head lab test	Barrow pit, Bouldin Island	1991, Washed sample
Brown sand w/ silt (SP-SM)	1.1×10^{-3}	-	Constant head lab test	Barrow pit, Bouldin Island	1991, Natural sample
Brown sand w/ silt (SP-SM)	1.2×10^{-4}	-	Constant head lab test	Barrow pit, Bouldin Island	1991, Natural sample
Brown poorly graded sand (SP)	1.0×10^{-3}	-	Constant head lab test	Barrow pit, Bouldin Island	1991, washed sample
Brown poorly graded sand (SP)	1.9×10^{-3}	-	Constant head lab test	Barrow pit, Bouldin Island	1991, washed sample
Brown silty sand (SM)	2.4×10^{-5}	-	Constant head lab test	Test Fill, Bouldin Island	1991, natural sample
Brown silty sand (SM)	1.1×10^{-6}	-	Falling head lab test	Test Fill, Bouldin Island	1991, natural sample
Brown poorly graded sand (SP)	7.5×10^{-4}	-	Constant head lab test	Test Fill, Bouldin Island	1991, washed sample
Brown poorly graded sand (SP)	1.1×10^{-3}	-	Constant head lab test	Test Fill, Bouldin Island	1991, washed sample
Poorly graded sand (SP), very fine to fine grained, contains some silt	5.4×10^{-3}	-	Field pump test	Holland Tract	1989, Pumping rate = 30 GPM, Depth = 20 ft
Poorly graded sand (SP), very fine to fine grained, contains some silt	6.4×10^{-3}	-	Field pump test	Holland Tract	1989, Pumping rate = 30 GPM, Depth = 30 ft
Blue gray silty sand (SM, fine grained)	1.4×10^{-1}	-	Field pump test	McDonald Island	1989, Pumping rate = 215 GPM
Blue-gray elastic silt (MH)	3.1×10^{-6}	3.8×10^{-6}	Falling head lab test	Wilkerson Dam-Bouldin Island	1989, Sample depth = 20 ft
Blue-gray sandy silt (ML)	-	3.9×10^{-7}	Falling head lab test	Wilkerson Dam-Bouldin Island	1989, Sample depth = 25 ft
Blue-gray silt (ML)	-	1.1×10^{-5}	Falling head lab test	Wilkerson Dam-Bouldin Island	1989, Sample depth = 20 ft

Table 5-3 Permeability Coefficients Used for Initial Seepage Analysis

Material	k_h (cm/s)			k_h/k_v
	Mean - σ	Mean	Mean + σ	
Fill				
CL-ML (fill)	-	1×10^{-5}	-	4
SM (fill)	-	1×10^{-3}	-	4
Peat & Organics				
Free Field	1×10^{-5}	1×10^{-4}	1×10^{-3}	10
Under Levee	1×10^{-6}	1×10^{-5}	1×10^{-4}	10
Other Foundation Soils				
Sand (SM/SP)	5×10^{-4}	1×10^{-3}	5×10^{-3}	4
ML	-	1×10^{-4}	-	4
CL	-	1×10^{-6}	-	4
Sediment (at slough bottom)	-	1×10^{-5}	-	1

Table 5-4 Initial Analysis Results for Terminous Tract

Slough Water Elevation (ft) [NAVD88]	Analysis Case-Permeability	Ditch		No Ditch		Remarks
		i_y below ditch (Point A)	Ave. i_y at Point B	i_y (near toe)	Ave. i_y at Point B	
0	k_{mean}	0.46	0.17	0.22	0.178	model with sediment
4	k_{mean}	0.64	0.24	0.30	0.249	model with sediment
7	k_{mean}	0.75	0.29	0.36	0.301	model with sediment
0	$k_{(mean-\sigma)peat}$	0.57	0.25			model with sediment
4	$k_{(mean-\sigma)peat}$	0.82	0.38	-	-	model with sediment
7	$k_{(mean-\sigma)peat}$	1	0.47			model with sediment
0	$k_{(mean+\sigma)peat}$	0.26	0.05			model with sediment
4	$k_{(mean+\sigma)peat}$	0.36	0.07	-	-	model with sediment
7	$k_{(mean+\sigma)peat}$	0.42	0.08			model with sediment
0	$k_{(mean-\sigma)\ sand}$	0.44	0.14			model with sediment
4	$k_{(mean-\sigma)\ sand}$	0.6	0.20	-	-	model with sediment
7	$k_{(mean-\sigma)\ sand}$	0.7	0.24			model with sediment
0	$k_{(mean+\sigma)\ sand}$	0.25	0.07			model with sediment
4	$k_{(mean+\sigma)\ sand}$	0.41	0.15	-	-	model with sediment
7	$k_{(mean+\sigma)\ sand}$	0.52	0.21			model with sediment
0	k_{mean}	0.58	0.22			model without sediment
4	k_{mean}	0.79	0.31	-	-	model without sediment
7	k_{mean}	0.94	0.38			model without sediment

Table 5-5 Estimated Vertical Gradients for Grand Island Under-seepage Problem

(k_h/k_v)peat	Analysis Case: No Ditch & No Sediment	
	Ave. i_y near toe	Ave. i_y at Point B
10	0.42	0.26
100	0.59	0.50
1000	0.63	0.56

Table 5-6 Evaluated Permeability Coefficients Used for Model Analyses

Material	k_h (cm/s)			k_h/k_v
	Mean - σ	Mean	Mean + σ	
Fill				
SM (fill)	-	1×10^{-3}	-	4
Peat & Organics				
Free Field	1×10^{-5}	1×10^{-4}	1×10^{-3}	100
Under Levee	1×10^{-6}	1×10^{-5}	1×10^{-4}	100
Other Foundation Soils				
Sand (SM/SP)	-	1×10^{-3}	-	4
CL	-	1×10^{-6}	-	4
Sediment (at slough bottom)	-	1×10^{-5}	-	1

Table 5-7 Vulnerability Classes Considered for Under-Seepage Analyses

Geographic Region	Vulnerability Class Index	Peat Thickness (ft)	Slough Width	Random Input Variables
Delta	1	0	Narrow	Ditch, Sediment
	2	0	Not Narrow	Ditch, Sediment
	3	0.1-5	Narrow	Ditch, Sediment, Peat Thickness, Peat Permeability
	4	0.1-5	Not Narrow	Ditch, Sediment, Peat Thickness, Peat Permeability
	5	5.1-10	Narrow	Ditch, Sediment, Peat Thickness, Peat Permeability
	6	5.1-10	Not Narrow	Ditch, Sediment, Peat Thickness, Peat Permeability
	7	10.1-15	Narrow	Ditch, Sediment, Peat Thickness, Peat Permeability
	8	10.1-15	Not Narrow	Ditch, Sediment, Peat Thickness, Peat Permeability
	9	15.1-30	Narrow	Ditch, Sediment, Peat Thickness, Peat Permeability
	10	15.1-30	Not Narrow	Ditch, Sediment, Peat Thickness, Peat Permeability
	11	>30	Narrow	Ditch, Sediment, Peat Thickness, Peat Permeability
	12	>30	Not Narrow	Ditch, Sediment, Peat Thickness, Peat Permeability
Suisan Marsh	13	0	Narrow	Sediment
	14	0	Not Narrow	Sediment
	15	0.1-5	Narrow	Sediment, Peat Thickness, Peat Permeability
	16	0.1-5	Not Narrow	Sediment, Peat Thickness, Peat Permeability
	17	5.1-10	Narrow	Sediment, Peat Thickness, Peat Permeability
	18	5.1-10	Not Narrow	Sediment, Peat Thickness, Peat Permeability
	19	10.1-15	Narrow	Sediment, Peat Thickness, Peat Permeability
	20	10.1-15	Not Narrow	Sediment, Peat Thickness, Peat Permeability
	21	15.1-30	Narrow	Sediment, Peat Thickness, Peat Permeability
	22	15.1-30	Not Narrow	Sediment, Peat Thickness, Peat Permeability
	23	>30	Narrow	Sediment, Peat Thickness, Peat Permeability
	24	>30	Not Narrow	Sediment, Peat Thickness, Peat Permeability

6.0 Seismic Vulnerability

6.1 Introduction

The present day Delta levees are at risk from many sources of failure including seepage (both under and through), overtopping, erosion, stability, seismic, and unforeseeable defects and rodents activities. This section addresses the seismic risk. There have been 166 Delta failures leading to island inundations since construction of levees a century ago. No reports could be found to indicate that seismic shaking had ever induced significant damage. However, the lack of historic damage should not be used to conclude that Delta levees are not vulnerable to earthquake shaking. The present day Delta levees have never been significantly tested under moderate to high seismic shaking since the levees have been at their current size. Floods and earthquakes have the potential to challenge the integrity of a large portion of Delta levees creating possibility of multiple failures.

This section provides an assessment of the Delta levee's current vulnerability to potential damage caused by an earthquake. The analyses and assessments presented in this technical memorandum are based on available information. No investigations or further research, to fill data gaps, were part of this study. As described in Section 4, several thousands of borings and laboratory tests describing subsurface conditions of Delta levees were reviewed to characterize the hundreds of miles of levees and foundations. The data from these borings were also digitized and entered into a database to support the GIS mapping needs for this section and others, as described in Section 4.

6.2 Definition of Vulnerability Classes and Random Input Variables

The system of levees in the Delta study area was divided into vulnerability classes using factors that differentiate the performance of the levees when subjected to the same seismic event. The definition of the vulnerability classes was based on available subsurface information, levee fill conditions and geometry, past performance, and maintenance history. This information was used to develop a GIS-based Delta levee catalogue providing data regarding the spatial and temporal variation in the levee and foundation conditions. This catalogue was then used to develop typical cross-sections based on an idealized geometry and subsurface materials.

The geo-database was integrated into the GIS system for creating and displaying several maps such as the peat/organic soil thickness map. Following are the GIS maps used to define the vulnerability classes under seismic loading:

1. Organic Thickness map (Figure 4-2)
2. Type of Levee Materials (Figure 4-3)
3. (N1)60-cs for Foundation Sand (Figure 4-4)

The following factors were considered in defining levee vulnerability classes for seismic analyses:

- Levee material type (clay levees, and sand levees with potential for liquefaction)
- Thickness of peat and organics (0, 0.1-10.0 ft, 10.1-20.0 ft, and > 20 ft)
- Liquefaction potential of foundation sand ((N1)60-cs of 0-5, 5.1-10, 10.1-20, and >20)
- Levee geometry (steep waterside slope, and non-steep water side slope)

The vulnerability classes for Delta were developed considering only possible combinations of above factors that would differentiate the seismic behavior of levees for the geographic region. For example, if a levee reach had liquefiable levee material with (N1)60-cs < 20, the seismic behavior of that levee reach would not be controlled by both the liquefaction potential of the foundation sand and levee geometry. The variations in peat properties (friction angle (f) and cohesion (c)), peat thickness, and corrected clean sand equivalent SPT blow count ((N1)60-cs) were treated as random variables, where applicable (see Table 6-1). (All Section 6 tables are located at the end of the section.) For example, vulnerability class 6 has (N1)60-cs of the foundation sand and peat thickness as random input variables; the variations in peat properties are not applicable for this class because it has relatively minimal influence on seismic behavior compared to the influence of (N1)60-cs of the foundation sand. Conversely, vulnerability class 15 has the soil properties (c, f) as random input variables; (N1)60-cs of the foundation sand and peat thickness are not applicable for this class because of their minimal influence on seismic behavior. Table 6-1 lists the vulnerability classes considered for seismic analyses for Delta along with the random variables considered for each vulnerability class.

The levees in Suisun Marsh were divided into two vulnerability classes mainly based on liquefaction potential of levee and foundation sand. Table 6-1 also lists the vulnerability classes considered for Suisun Marsh along with the details of random variables.

For each vulnerability class, the earthquake-induced permanent deformation from the various earthquake events was estimated using the logic tree approach presented in Figure 6-1. The logic tree approach requires identifying the material properties that should be treated as random variables and characterized in terms of their probability distributions. Several potential material properties were considered and the sensitivity of the estimated deformations to the variations in each property was assessed. The material properties whose variations showed relatively little effect on deformation were considered to be deterministic in the probabilistic analysis and best point estimates of these properties were used in the calculation of deformation for different vulnerability classes. The material properties whose variations showed a significant effect on deformation were considered to be random variables and their probability distributions were defined based on a statistical analysis of available data. These probability distributions quantify the aleatory uncertainty in the materials properties.

A lognormal distribution was assumed for each random input variable because it is a commonly accepted probability distribution of soil properties and the shape of this distribution provides a reasonable fit to the distribution of field data. A lognormal

distribution is completely defined by two statistical parameters - the median and the logarithmic standard deviation.

The following section describes the selection of material properties that were defined to be random variables, and the estimation of the statistical parameters that define their probability distributions.

6.2.1 Selection of Random Variables and Estimation of Their Statistical Distribution

Non Liquefiable case

For the non-liquefiable case, the following variables were considered in the sensitivity analysis:

- Strength parameters of peat
- Variation of water side slope
- Variation of land side slope
- Variation of water level elevation
- Variation of G/Gmax and Damping curves of peat

Variation in the land side slope assumed to have insignificant effects on the calculations seismic deformations, since deep sliding surfaces through peat controls the seismic deformations. The variation of water level elevation of the slough also will not have much impact on calculations seismic deformations, since island side sliding surfaces controls the deformations.

The effect of variation of G/Gmax and Damping curves of PEAT were considered using the set of curves provided by Wehling (2001) for uncertainty in their estimation. It was found out from these analyses that the variation of G/Gmax and Damping curves of PEAT has almost no effect on the calculated deformations.

The variation of strength parameters of peat will have some impact on calculation of seismic deformations. Therefore, the available p-q data of peat were utilized to calculate the standard deviations in cohesion and friction of peat. Results are shown in Figures 6-2 and 6-3. These standard deviations were applied to the calibrated strength parameters of peat.

The steep water side slopes are expected to yield large displacements during seismic event. We have performed sensitivity analyses assuming steep waterside slope of 1.5:1, for all the idealized cross sections considered.

Liquefiable Case

For the liquefiable cases deformation is mainly controlled by the residual strength of the liquefiable sand layer. Since, we have used the correlation with $(N1)_{60\text{-}CS}$ to estimate residual strength of liquefiable sand layer, variation in $(N1)_{60\text{-}CS}$ value was used to estimate the standard deviation of residual strength values. $(N1)_{60\text{-}CS}$ values for both levee fill and foundation sand were calculated using available borings and cone penetrometer tests (CPT) data.

CPT data obtained within the top 20 feet through the levee were digitized and converted to (N1)60-cs using the procedure proposed by Boulanger and Idriss (2004). A total of 69 (N1)60-cs values (converted from CPT data) are available, out of which 52 of them were less than 15 and rest (i.e., 17) were greater than 15. For the case of boring data, only blowcount data obtained using either a SPT or a modified California drive samplers were considered. A total of 905 (N1)60-cs values were available, out of which 657 of them were less than 15 and the rest (i.e., 248) were greater than 15. The ratio of (N1)60-cs less than 15 to the numbers for SPT borings and CPT soundings (converted values) are about 72% and 75%, respectively.

The distribution of the (N1)60-cs from the SPT blow counts and the converted CPT blow count are shown on Figures 6-4a and 6-4b, respectively for levee fill. Figure 6-5 shows the data distribution of the $(N1)_{60\text{-}CS}$ values of the foundation sand within the Delta.

Sensitivity analyses were performed for variation in residual strength values of the liquefiable foundation layer and liquefiable embankment fill.

6.2.2 Seismic Fragility Curve

It was agreed during the TAC meeting that probability of failure during seismic event should be correlated to both the calculated vertical deformation and initial free board. For simplicity, probability of failure was correlated to a ratio between vertical deformation and initial free board. Expert elicitation was sought to provide input for this correlation. Using this input from the experts, three curves corresponding to the probabilities of 16%, 50%, and 84% were developed relating the probability of failure to the relative loss of freeboard (i.e., ratio of vertical deformation/initial freeboard). Figure 6-6 shows the three curves. These curves define the epistemic uncertainty in the seismic fragility curve.

6.3 Analysis Methods

The earthquake-induced levee deformations can result either in liquefaction-induced flow slides, inertia-induced seismic deformation in non-Liquefiable case, or a combination of the two. The potential seismic-induced modes of failure include: overtopping as a result of crest slumping and settlement, internal piping and erosion caused earthquake-induced differential deformations, sliding blocks and lateral spreading resulting in transverse cracking, and exacerbation of existing seepage problems due to deformations and cracking.

6.3.1 Dynamic Response Analysis

The levees form a large and finite embankment mass supported by the soil foundation half-space. Strong two-dimensional effects characterize the dynamic response and interaction between the levee and foundation soil. An analysis comparing the one-dimensional dynamic response through the levee crest to the two-dimensional response for a range of earthquake magnitude and peak ground accelerations is shown in Figure 6-7. Because of the strong 2-D effects on the site response, the seismic vulnerability analyses presented below were all carried used 2-D numerical models.

Various computer numerical models were used to carry out specific tasks. In the remaining part of this section, these models and analysis methods are described.

The computer program QUAD4M (Hudson et al. 1994) is a two-dimensional, plane-strain, finite element code for dynamic response analysis. It uses an equivalent linear procedure (Seed and Idriss, 1970) to model the nonlinear behavior of soils. The softening of the soil stiffness is represented by shear modulus degradation curves (G/G_{max}) and damping ratios (ξ) vs. shear strain curves. QUAD4M also incorporates a compliant base (energy-transmitting base), which can be used to model the elastic half-space. QUAD4M was used to calculate shear stresses and acceleration time histories within the levee and foundation mass under a given earthquake input motions.

In order to obtain the earthquake-induced levee deformations, the results from the computer program QUAD4M (which calculate the average acceleration time histories within the slip surface [k_{ave}]) are combined with the calculated yield acceleration (K_y) obtained from a limit-equilibrium slope stability analysis model (UTEXAS3 [Wright, 1992]) which are then both used as input into the Newmark sliding block routine to produce the expected levee and foundation deformation. The description of UTEXAS3 and the Newmark sliding block method are discussed in the following sections 6.3.2 and 6.3.3.

FLAC (Itasca 2005) is a two-dimensional explicit finite difference commercial code, which offers a wide range of capabilities to solve complex problems in geomechanics, including nonlinear static and dynamic stress-strain analysis of soil continua, soil-structure interaction, and groundwater flow. Soil behavior was simulated by a Mohr-Coulomb, linear elastic/perfectly plastic model. Because the program has the capability to represent the coupled pore pressure generation during the seismic shaking, it was used to calculate directly the total deformation and slumping induced by the earthquake events in both liquefiable and non-liquefiable conditions. The computer program FLAC was also used to evaluate the post-seismic static slumping (when a full time domain analysis is not required). However, when a full characterization of flow failure, slumping, and lateral sliding are required, a time-domain non-linear with coupled pore pressure analysis was performed (Salah-Mars et al. 2004).

Non-Liquefaction Conditions – In the cases of non-liquefiable site conditions, a limited number of verification runs were performed to compare the earthquake-induced deformation results between QUAD4M-K_y –Newmak on one hand and FLAC on the other. The analysis was conducted for a magnitude 7.5 earthquake for a range of peak ground accelerations between 0.1g to 0.5g as shown in Figure 6-8. For this particular condition (non-liquefaction) the results compare well and QUAD4M was then selected to peform these calculations. QUAD4M offers more ease in its use and the ability to produce multiple runs in a shorter time frame.

Foundation Liquefaction Conditions – For levees with potentially liquefiable foundation layer, a time domain fully coupled analysis was performed using the computer program FLAC. Soil behavior was simulated by a Mohr-Coulomb, linear elastic/perfectly plastic model. For the liquefiable foundation layer, this model was coupled with an empirical pore pressure generation scheme. Pore pressure is generated in response to shear stress cycles, following the cyclic-stress approach of H.B. Seed (Seed, 1979).

However, unlike the standard cyclic-stress approach, pore pressure is generated incrementally during shaking. Thus, pore-pressure generation is fully integrated with the

dynamic effective-stress analysis. In the standard cyclic-stress approach, pore pressures are computed in a post-processing mode based on shear-stress time histories resulting from a total-stress equivalent linear analysis.

In the current analyses, pore pressures are updated continuously for each element in response to shear stress cycles. As pore pressures increase, effective stresses decrease and a state of liquefaction is approached for frictional materials. As the available shear strength of the material decreases, increments of permanent deformation are accumulated. The simultaneous coupling of pore-pressure generation with the stress analysis results in a more realistic dynamic response of the model. Specifically, the plastic strains generated as a result of increased pore pressures significantly contribute to the internal damping of the modeled earth structure.

Levee fill Liquefaction Conditions – When the levee fill or when both the levee fill and foundation materials are susceptible to liquefaction the earthquake-induced deformations tend to be very large and may cause the computer program not converge. To mitigate these conditions, a simplified use of the FLAC model was considered to capture the "post-liquefaction static slumping". In this simplified method, the levee fill was first modeled using the pre-liquefied shear strength values, then in a quasi-static fashion, these strength values were reduced in a step-wise function to the post-liquefactions residual shear strength values. The deformations obtained by this approach would then be combined with the inertia-induced deformations from the QUAD4M-Ky-Newmark results to form the total levee-foundation deformation.

6.3.2 Slope Stability Analysis and Computation of Yield Acceleration

The limit-equilibrium slope stability program UREXAS3 was used to calculate the factors of safety of the levee slopes and the yield accelerations associated with each potential slip surface. The yield acceleration values are then used as input parameters in the Newmark sliding block procedure to estimate the seismic-induced inertial deformations.

The computer program UTEXAS3 is capable of performing two and three stage computations to simulate seismic loading and rapid drawdown conditions, respectively. To perform two or three stage computations, both effective (S-envelope) and total (R-envelope) strength envelopes need to be defined for fine-grained soils. Two-stage stability computations consist of two complete sets of stability calculations; of which the first step is performed to calculate the long term steady-state stresses along the shear surface and the second step is performed to compute the factor of safety for the undrained loading due to earthquake or any other rapidly occurring event.

In general, two-stage stability computations are appropriate for earthquake loadings, where the loads produced by the earthquake will not remain for a long enough time for pore pressures to dissipate. The seismic coefficient representing the earthquake load is applied and a pseudo-static factor of safety is calculated. The seismic coefficient that results in a pseudo-static factor of safety of 1.0 is referred to as yield acceleration (K_y).

Typical analysis cross sections were developed to represent range of conditions expected in the Delta.

The yield acceleration values for potential sliding masses both on the landside and the waterside were estimated using the calibrated shear strength parameters discussed in the following sections.

For conditions of potentially liquefiable layer the strength parameters used in the analysis correspond to the residual undrained shear strength for the purpose of assessing the post-seismic stability of levee embankments. The development of the post-liquefaction residual strength parameters are discussed in the following sections.

6.3.3 Newmark Type Deformation Analysis

Seismic-induced permanent deformations of the embankment slopes were estimated using the Newmark Double Integration Method (1965). The Newmark Double Integration Method is based on the concept that deformations of an embankment will result from incremental sliding during the short periods when earthquake inertia forces in the critical slide mass exceed the available resisting forces. This method involves the calculation of the displacement (deformation) increment of a critical slide mass at each time step using the average horizontal acceleration (k_{ave}) and the value of yield acceleration (k_y) calculated for the slide mass. The development of the k_y is discussed in the Embankment Design Analysis Report. The displacement increment is calculated by double integrating the difference between k_{ave} and k_y values acting on the slide mass. The estimated permanent deformation of the slide mass is then taken as the sum of the displacement increments at the end of ground shaking.

6.3.4 Liquefaction Triggering Analysis (Cyclic Resistance Ratio – CRR)

A liquefaction triggering analysis was conducted to map the "cyclic resistance ratio" (CRR) in the Delta. The CRR was defined as the cyclic stress ratio that would be back-calculated from the liquefaction potential chart (Seed et al., 2003) for a given SPT blow count ($(N1)_{60\text{-}CS}$). A Total of about 900, 6000 standard penetration tests (SPT) and modified California sampler (MC) blow counts (N) were found in the master database for the sandy fill and foundation layers, respectively. These blow count data were first converted to an equivalent normalized clean-sand blow count ($(N1)_{60\text{-}CS}$). These normalized blow counts were then correlated to the CRR (the capacity of the soil to resist liquefaction). The CRR calculations were performed for three Magnitude levels: **M** 7.5, 6.5, and 5.5. The results are presented in Figures 6-9 through 6-11.

6.4 Material Properties and Characterization

The main engineering properties required for the site response and seismic risk analyses include: shear wave velocities, unit weights, undrained shear strengths, cyclic strengths, and modulus reduction and damping relationships for the levee embankment and foundation materials. In the following subsections, the raw data and the characterization of the engineering properties are presented.

Several geotechnical and environmental studies have been performed in the Delta. A list of these past studies and the compilation and interpretation of the data are presented in Section 4.0. These studies included several field investigations and laboratory tests dating back to 1950's (early data developed for the salinity control projects). The field investigations included exploratory borings, cone penetration tests, and down-hole

geophysical surveys. Laboratory test results pertaining to seismic analysis were reviewed to develop both static and dynamic properties. The aleatory uncertainties associated with the dynamic properties of the levee and foundation soils (e.g., modulus reduction and damping as a function of shear strain, shear wave velocity, c, ϕ, Su, unit weight) were considered in the seismic analyses as described in Section 2.0.

In addition, reports containing levee cross sections with subsurface conditions (two to three borings across the levees) were reviewed to develop an understanding of the degree of randomness and heterogeneity of the fills composition of the levees. Selected and representative levee cross sections are presented in the Appendix A of this memorandum.

Available shear strength data for peat/organic soils consisting mainly of unconsolidated undrained (UU) and consolidated undrained (CU) triaxial strengths (see Appendix B). These test data showed progressive increase in deviator stress as axial strain increased, often resulting in large strain levels as high as 15 %. Shear strength data suggest that large strains are needed to cause shear failure in peat and peaty soils. The levee fill materials are in general stiffer and stronger than the soft foundation peat and organic marsh deposits. This could lead to potential cracking of the levee embankments while the foundation peat is still undergoing larger deformation but not failing under the weight of embankment, resulting in strong strain incompatibility as shown in Figure 6-12. Because the levee embankment may reach failure while the peat foundation is still below the failure state is was estimated that the shear strength of peat/organic soils at 5% stain or less would represent the "apparent" strength for use in these analyses.

Static Strength Data Analysis - The mean principal stresses versus maximum shear stress for each of the tests were plotted for both total stress and effective stress at 5 % strain level. This is referred to as a p-q plot. The best linear fit of the total stress p-q data has an intercept of 130 psf and a slope angle of 18 degrees. This corresponds to a Mohr-Coulomb envelope with cohesion intercept (c) of 140 psf and a slope angle (ϕ) of 19 degrees. Similarly for the effective stresses, the best linear fit of p'-q data, has an intercept (c') of 205 psf and a slope angle (ϕ ') of 30 degrees. This corresponds to a Mohr-Coulomb envelope with a cohesion intercept of 250 psf and a slope angle of 35 degrees.

Post-Liquefaction Residual Strength - The liquefaction of loose saturated sandy materials in the foundation and levees will result in substantial loss of strength as a result of increasing pore pressure. The residual shear strength values were estimated using the relationships published by Seed and Harder (1990). At a given $(N1)_{60\text{-}CS,}$ the residual shear strength corresponding to the 25^{th} percentile of the data range was adopted for conditions representative of the Delta. The undrained residual shear strength of 250 psf was estimated for an average $(N1)_{60\text{-}CS}$, of 11.

Liquefaction Potential - Cohesionless soils, such as sands, are generally considered susceptible to liquefaction. Fine-grained soils of moderately to high plasticity, such as CL or CH clays, are generally considered not susceptible to liquefaction. However, fine-grained soils of low plasticity, such as ML silts, are potentially liquefiable. Both SPT and CPT data were used to evaluate the liquefaction potential of the fill and foundation materials using the Seed et al. (2003) procedure.

Shear Wave Velocity and Maximum Shear Modulus (Vs, G_{max}) – DWR conducted shear (S) and Body (P) wave velocities measurements of levee and foundation materials in at least five locations, extending about 100 to 120 feet below the crest of the levees. Most of these velocity measurements were conducted during the installation of downhole array of accelerometers at Sherman Island, Clifton Court Forebay, Staten Island, and Montezuma slough. Although there is significant variability throughout the Delta, the data suggests that the shear wave velocity (Vs) is less that 100 feet/sec for the free field peat, and over 200 feet/sec for peat confined under the levees. The shear wave velocity profiles tend to increase with depth, reaching values of about 1100 to 1200 feet/sec in the lower dense sand and stiff clay stratum. A representative shear wave velocity profile at Sherman Island is shown in Figure 6-13. The shear wave velocity profiles along with the boring data were used to identify the stiff soil layer for the site response analysis. A review of site geology indicates that the bedrock within Delta study area is at great depth, more than 400 feet below ground surface. Therefore, it was necessary to identify a stiff soil layer, which can then be modeled as an elastic half space for the site response analysis.

Depending on the location of the near surface soft deposits (peat and organic marsh deposits) relationships that relate maximum shear modulus, over consolidation ratio (OCR) and effective pressure proposed by Wehling (2001) for peat were used to account for the dependency of shear modulus (or shear wave velocity) on effective pressure.

$$\frac{G_{\max}}{Pa} = 75.7\left[\frac{\sigma'_{1c}}{Pa}\right]^{0.87} OCR^{0.65}$$

Where Pa and σ'_{1c} are the atmospheric and effective vertical pressures, respectively

Modulus Reduction and Damping Ratio (G/G_{max}, ζ) – The variations of shear modulus and damping with shear strain for the various soil profiles were represented by modulus reduction and damping relationships. The modulus reduction relationship with shear strain corresponds to the variation of normalized secant shear modulus, G/Gmax, with strain.

G/Gmax and damping curves were obtained from UC Davis (Wehling et al., 2001) for the peat/organic soils, as shown in Figures 6-14a and 6-14b. The series of curves along with their distribution around the mean were used in the statistical model to generate mean and standard deviations for the probabilistic seismic deformation analysis.

The shear modulus reduction curves (G/G_{max}) and damping curves of Seed and Idriss (1970) and Vucetic and Dobry (1991) were applied for the sandy soils (embankment fill and alluvium) and clay, respectively. The selected dynamic soil properties used for the response analyses are summarized in Table 6-2. Plots of the selected G/G_{max} and damping vs. shear strain relationships are presented in Figure 6-15.

6.5 Earthquake Ground Motions

Development of Response spectra – Acceleration response spectra (ARS) were generated for a reference site with an average 30-meter shear wave velocity profile V_{S-30} of about 1100 feet/sec. Three magnitudes were considered, **M** 5.5 , 6.5 and 7.5 at distances of 20 km, 20 km, and 75 km respectively to represent a small and local

earthquake, a medium earthquake within the Delta or further to the east , and a larger earthquake on the Hayward or the San Andreas faults. The same attenuation relationships used in the probabilistic seismic hazard analysis (PSHA Technical Memorandum, 2007) were also used to develop these response spectra. The response spectra were then scaled up and down to generate a suite of peak ground acceleration values to allow for variation in distances from the sources to different parts of the Delta and Suisun Marsh.

Figure 6-16 shows the 5%-damped response spectra corresponding to these ground motions. These response spectra represent free-field motions for the outcropping reference stiff soil site condition mentioned above.

Development of Time Histories for Dynamic Analyses – To perform the dynamic response analyses of the levee and foundation system, earthquake acceleration time histories were developed as input to the QUAD4M, Newmark, and FLAC analyses. Recorded motions from past earthquakes were selected to match the magnitudes and distances used for the analysis. The selected records were: the **M** 5.5 1991 Sierra Madre Earthquake recorded at Station USGS 4734, the **M** 6.5 1987 Superstition Hills earthquake recorded at the Wildlife station, and the 1992 **M** 7.3 Landers earthquake, recorded at Hemet fire station. The site conditions at these strong motion recording stations are classified as stiff soil sites. The record from the 1992 Landers earthquake was selected to represent the **M** 7.5 events on the San Andreas and Hayward faults. The 1991 Sierra Madre and 1987 and the Superstition Hills earthquakes were selected to represent the **M** 5.5, 6.5 seismic events on the local seismic sources, respectively.

The selected acceleration time histories were spectrally matched to the response spectra (**M** 7.5, 6.5 and 5.5 events) using the method proposed by Lilhanand and Tseng (1988) and modified by Abrahamson (1993). The plots of the acceleration, velocity, and displacement time histories of the spectrally matched motions are presented in Figures 6-17 through 6-22. The 5% damped response spectra for the modified motions are shown in Figures 6-23 through 6-25 along with the target spectra.

The modified time histories were then scaled to PGA of 0.05g, 0.1g, 0.2g, 0.3g, 0.4g, and 0.5g to cover the range of possible events and to cover the entire study area.

6.6 Calibration Analysis

Very often data collected in the filed and tests performed in the laboratories do not represent fully the levee and foundation conditions, particularly when dealing with 100s of miles of levees across varying geomorphic and geologic site conditions. Although a large number of data sets for each engineering soil parameter were compiled, it was desirable to perform a calibration (or ground-truthing) of the soil parameters using the best estimate values at known problem areas in the Delta and compare the results with the field observations. Based on discussions with the local geotechnical engineers and maintenance agencies, two sites were identified as prime candidates. The site at Bradford Island is experiencing tension crack and vertical offset at the levee crest while the site at Holland Tract is experiencing erosion induced over-steepened water side slope. The calibration results are discussed below.

6.6.1 Bradford Island Station 169+00

Stability-induced cracking was reported at the Station 169+00 in Bradford Island. Figure 6-26 shows the approximate location of this site, located at the midpoint of the northern boundary of the island. It is believed that the cracking resulted from placing approximately 2-ft of fill on the levee crest in late 2002. No fill was placed on the slopes. Cracking was first observed in 2005 with some vertical and horizontal offsets in the crest. It appears that the crest movement has been gradually increasing since 2005. A vertical offset in the range of 6 to 12 inches was observed in the summer of 2006. Some horizontal offsets have also occurred. The movement of the crest may be attributed to the consolidation of soft foundation materials such as peat/organic and soft clays resulting from additional weight of the new fill and creeping of the peat/organic soils under sustained shear stresses.

An analysis cross section was developed at this location based on available topographical and subsurface data. Since cracking was observed at this location, it was assumed that this levee section is at best marginally stable. A static factor of safety of 1.1 to 1.15 was considered to represent appropriately the observed condition. The stability of the levees was analyzed using the limit equilibrium method based on Spencer's procedure as coded in the computer program UTEXAS3. UTEXAS3 was used to compute factors of safety using circular shaped shear surfaces.

The slope stability analysis was first performed using the best estimate shear strength parameters for the peat/organic soils from previous laboratory tests. Subsequently, the shear strength was adjusted until it yielded a factor of safety of about 1.1, as shown in Figure 6-26.

6.6.2 Holland Island station 60+00

The waterside slope at this location is very steep and therefore this section was selected for testing the reasonableness of he calibrated shear strength parameters of peat/organic soils. The results of the slope stability analysis for this section are presented in Figure 6-27. Results indicate that the calibrated shear strength parameters are reasonable.

These "calibrated" strength parameters were then used for the rest of the stability analyses for this project.

6.7 Analysis Results

6.7.1 Analysis Results for Sherman Island

A cross-section was developed at station 650+00 at Sherman Island (south side of the island) to verify the factors of safety and yield acceleration against previous studies. At that location the peat layer forming the foundation is in excess of 40 feet in thickness. As shown in Figures 6-28 and 6-29, the long term factors of safety for the best estimate material parameters are equal to 1.29 and 1.60 and the corresponding yield accelerations are 0.05 and 0.07for the land side and water side slopes, respectively. The results are generally consistent with the pervious studies of Sherman Island.

Seismic deformation analysis was also conducted for the same cross-section. The analysis was performed for three earthquake magnitudes (**M** 5.5, 6.5, and 7.5) and a range of

reference site peak ground accelerations ranging from 0.1 to 0.5 g. The dynamic analysis was conducted using both FLAC and QUAD4M-Newmark type procedures. The finite element mesh is illustrated in Figure 6-30. The results of the dynamic analysis indicate that the two methods produce generally similar results as shown in Figures 6-31 and 6-32. The results indicate further that under large earthquake shaking, the south levee could undergo more than 6 feet of deformation, while under small to moderate earthquake the levee could experience up to 2 feet of deformation.

6.7.2 Pseudo-Static Analyses for the Idealized Cross-Sections

After the calibration analysis at Bradford Island and Holland Tract, and the verification against Sherman Island, the analysis of the typical/idealized cross-section representing the range of the vulnerability classes was initiated.

The pseudo-static analyses were performed to estimate the yield accelerations (K_y) to be used in the seismic deformation calculations. Yield accelerations were estimated for non-liquefaction and liquefaction in the upper sand layer. The K_y values for the upper sand liquefying are significantly lower than non-liquefaction because they are based on the consideration that the entire loose sand layer across the section has liquefied.

Non-liquefaction Conditions – For the foundation peat conditions, five classes were used. They included: No peat, 5-foot thick, 15-foot, 25-foot, and a typical section for Suisun Marsh. These conditions assume that the underlying sand deposits are not susceptible to liquefaction. The same cases with potentially liquefiable sand deposits are discussed later.

The static stability analyses for long-term conditions were performed for these five idealized cross sections (Sherman Island would represent the sixth class). The results are summarized in Table 6-3 and the cross-section with the most critical slip surfaces and factors of safety are shown in Figure 6-33 through 6-37. The results of these analyses indicate that the yield acceleration deceases as the peat thickness increases. For Suisun Marsh, the yield accelerations range from 0.03 to 0.09g. For the Delta levees, the yield accelerations range from as low as 0.05g for peat thicker than 40 feet (Sherman Island) and as high as 0.24g in places, where peat is not present.

Potentially Liquefiable Foundation Conditions – For the conditions where foundation sands are susceptible to liquefaction, the seismic deformation analysis was carried out using FLAC. Consequently the yield accelerations were not required. We have, nonetheless calculated the yield acceleration to offer a comparison with the non-liquefaction cases. The results of the pseudo-static analyses are presented in Table 6-4. The comparison of the results shows that the yield accelerations are lower for the liquefiable cases. The difference is more pronounced for the landside slopes.

6.7.3 Seismic Deformation Analysis Results

6.7.3.1 Non-Liquefiable Case

The QUAD4M-Newmark type deformation analyses were conducted for the five idealized cross-sections for the best estimate values. Their respective finite element meshes are shown in Figures 6-38 through 6-42, respectively. The acceleration time histories recorded from the base of the mesh to the crest of the levee or the free field

surface are presented in Figures 6-43 through 6-57. Figure 6-58 presents a typical displacement time history from the Newmark sliding block analysis. The results of the deformation analyses are presented in Figures 6-59 through 6-63, for the five idealized sections. The calculated displacements range from fraction of an inch for the cross-section with no peat, to several feet (up to 14 feet) for Suisun Marsh. The results are also summarized in Tables 6-5a and 6-5b. These calculated displacements correspond to horizontal translations of the center of mass of each sliding block. The corresponding vertical displacements can be obtained from the rotation of the block necessary to accommodate the horizontal displacements. A factor of ½ was used for this conversion.

The same deformation analyses were performed for the condition of steep (eroded) waterside slopes. The results are presented in Figures 6-64 through 6-67.

6.7.3.2 Liquefiable Case

Similar analyses to the cases presented above were conducted assuming the upper loose saturated sands are present and are susceptible to liquefaction. In this case the analysis method consisted of running the computer program FLAC. Within the potentially liquefiable materials, there two subsets: 1) liquefiable foundations and 2) liquefiable levee fill. The results presented below address the first subset (foundation liquefaction only).

Foundation Liquefaction Cases – The FLAC meshes developed to model the four idealized sections are shown in Figures 6-68 through 6-71. The time history of the cyclic stress ratio (CSR) and the pore pressure generation in the liquefiable sand layer are shown in Figures 6-72 through 6-89 for the low (**M** 5.5), moderate (**M** 6.5), and large (**M** 7.5) earthquakes and a reference peak ground acceleration of 0.2g. The seismic-induced post-liquefaction deformation contours are shown in Figures 6-90 through Figure 6-98. As shown in these figures, the analyses results for this case show high excess pore pressure and therefore high strength degradation in the liquefiable sand layer resulting in excessive deformations (8 to 10 feet). The total displacements are also summarized in Table 6-6 and shown in Figures 6-99 through 6-101. It should be noted that for the section with no peat, the deformation are very large and the computer model could not converge, indicating flow failures beyond 10 feet.

Levee Fill Liquefaction Cases – For the case of the potentially liquefiable levee fill, the computer program FLAC was utilized. It was noted however, that in this case, again, the deformation were very large (beyond 10 feet) and hence the non-linear time-domain analysis could not converge because of the excessive deformations. A simplified approach using the post-liquefaction static-slumping method (discussed in an early section) was used as a substitute, recognizing that it does not represent the inertia-induced deformations. An example of the pre- and post static slump deformation is illustrated in Figure 6-102 showing 10 feet of vertical slump for a levee fill with residual strength of 230 psf. Below 230 psf residual strength, the computer program did not converge, indicating deformations in excess of 10 feet.

6.8 Probability of Breach due to Seismic Deformation

Each vulnerability class of levee and foundation is characterized by a set of random variables and their statistical distributions. Based on statistical analysis of available data

and published information, probability distribution functions of the input variables that exhibit random spatial variability were developed. Monte Carlo simulations were used to generate values of the input random variables. The seismic response of each vulnerability class (idealized cross-section) was estimated for the range of earthquake magnitudes and reference site PGA's as described in Section 6.2. Multiple regression equations were developed (mean value and distribution around the mean) to represent the seismic-induced deformation as a function of earthquake magnitude and reference site PGA's for various confidence levels (called levee "response" curves, Figure 6-103a).

In order to estimate the probability of levee failure under a seismic loading, the response curves need to be combined with a "fragility" curve that represents the probability of failure as function of the levee response, Figure 6-103b.

Using input from a panel of geotechnical experts, relationship between probabilities of levee breach as a function of levee response were obtained. The range of data from experts was used to define a median curve and upper and lower confidence bounds around the median value. These curves quantify the epistemic uncertainty in the estimated breach probability Figure 6-103b.

The product of the two sets of functions (response and fragility curves) resulted in the estimation of the levee probability of failure as a function of the seismic loading, Figure 6-103c. Examples of product output from the levee seismic vulnerability task are shown in Tables 6-5a, 6-5b, and 6-6. The data will be fed into the risk model and combined with the probability of occurrence of the various stressing events to produce the expected probability of failures of the Delta and Suisun Marsh levees.

Table 6-1 Vulnerability Class Details for Seismic Fragility

Geographic Area	Vulnerability Class Index	Waterside Levee Slope	$(N_1)_{60\text{-}cs}$ Fill	$(N_1)_{60\text{-}cs}$ Foundation	Peat Thickness (ft)	Random Input Variables
Delta	1	Any	0-20	Any	0	No analysis is needed
	2	Any	0-20	Any	0.1-10	
	3	Any	0-20	Any	10.1-20	
	4	Any	0-20	Any	>20	
	5	Any	>20	0-20	0	No analysis is needed
	6	Any	>20	0-5	0.1-10	$(N_1)_{60\text{-}cs}$ Foundation, Peat Thickness
	7	Any	>20	0-5	10.1-20	$(N_1)_{60\text{-}cs}$ Foundation, Peat Thickness
	8	Any	>20	0-5	>20	$(N_1)_{60\text{-}cs}$ Foundation, Peat Thickness
	9	Any	>20	5.1-10	0.1-10	$(N_1)_{60\text{-}cs}$ Foundation, Peat Thickness
	10	Any	>20	5.1-10	10.1-20	$(N_1)_{60\text{-}cs}$ Foundation, Peat Thickness
	11	Any	>20	5.1-10	>20	$(N_1)_{60\text{-}cs}$ Foundation, Peat Thickness
	12	Any	>20	10.1-20	0.1-10	$(N_1)_{60\text{-}cs}$ Foundation, Peat Thickness
	13	Any	>20	10.1-20	10.1-20	$(N_1)_{60\text{-}cs}$ Foundation, Peat Thickness
	14	Any	>20	10.1-20	>20	$(N_1)_{60\text{-}cs}$ Foundation, Peat Thickness
	15	Steep	>20	>20	0	
	16	Steep	>20	>20	0.1-10	c, ϕ, Peat Thickness
	17	Steep	>20	>20	10.1-20	c, ϕ, Peat Thickness
	18	Steep	>20	>20	>20	c, ϕ, Peat Thickness
	19	Non-Steep	>20	>20	0	
	20	Non-Steep	>20	>20	0.1-10	cϕ, Peat Thickness
	21	Non-Steep	>20	>20	10.1-20	cv Peat Thickness
	22	Non-Steep	>20	>20	>20	c, ϕ, Peat Thickness
Suisun Marsh	23	Any	>20	>20	Thin layer	c
	24	Any	<=20	<=20	Thin Layer	No analysis is needed

Note:

$(N_1)_{60\text{-}cs}$ – corrected clean sand equivalent SPT blow count, c – cohesion, ϕ, - friction angle

Table 6-2 Dynamic Soil Parameters Selected for Analysis

Description		Moist Unit Weight (pcf)	K_{2max}	Shear Wave Velocity (ft/sec)	Modulus and Damping Curves
Embankment Materials					
Sandy Fill		115	35	-	Sand[1]
Peat	- free-field	70	-	100	Peat[2]
	- under embankment			300	Peat[3]
Sand		125	65	-	Sand[1]
Bay Deposits		110		400	Clay[4]
Clay		125	-	900	Clay[4]

Note:
1. Relationships of Seed and Idriss (1970)
2: Relationships of Wehling et al (2001) for 12 kPa
3: Relationships of Wehling et al (2001) for 40 kPa
4: Relationships of Vucetic and Dobry (1991) for PI = 30

Table 6-3 Stability Analysis Results – Non-Liquefiable Sand Layer

Section	Factor of Safety		Yield Acceleration, K_y	
	Landside	Waterside	Landside	Waterside
No Peat	1.79	1.85	0.24	0.19
5 feet Peat	1.57	2.02	0.16	0.16
15 feet Peat	1.39	1.79	0.11	0.11
>25 feet Peat	1.38	1.79	0.09	0.11
Suisun Marsh	1.77	1.15	0.09	0.03

Table 6-4 Stability Analysis Results – Liquefiable Sand Layer

Section	Factor of Safety		Yield Acceleration, K_y	
	Landside	Waterside	Landside	Waterside
No Peat	1.21	1.70	0.05	0.13
5 feet Peat	1.12	1.77	0.03	0.13
15 feet Peat	1.10	1.69	0.01	0.11
>25 feet Peat	1.36	1.77	0.03	0.11

Table 6-5a Calculated Newmark Deformations – Idealized Sections Non-Liquefiable

Earthquake Magnitude	PGA	Peat Thickness, ft	C	phi	Deformation (ft)
5.5	0.05	0	median	median	<0.1
			median	median*exp(log10 sigma)	<0.1
			median	median/exp(Log10 sigma)	<0.1
			median*exp(log10 sigma)	median	<0.1
			median/exp(Log10 sigma)	median	<0.1
5.5	0.1	0	median	median	<0.1
			median	median*exp(log10 sigma)	<0.1
			median	median/exp(Log10 sigma)	<0.1
			median*exp(log10 sigma)	median	<0.1
			median/exp(Log10 sigma)	median	<0.1
5.5	0.2	0	median	median	<0.1
			median	median*exp(log10 sigma)	<0.1
			median	median/exp(Log10 sigma)	<0.1
			median*exp(log10 sigma)	median	<0.1
			median/exp(Log10 sigma)	median	<0.1
5.5	0.3	0	median	median	<0.1
			median	median*exp(log10 sigma)	<0.1
			median	median/exp(Log10 sigma)	<0.1
			median*exp(log10 sigma)	median	<0.1
			median/exp(Log10 sigma)	median	<0.1
5.5	0.4	0	median	median	<0.1
			median	median*exp(log10 sigma)	<0.1
			median	median/exp(Log10 sigma)	<0.1
			median*exp(log10 sigma)	median	<0.1
			median/exp(Log10 sigma)	median	<0.1

Table 6-5a Calculated Newmark Deformations – Idealized Sections Non-Liquefiable

Earthquake Magnitude	PGA	Peat Thickness, ft	C	phi	Deformation (ft)
5.5	0.5	0	median	median	<0.1
			median	median*exp(log10 sigma)	<0.1
			median	median/exp(Log10 sigma)	<0.1
			median*exp(log10 sigma)	median	<0.1
			median/exp(Log10 sigma)	median	<0.1
6.5	0.05	0	median	median	<0.1
			median	median*exp(log10 sigma)	<0.1
			median	median/exp(Log10 sigma)	<0.1
			median*exp(log10 sigma)	median	<0.1
			median/exp(Log10 sigma)	median	<0.1
6.5	0.1	0	median	median	<0.1
			median	median*exp(log10 sigma)	<0.1
			median	median/exp(Log10 sigma)	<0.1
			median*exp(log10 sigma)	median	<0.1
			median/exp(Log10 sigma)	median	<0.1
6.5	0.2	0	median	median	<0.1
			median	median*exp(log10 sigma)	<0.1
			median	median/exp(Log10 sigma)	<0.1
			median*exp(log10 sigma)	median	<0.1
			median/exp(Log10 sigma)	median	<0.1
6.5	0.3	0	median	median	<0.1
			median	median*exp(log10 sigma)	<0.1
			median	median/exp(Log10 sigma)	<0.1
			median*exp(log10 sigma)	median	<0.1
			median/exp(Log10 sigma)	median	<0.1

Table 6-5a Calculated Newmark Deformations – Idealized Sections Non-Liquefiable

Earthquake Magnitude	PGA	Peat Thickness, ft	C	phi	Deformation (ft)
6.5	0.4	0	median	median	<0.1
			median	median*exp(log10 sigma)	<0.1
			median	median/exp(Log10 sigma)	<0.1
			median*exp(log10 sigma)	median	<0.1
			median/exp(Log10 sigma)	median	<0.1
6.5	0.5	0	median	median	<0.1
			median	median*exp(log10 sigma)	<0.1
			median	median/exp(Log10 sigma)	<0.1
			median*exp(log10 sigma)	median	<0.1
			median/exp(Log10 sigma)	median	<0.1
7.5	0.05	0	median	median	<0.1
			median	median*exp(log10 sigma)	<0.1
			median	median/exp(Log10 sigma)	<0.1
			median*exp(log10 sigma)	median	<0.1
			median/exp(Log10 sigma)	median	<0.1
7.5	0.1	0	median	median	<0.1
			median	median*exp(log10 sigma)	<0.1
			median	median/exp(Log10 sigma)	<0.1
			median*exp(log10 sigma)	median	<0.1
			median/exp(Log10 sigma)	median	<0.1
7.5	0.2	0	median	median	<0.1
			median	median*exp(log10 sigma)	<0.1
			median	median/exp(Log10 sigma)	<0.1
			median*exp(log10 sigma)	median	<0.1
			median/exp(Log10 sigma)	median	<0.1

Table 6-5a Calculated Newmark Deformations – Idealized Sections Non-Liquefiable

Earthquake Magnitude	PGA	Peat Thickness, ft	C	phi	Deformation (ft)
7.5	0.3	0	median	median	<0.1
			median	median*exp(log10 sigma)	<0.1
			median	median/exp(Log10 sigma)	<0.1
			median*exp(log10 sigma)	median	<0.1
			median/exp(Log10 sigma)	median	<0.1
7.5	0.4	0	median	median	<0.1
			median	median*exp(log10 sigma)	<0.1
			median	median/exp(Log10 sigma)	<0.1
			median*exp(log10 sigma)	median	<0.1
			median/exp(Log10 sigma)	median	<0.1
7.5	0.5	0	median	median	0.11
			median	median*exp(log10 sigma)	0.11
			median	median/exp(Log10 sigma)	0.11
			median*exp(log10 sigma)	median	0.11
			median/exp(Log10 sigma)	median	0.11
5.5	0.05	5	median	median	<0.1
			median	median*exp(log10 sigma)	<0.1
			median	median/exp(Log10 sigma)	<0.1
			median*exp(log10 sigma)	median	<0.1
			median/exp(Log10 sigma)	median	<0.1
5.5	0.1	5	median	median	<0.1
			median	median*exp(log10 sigma)	<0.1
			median	median/exp(Log10 sigma)	<0.1
			median*exp(log10 sigma)	median	<0.1
			median/exp(Log10 sigma)	median	<0.1

Table 6-5a Calculated Newmark Deformations – Idealized Sections Non-Liquefiable

Earthquake Magnitude	PGA	Peat Thickness, ft	C	phi	Deformation (ft)
5.5	0.2	5	median	median	<0.1
			median	median*exp(log10 sigma)	<0.1
			median	median/exp(Log10 sigma)	<0.1
			median*exp(log10 sigma)	median	<0.1
			median/exp(Log10 sigma)	median	<0.1
5.5	0.3	5	median	median	<0.1
			median	median*exp(log10 sigma)	<0.1
			median	median/exp(Log10 sigma)	<0.1
			median*exp(log10 sigma)	median	<0.1
			median/exp(Log10 sigma)	median	<0.1
5.5	0.4	5	median	median	<0.1
			median	median*exp(log10 sigma)	<0.1
			median	median/exp(Log10 sigma)	<0.1
			median*exp(log10 sigma)	median	<0.1
			median/exp(Log10 sigma)	median	<0.1
5.5	0.5	5	median	median	<0.1
			median	median*exp(log10 sigma)	<0.1
			median	median/exp(Log10 sigma)	<0.1
			median*exp(log10 sigma)	median	<0.1
			median/exp(Log10 sigma)	median	<0.1
6.5	0.05	5	median	median	<0.1
			median	median*exp(log10 sigma)	<0.1
			median	median/exp(Log10 sigma)	<0.1
			median*exp(log10 sigma)	median	<0.1
			median/exp(Log10 sigma)	median	<0.1

Table 6-5a Calculated Newmark Deformations – Idealized Sections Non-Liquefiable

Earthquake Magnitude	PGA	Peat Thickness, ft	C	phi	Deformation (ft)
6.5	0.1	5	median	median	<0.1
			median	median*exp(log10 sigma)	<0.1
			median	median/exp(Log10 sigma)	<0.1
			median*exp(log10 sigma)	median	<0.1
			median/exp(Log10 sigma)	median	<0.1
6.5	0.2	5	median	median	<0.1
			median	median*exp(log10 sigma)	<0.1
			median	median/exp(Log10 sigma)	<0.1
			median*exp(log10 sigma)	median	<0.1
			median/exp(Log10 sigma)	median	<0.1
6.5	0.3	5	median	median	<0.1
			median	median*exp(log10 sigma)	<0.1
			median	median/exp(Log10 sigma)	<0.1
			median*exp(log10 sigma)	median	<0.1
			median/exp(Log10 sigma)	median	<0.1
6.5	0.4	5	median	median	<0.1
			median	median*exp(log10 sigma)	<0.1
			median	median/exp(Log10 sigma)	0.11
			median*exp(log10 sigma)	median	<0.1
			median/exp(Log10 sigma)	median	0.12
6.5	0.5	5	median	median	0.16
			median	median*exp(log10 sigma)	0.15
			median	median/exp(Log10 sigma)	0.21
			median*exp(log10 sigma)	median	0.13
			median/exp(Log10 sigma)	median	0.22

Table 6-5a Calculated Newmark Deformations – Idealized Sections Non-Liquefiable

Earthquake Magnitude	PGA	Peat Thickness, ft	C	phi	Deformation (ft)
7.5	0.05	5	median	median	<0.1
			median	median*exp(log10 sigma)	<0.1
			median	median/exp(Log10 sigma)	<0.1
			median*exp(log10 sigma)	median	<0.1
			median/exp(Log10 sigma)	median	<0.1
7.5	0.1	5	median	median	<0.1
			median	median*exp(log10 sigma)	<0.1
			median	median/exp(Log10 sigma)	<0.1
			median*exp(log10 sigma)	median	<0.1
			median/exp(Log10 sigma)	median	<0.1
7.5	0.2	5	median	median	<0.1
			median	median*exp(log10 sigma)	<0.1
			median	median/exp(Log10 sigma)	<0.1
			median*exp(log10 sigma)	median	<0.1
			median/exp(Log10 sigma)	median	<0.1
7.5	0.3	5	median	median	<0.1
			median	median*exp(log10 sigma)	<0.1
			median	median/exp(Log10 sigma)	0.13
			median*exp(log10 sigma)	median	<0.1
			median/exp(Log10 sigma)	median	0.14
7.5	0.4	5	median	median	0.25
			median	median*exp(log10 sigma)	0.22
			median	median/exp(Log10 sigma)	0.36
			median*exp(log10 sigma)	median	0.16
			median/exp(Log10 sigma)	median	0.38

Table 6-5a Calculated Newmark Deformations – Idealized Sections Non-Liquefiable

Earthquake Magnitude	PGA	Peat Thickness, ft	C	phi	Deformation (ft)
7.5	0.5	5	median	median	0.61
			median	median*exp(log10 sigma)	0.56
			median	median/exp(Log10 sigma)	0.86
			median*exp(log10 sigma)	median	0.44
			median/exp(Log10 sigma)	median	0.91
5.5	0.05	15	median	median	<0.1
			median	median*exp(log10 sigma)	<0.1
			median	median/exp(Log10 sigma)	<0.1
			median*exp(log10 sigma)	median	<0.1
			median/exp(Log10 sigma)	median	<0.1
5.5	0.1	15	median	median	<0.1
			median	median*exp(log10 sigma)	<0.1
			median	median/exp(Log10 sigma)	<0.1
			median*exp(log10 sigma)	median	<0.1
			median/exp(Log10 sigma)	median	<0.1
5.5	0.2	15	median	median	<0.1
			median	median*exp(log10 sigma)	<0.1
			median	median/exp(Log10 sigma)	<0.1
			median*exp(log10 sigma)	median	<0.1
			median/exp(Log10 sigma)	median	<0.1
5.5	0.3	15	median	median	<0.1
			median	median*exp(log10 sigma)	<0.1
			median	median/exp(Log10 sigma)	<0.1
			median*exp(log10 sigma)	median	<0.1
			median/exp(Log10 sigma)	median	<0.1

Table 6-5a Calculated Newmark Deformations – Idealized Sections Non-Liquefiable

Earthquake Magnitude	PGA	Peat Thickness, ft	C	phi	Deformation (ft)
5.5	0.4	15	median	median	0.11
			median	median*exp(log10 sigma)	<0.1
			median	median/exp(Log10 sigma)	0.16
			median*exp(log10 sigma)	median	<0.1
			median/exp(Log10 sigma)	median	0.21
5.5	0.5	15	median	median	0.19
			median	median*exp(log10 sigma)	0.17
			median	median/exp(Log10 sigma)	0.27
			median*exp(log10 sigma)	median	0.14
			median/exp(Log10 sigma)	median	0.34
6.5	0.05	15	median	median	<0.1
			median	median*exp(log10 sigma)	<0.1
			median	median/exp(Log10 sigma)	<0.1
			median*exp(log10 sigma)	median	<0.1
			median/exp(Log10 sigma)	median	<0.1
6.5	0.1	15	median	median	<0.1
			median	median*exp(log10 sigma)	<0.1
			median	median/exp(Log10 sigma)	<0.1
			median*exp(log10 sigma)	median	<0.1
			median/exp(Log10 sigma)	median	<0.1
6.5	0.2	15	median	median	<0.1
			median	median*exp(log10 sigma)	<0.1
			median	median/exp(Log10 sigma)	<0.1
			median*exp(log10 sigma)	median	<0.1
			median/exp(Log10 sigma)	median	0.14

Table 6-5a Calculated Newmark Deformations – Idealized Sections Non-Liquefiable

Earthquake Magnitude	PGA	Peat Thickness, ft	C	phi	Deformation (ft)
6.5	0.3	15	median	median	0.21
			median	median*exp(log10 sigma)	0.18
			median	median/exp(Log10 sigma)	0.34
			median*exp(log10 sigma)	median	0.14
			median/exp(Log10 sigma)	median	0.49
6.5	0.4	15	median	median	0.50
			median	median*exp(log10 sigma)	0.42
			median	median/exp(Log10 sigma)	0.78
			median*exp(log10 sigma)	median	0.30
			median/exp(Log10 sigma)	median	1.06
6.5	0.5	15	median	median	0.98
			median	median*exp(log10 sigma)	0.84
			median	median/exp(Log10 sigma)	1.39
			median*exp(log10 sigma)	median	0.59
			median/exp(Log10 sigma)	median	1.77
7.5	0.05	15	median	median	<0.1
			median	median*exp(log10 sigma)	<0.1
			median	median/exp(Log10 sigma)	<0.1
			median*exp(log10 sigma)	median	<0.1
			median/exp(Log10 sigma)	median	<0.1
7.5	0.1	15	median	median	<0.1
			median	median*exp(log10 sigma)	<0.1
			median	median/exp(Log10 sigma)	<0.1
			median*exp(log10 sigma)	median	<0.1
			median/exp(Log10 sigma)	median	<0.1

Table 6-5a Calculated Newmark Deformations – Idealized Sections Non-Liquefiable

Earthquake Magnitude	PGA	Peat Thickness, ft	C	phi	Deformation (ft)
7.5	0.2	15	median	median	0.26
			median	median*exp(log10 sigma)	0.19
			median	median/exp(Log10 sigma)	0.42
			median*exp(log10 sigma)	median	0.13
			median/exp(Log10 sigma)	median	0.59
7.5	0.3	15	median	median	1.03
			median	median*exp(log10 sigma)	0.87
			median	median/exp(Log10 sigma)	1.47
			median*exp(log10 sigma)	median	0.63
			median/exp(Log10 sigma)	median	1.90
7.5	0.4	15	median	median	2.35
			median	median*exp(log10 sigma)	2.07
			median	median/exp(Log10 sigma)	3.35
			median*exp(log10 sigma)	median	1.54
			median/exp(Log10 sigma)	median	4.23
7.5	0.5	15	median	median	5.17
			median	median*exp(log10 sigma)	4.51
			median	median/exp(Log10 sigma)	6.81
			median*exp(log10 sigma)	median	3.39
			median/exp(Log10 sigma)	median	8.20
5.5	0.05	>25	median	median	<0.1
			median	median*exp(log10 sigma)	<0.1
			median	median/exp(Log10 sigma)	<0.1
			median*exp(log10 sigma)	median	<0.1
			median/exp(Log10 sigma)	median	<0.1

Table 6-5a Calculated Newmark Deformations – Idealized Sections Non-Liquefiable

Earthquake Magnitude	PGA	Peat Thickness, ft	C	phi	Deformation (ft)
5.5	0.1	>25	median	median	<0.1
			median	median*exp(log10 sigma)	<0.1
			median	median/exp(Log10 sigma)	<0.1
			median*exp(log10 sigma)	median	<0.1
			median/exp(Log10 sigma)	median	<0.1
5.5	0.2	>25	median	median	<0.1
			median	median*exp(log10 sigma)	<0.1
			median	median/exp(Log10 sigma)	<0.1
			median*exp(log10 sigma)	median	<0.1
			median/exp(Log10 sigma)	median	<0.1
5.5	0.3	>25	median	median	<0.1
			median	median*exp(log10 sigma)	<0.1
			median	median/exp(Log10 sigma)	<0.1
			median*exp(log10 sigma)	median	<0.1
			median/exp(Log10 sigma)	median	0.11
5.5	0.4	>25	median	median	0.13
			median	median*exp(log10 sigma)	<0.1
			median	median/exp(Log10 sigma)	0.18
			median*exp(log10 sigma)	median	<0.1
			median/exp(Log10 sigma)	median	0.22
5.5	0.5	>25	median	median	0.20
			median	median*exp(log10 sigma)	0.14
			median	median/exp(Log10 sigma)	0.26
			median*exp(log10 sigma)	median	0.11
			median/exp(Log10 sigma)	median	0.31

Table 6-5a Calculated Newmark Deformations – Idealized Sections Non-Liquefiable

Earthquake Magnitude	PGA	Peat Thickness, ft	C	phi	Deformation (ft)
6.5	0.05	>25	median	median	<0.1
			median	median*exp(log10 sigma)	<0.1
			median	median/exp(Log10 sigma)	<0.1
			median*exp(log10 sigma)	median	<0.1
			median/exp(Log10 sigma)	median	<0.1
6.5	0.1	>25	median	median	<0.1
			median	median*exp(log10 sigma)	<0.1
			median	median/exp(Log10 sigma)	<0.1
			median*exp(log10 sigma)	median	<0.1
			median/exp(Log10 sigma)	median	<0.1
6.5	0.2	>25	median	median	<0.1
			median	median*exp(log10 sigma)	<0.1
			median	median/exp(Log10 sigma)	<0.1
			median*exp(log10 sigma)	median	<0.1
			median/exp(Log10 sigma)	median	0.14
6.5	0.3	>25	median	median	0.24
			median	median*exp(log10 sigma)	0.13
			median	median/exp(Log10 sigma)	0.37
			median*exp(log10 sigma)	median	0.10
			median/exp(Log10 sigma)	median	0.50
6.5	0.4	>25	median	median	0.49
			median	median*exp(log10 sigma)	0.27
			median	median/exp(Log10 sigma)	0.76
			median*exp(log10 sigma)	median	0.20
			median/exp(Log10 sigma)	median	1.01

Table 6-5a Calculated Newmark Deformations – Idealized Sections Non-Liquefiable

Earthquake Magnitude	PGA	Peat Thickness, ft	C	phi	Deformation (ft)
6.5	0.5	>25	median	median	0.98
			median	median*exp(log10 sigma)	0.58
			median	median/exp(Log10 sigma)	1.38
			median*exp(log10 sigma)	median	0.42
			median/exp(Log10 sigma)	median	1.68
7.5	0.05	>25	median	median	<0.1
			median	median*exp(log10 sigma)	<0.1
			median	median/exp(Log10 sigma)	<0.1
			median*exp(log10 sigma)	median	<0.1
			median/exp(Log10 sigma)	median	<0.1
7.5	0.1	>25	median	median	<0.1
			median	median*exp(log10 sigma)	<0.1
			median	median/exp(Log10 sigma)	<0.1
			median*exp(log10 sigma)	median	<0.1
			median/exp(Log10 sigma)	median	<0.1
7.5	0.2	>25	median	median	0.25
			median	median*exp(log10 sigma)	0.10
			median	median/exp(Log10 sigma)	0.43
			median*exp(log10 sigma)	median	<0.1
			median/exp(Log10 sigma)	median	0.59
7.5	0.3	>25	median	median	0.98
			median	median*exp(log10 sigma)	0.47
			median	median/exp(Log10 sigma)	1.47
			median*exp(log10 sigma)	median	0.33
			median/exp(Log10 sigma)	median	1.92

Table 6-5a Calculated Newmark Deformations – Idealized Sections Non-Liquefiable

Earthquake Magnitude	PGA	Peat Thickness, ft	C	phi	Deformation (ft)
7.5	0.4	>25	median	median	2.27
			median	median*exp(log10 sigma)	1.14
			median	median/exp(Log10 sigma)	3.39
			median*exp(log10 sigma)	median	0.82
			median/exp(Log10 sigma)	median	4.30
7.5	0.5	>25	median	median	5.43
			median	median*exp(log10 sigma)	3.07
			median	median/exp(Log10 sigma)	6.61
			median*exp(log10 sigma)	median	2.32
			median/exp(Log10 sigma)	median	7.86

Table 6-5b Calculated Newmark Deformations – Suisun Marsh Non-Liquefiable

Earthquake Magnitude	PGA	Bay Deposit Thickness	C	Deformation
5.5	0.05	40	median	0.003
			median*exp(log10 sigma)	0
			median/exp(Log10 sigma)	>10
5.5	0.1	40	median	0.026
			median*exp(log10 sigma)	0
			median/exp(Log10 sigma)	>10
5.5	0.2	40	median	0.208
			median*exp(log10 sigma)	0
			median/exp(Log10 sigma)	>10
5.5	0.3	40	median	0.408
			median*exp(log10 sigma)	0.015
			median/exp(Log10 sigma)	>10
5.5	0.4	40	median	0.746
			median*exp(log10 sigma)	0.049
			median/exp(Log10 sigma)	>10
5.5	0.5	40	median	1.185
			median*exp(log10 sigma)	0.096
			median/exp(Log10 sigma)	>10
6.5	0.05	40	median	0.008
			median*exp(log10 sigma)	0
			median/exp(Log10 sigma)	>10
6.5	0.1	40	median	0.104
			median*exp(log10 sigma)	0
			median/exp(Log10 sigma)	>10
6.5	0.2	40	median	0.593
			median*exp(log10 sigma)	0.007
			median/exp(Log10 sigma)	>10
6.5	0.3	40	median	1.764
			median*exp(log10 sigma)	0.049
			median/exp(Log10 sigma)	>10
6.5	0.4	40	median	3.28
			median*exp(log10 sigma)	0.121
			median/exp(Log10 sigma)	>10
6.5	0.5	40	median	4.841
			median*exp(log10 sigma)	0.276
			median/exp(Log10 sigma)	>10
7.5	0.05	40	median	0.016
			median*exp(log10 sigma)	0
			median/exp(Log10 sigma)	>10
7.5	0.1	40	median	0.328
			median*exp(log10 sigma)	0
			median/exp(Log10 sigma)	>10
7.5	0.2	40	median	2.19
			median*exp(log10 sigma)	0.02
			median/exp(Log10 sigma)	>10
7.5	0.3	40	median	4.927
			median*exp(log10 sigma)	0.135
			median/exp(Log10 sigma)	>10

Table 6-5b Calculated Newmark Deformations – Suisun Marsh Non-Liquefiable

Earthquake Magnitude	PGA	Bay Deposit Thickness	C	Deformation
7.5	0.4	40	median	9.083
			median*exp(log10 sigma)	0.483
			median/exp(Log10 sigma)	>10
7.5	0.5	40	median	13.989
			median*exp(log10 sigma)	1.207
			median/exp(Log10 sigma)	>10

Table 6-6 Calculated FLAC Deformations – Idealized Sections Liquefiable

Earthquake Magnitude	PGA	Peat Thickness	(N1-60), Foundation	Deformation
5.5	0.05	0	median	>10
			median*exp(log10 sigma)	>10
			median/exp(Log10 sigma)	>10
5.5	0.1	0	median	>10
			median*exp(log10 sigma)	>10
			median/exp(Log10 sigma)	>10
5.5	0.2	0	median	>10
			median*exp(log10 sigma)	>10
			median/exp(Log10 sigma)	>10
5.5	0.3	0	median	>10
			median*exp(log10 sigma)	>10
			median/exp(Log10 sigma)	>10
5.5	0.4	0	median	>10
			median*exp(log10 sigma)	>10
			median/exp(Log10 sigma)	>10
5.5	0.5	0	median	>10
			median*exp(log10 sigma)	>10
			median/exp(Log10 sigma)	>10
6.5	0.05	0	median	>10
			median*exp(log10 sigma)	>10
			median/exp(Log10 sigma)	>10
6.5	0.1	0	median	>10
			median*exp(log10 sigma)	>10
			median/exp(Log10 sigma)	>10
6.5	0.2	0	median	>10
			median*exp(log10 sigma)	>10
			median/exp(Log10 sigma)	>10
6.5	0.3	0	median	>10
			median*exp(log10 sigma)	>10
			median/exp(Log10 sigma)	>10
6.5	0.4	0	median	>10
			median*exp(log10 sigma)	>10
			median/exp(Log10 sigma)	>10

Table 6-6 Calculated FLAC Deformations – Idealized Sections Liquefiable

Earthquake Magnitude	PGA	Peat Thickness	(N1-60), Foundation	Deformation
6.5	0.5	0	median	>10
			median*exp(log10 sigma)	>10
			median/exp(Log10 sigma)	>10
7.5	0.05	0	median	>10
			median*exp(log10 sigma)	>10
			median/exp(Log10 sigma)	>10
7.5	0.1	0	median	>10
			median*exp(log10 sigma)	>10
			median/exp(Log10 sigma)	>10
7.5	0.2	0	median	>10
			median*exp(log10 sigma)	>10
			median/exp(Log10 sigma)	>10
7.5	0.3	0	median	>10
			median*exp(log10 sigma)	>10
			median/exp(Log10 sigma)	>10
7.5	0.4	0	median	>10
			median*exp(log10 sigma)	>10
			median/exp(Log10 sigma)	>10
7.5	0.5	0	median	>10
			median*exp(log10 sigma)	>10
			median/exp(Log10 sigma)	>10
5.5	0.05	5	median	0.1
			median*exp(log10 sigma)	0.1
			median/exp(Log10 sigma)	0.1
5.5	0.1	5	median	0.2
			median*exp(log10 sigma)	0.1
			median/exp(Log10 sigma)	0.5
5.5	0.2	5	median	0.6
			median*exp(log10 sigma)	0.4
			median/exp(Log10 sigma)	1.5
5.5	0.3	5	median	2
			median*exp(log10 sigma)	0.8
			median/exp(Log10 sigma)	4
5.5	0.4	5	median	3
			median*exp(log10 sigma)	1
			median/exp(Log10 sigma)	6
5.5	0.5	5	median	3.5
			median*exp(log10 sigma)	1.5
			median/exp(Log10 sigma)	8
6.5	0.05	5	median	0.1
			median*exp(log10 sigma)	0.1
			median/exp(Log10 sigma)	0.1
6.5	0.1	5	median	0.2
			median*exp(log10 sigma)	0.1
			median/exp(Log10 sigma)	1
6.5	0.2	5	median	1
			median*exp(log10 sigma)	0.7
			median/exp(Log10 sigma)	3

Table 6-6 Calculated FLAC Deformations – Idealized Sections Liquefiable

Earthquake Magnitude	PGA	Peat Thickness	(N1-60), Foundation	Deformation
6.5	0.3	5	median	2
			median*exp(log10 sigma)	1.5
			median/exp(Log10 sigma)	6
6.5	0.4	5	median	3
			median*exp(log10 sigma)	2
			median/exp(Log10 sigma)	8
6.5	0.5	5	median	4
			median*exp(log10 sigma)	2.5
			median/exp(Log10 sigma)	10
7.5	0.05	5	median	0.4
			median*exp(log10 sigma)	0.2
			median/exp(Log10 sigma)	2
7.5	0.1	5	median	3
			median*exp(log10 sigma)	1.5
			median/exp(Log10 sigma)	7.5
7.5	0.2	5	median	6
			median*exp(log10 sigma)	4
			median/exp(Log10 sigma)	10
7.5	0.3	5	median	10
			median*exp(log10 sigma)	8
			median/exp(Log10 sigma)	>10
7.5	0.4	5	median	>10
			median*exp(log10 sigma)	>10
			median/exp(Log10 sigma)	>10
7.5	0.5	5	median	>10
			median*exp(log10 sigma)	>10
			median/exp(Log10 sigma)	>10
5.5	0.05	15	median	0.1
			median*exp(log10 sigma)	0.1
			median/exp(Log10 sigma)	0.1
5.5	0.1	15	median	0.1
			median*exp(log10 sigma)	0.1
			median/exp(Log10 sigma)	0.2
5.5	0.2	15	median	0.6
			median*exp(log10 sigma)	0.2
			median/exp(Log10 sigma)	1.5
5.5	0.3	15	median	1.3
			median*exp(log10 sigma)	0.5
			median/exp(Log10 sigma)	3
5.5	0.4	15	median	1.8
			median*exp(log10 sigma)	0.6
			median/exp(Log10 sigma)	4
5.5	0.5	15	median	2
			median*exp(log10 sigma)	0.8
			median/exp(Log10 sigma)	5
6.5	0.05	15	median	0.1
			median*exp(log10 sigma)	0.1
			median/exp(Log10 sigma)	0.1

Table 6-6 Calculated FLAC Deformations – Idealized Sections Liquefiable

Earthquake Magnitude	PGA	Peat Thickness	(N1-60), Foundation	Deformation
6.5	0.1	15	median	0.1
			median*exp(log10 sigma)	0.1
			median/exp(Log10 sigma)	0.4
6.5	0.2	15	median	0.7
			median*exp(log10 sigma)	0.2
			median/exp(Log10 sigma)	1.8
6.5	0.3	15	median	1.5
			median*exp(log10 sigma)	0.6
			median/exp(Log10 sigma)	3.5
6.5	0.4	15	median	2
			median*exp(log10 sigma)	0.8
			median/exp(Log10 sigma)	5
6.5	0.5	15	median	2.5
			median*exp(log10 sigma)	1.3
			median/exp(Log10 sigma)	6
7.5	0.05	15	median	0.4
			median*exp(log10 sigma)	0.2
			median/exp(Log10 sigma)	1.8
7.5	0.1	15	median	2
			median*exp(log10 sigma)	0.6
			median/exp(Log10 sigma)	5
7.5	0.2	15	median	4
			median*exp(log10 sigma)	2
			median/exp(Log10 sigma)	8
7.5	0.3	15	median	5
			median*exp(log10 sigma)	4
			median/exp(Log10 sigma)	10
7.5	0.4	15	median	6
			median*exp(log10 sigma)	5
			median/exp(Log10 sigma)	>10
7.5	0.5	15	median	8
			median*exp(log10 sigma)	6
			median/exp(Log10 sigma)	>10
5.5	0.05	>25	median	0.1
			median*exp(log10 sigma)	0.1
			median/exp(Log10 sigma)	0.1
5.5	0.1	>25	median	0.1
			median*exp(log10 sigma)	0.1
			median/exp(Log10 sigma)	0.3
5.5	0.2	>25	median	0.7
			median*exp(log10 sigma)	0.3
			median/exp(Log10 sigma)	1.5
5.5	0.3	>25	median	1.3
			median*exp(log10 sigma)	0.6
			median/exp(Log10 sigma)	2.5
5.5	0.4	>25	median	1.5
			median*exp(log10 sigma)	0.8
			median/exp(Log10 sigma)	3

Table 6-6 Calculated FLAC Deformations – Idealized Sections Liquefiable

Earthquake Magnitude	PGA	Peat Thickness	(N1-60), Foundation	Deformation
5.5	0.5	>25	median	1.8
			median*exp(log10 sigma)	1
			median/exp(Log10 sigma)	3.5
6.5	0.05	>25	median	0.1
			median*exp(log10 sigma)	0.1
			median/exp(Log10 sigma)	0.1
6.5	0.1	>25	median	0.1
			median*exp(log10 sigma)	0.1
			median/exp(Log10 sigma)	0.4
6.5	0.2	>25	median	0.8
			median*exp(log10 sigma)	0.3
			median/exp(Log10 sigma)	1.8
6.5	0.3	>25	median	1.3
			median*exp(log10 sigma)	0.6
			median/exp(Log10 sigma)	3
6.5	0.4	>25	median	1.8
			median*exp(log10 sigma)	1
			median/exp(Log10 sigma)	3.5
6.5	0.5	>25	median	2.3
			median*exp(log10 sigma)	1.5
			median/exp(Log10 sigma)	4.5
7.5	0.05	>25	median	0.4
			median*exp(log10 sigma)	0.2
			median/exp(Log10 sigma)	1.5
7.5	0.1	>25	median	1.8
			median*exp(log10 sigma)	0.6
			median/exp(Log10 sigma)	3.5
7.5	0.2	>25	median	3.5
			median*exp(log10 sigma)	2.5
			median/exp(Log10 sigma)	7
7.5	0.3	>25	median	4
			median*exp(log10 sigma)	3
			median/exp(Log10 sigma)	10
7.5	0.4	>25	median	7.5
			median*exp(log10 sigma)	6
			median/exp(Log10 sigma)	>10
7.5	0.5	>25	median	10
			median*exp(log10 sigma)	8
			median/exp(Log10 sigma)	>10

7.0 Summary of Findings

7.1 Historic Failures in The Delta and Suisun Marsh

- During the past 56 there were 68 storm related island failures corresponding to a mean annual frequency of failure of about 1.21.
- The annual mean number of events in the last 26 years indicate an increasing trend of island flooding and corresponds to about 1.62 or 162 percent.
- The increased rate of island flooding appears to be correlated to higher peak storm inflows experienced in the last 26 years. Peak total Delta inflows of 670,000 cfs and 570,000 cfs occurred during the past 26 years compared to 480,000 cfs and 400,000 cfs for the period between 1955 and 1980. The increased recent peak inflows are about 28% higher than those recorded during the period between 1950 and 1980. Higher peak inflow result in higher water stage in the Delta and Suisun Marsh increasing the hydraulic head on the levees.
- Six sunny weather failures were reported in the Delta. Sunny weather failure in Suisun Marsh are not well documented at this stage. The corresponding annual frequency of sunny weather failure is estimated at 0.107 or one failure every 9.3 years.

7.2 Flood Vulnerability

- In areas where the upper blanket (impervious layer) is 5-foot thick or less, the vertical exit gradients are expected to be excessive (above 1.0) indicating incipient state of under-seepage failure.
- The presence of the drainage ditch near the toe of the levee contributes t significantly to the exacerbation of the under-seepage conditions.
- Generally the results of the under-seepage calculations for a blanket thickness of 25 feet or higher indicate that the vertical gradients are below 0.8 with ditch and below 0.6 without the ditch and hence indicating a lesser potential for under-seepage failures.
- The calculated gradients for Suisun Marsh are much smaller that those calculated for the main Delta. For example, the calculated vertical gradients for the 5-foot thick blanket range from 0.4 to 1.1 at Suisun Marsh compared to 1.2 to 2.4 in the main Delta. The main reason for the difference is the higher surface elevation of the interior island floors in Suisun Marsh.
- Under-seepage at Suisun Marsh appears to be of a lesser concern compared to the main Delta.
- Through-seepage contribute to 40 percent of the total risk of levee failures. It is estimated that that the annual frequency of through-seepage failure corresponds to about 0.53 or about one failure every two years.

7.3 Seismic Vulnerability

- For the areas not susceptible to liquefaction, the earthquake induced levee deformations are expected to be as high as six feet for the vulnerability classes with 25 feet or more of peat and organic deposits. These included islands such as: Sherman, Brannan Andrus, Twetchel, Webb, Venice, Bouldin. For areas with 15 feet of peat and organic deposits, the estimated levee deformations are as high as five feet, and the deformations are on the order of one foot for peat/organic deposit thickness of 5 feet.
- Where waterside slopes are steeper then 1.5H:1V, the earthquake-induced deformations are expected to be as high as 15 feet.
- For the same conditions (no liquefaction) at Suisun Marsh, the earthquake-induced deformations are estimated to be as high as 14 feet.
- The areas most prone to liquefaction potential are the northern region and the south eastern regions of the Delta. The central and western regions of the Delta and Suisun Marsh show discontinuous areas of moderate to low liquefaction potential.
- Levees composed of liquefiable fill are likely to undergo extensive damage as a result of a moderate to large earthquake in the region.
- Levees founded on liquefiable foundations are expected to experience large deformations (in excess of 10 feet) under a moderate to large earthquake in the region

8.0 References

Abrahamson N., 1993, Non-stationary spectral matching program, personnel communication.

Atwater, B.F. and Belknap, D.F. 1980. Tidal-wetland deposits of the Sacramento-San Joaquin Delta, California. In Field, M.E., Bouma, A.H., Colburn, I.P., Douglas, R.G. and Ingle, J.C. (eds) Quaternary Depositional Environments of the Pacific Coast. Proceedings of the Pacific Coast Paleogeography Symposium, 4. Society of Economic Paleontologists and Mineralogists, Pacific Section, Los Angeles, CA, 89-103.

California Data Exchange Center (CDEC), Water level database http://cdec.water.ca.gov

California Department of Water Resources (1958) "Report: Salinity Control Structures Study"

California Department of Water Resources (1994) "Geology report – Grant Line Canal Barrier," Division of Design and Construction

Cedergren, H. (1967), "Seepage, Drainage and Flow Nets"

Converse, Ward, Davis, and Dixon (CWDD), 1981. Partial technical background data for the Mokelumne aqueduct security plan for EMBUD, Oakland, CA.

Cosio, G. (2007) Personal Communication

Department of Water Resources Water Data Library (WDL) http://wdl.water.ca.gov

Department of Water Resources (DWR), 1958. Salinity Control Barrier Investigation, DWR, CA.

Department of Water Resources (DWR), 1994. Geology report – Grant line canal barrier, Division of design and construction, DWR, CA.

Department of Water Resources, DWR Bay-Delta Office, Delta Levees Program "Historic Inundation of Delta Island" http://baydeltaoffice.water.ca.gov/ndelta/levees/historic_inundation_delta.htm

Department of Water Resources, DRMS, Comparison of Repairs of Major Levee Breaks in Delta http://www.drms.water.ca.gov/docs/Comparison_of_Major_Levee_Breaks_in_Delta.pdf

DWR IFSAR Provided with the GIS Data Base

Freeze, R. A., and J. A. Cherry (1979), "Groundwater," Prentice Hall, New Jersey

Geo-Slope International, 2004. SEEP/W for finite element seepage analysis, Version 6.17, Calgary, Alberta, Canada.

Google Maps - http://maps.google.com/maps

Harding Lawson Associates, 1989. Delta Wetlands Project, Sacramento - San Joaquin River, HLA job # 18749 001.03.

Harding Lawson Associates, 1992. Geotechnical Investigation and Design, Wilkerson Dam, Bouldin Island, HLA job # 11472-008.

Harding Lawson Associates, 1991, Interceptor well modeling, Delta Wetlands Project, Sacramento - San Joaquin River Delta, HLA job # 18749016.03.

Harding Lawson Associates (HLA) (1989) "Report: Delta Wetlands Project, Sacramento - San Joaquin River," HLA job # 18749 001.03.

Harding Lawson Associates (HLA) (1992) "Report: Geotechnical Investigation and Design, Wilkerson Dam, Bouldin Island," HLA job # 11472-008.

Harding Lawson Associates (HLA) (1991) "Report: Interceptor well modeling, Delta Wetlands Project, Sacramento - San Joaquin River Delta, HLA job # 18749016.03.

Hudson, M., Idriss, I.M., Beikae, M., 1994, User's Manual for QUAD4M, Center for Geotechnical Modeling, Department of Civil & Environmental Engineering, University of California, Davis, California, May.

Itasca, (2005). "FLAC, fast lagrangian analysis of continua, version 5.0, user's guide," Itasca Consulting Group, Inc., Thrasher Square East, 708 South Third Street, Suite 310, Minneapolis, Minnesota.

Lilhanand, K. and Tseng, W.S., 1988, Development and application of realistic earthquake time histories compatible with multiple-damping design spectra, Proceeding of the 9th World Conference on Earthquake Engineering, Tokyo-Kyoto, Japan, August.

Miller AW, RS Miller, HC Cohen, and RF Schultze. 1975. Suisun Marsh Study, Solano County, California. U.S. Department of Agriculture, Soil Conservation Service. 186 p.

Newmark N.M., 1965, 'Effects of earthquakes on dams and embankments', Geotechnique, Vol. 15, No. 2, June.

Salah-Mars S., Arulnathan R., Roth W., Dawson E., (2004), "Seismic Evaluation Of Wharf And Embankment At The Port Of Oakland, California," Proceedings of 11th International Conference on Soil Dynamics and Earthquake Engineering, Berkeley, California, January.

Seed, R.B., Cetin, K.O., Moss, R.E.S., Kammerer, A., Wu, J., Pestana, J., Riemer, M., Sancio, R.B., Bray, J.D., Kayen, R.E. and Faris, A. (2003) "Recent advances in soil liquefaction engineering: a unified and consistent framework," Report No. EERC 2003-06, (originally presented at 26th Annual ASCE Los Angeles Geotechnical Spring Seminar, Keynote Presentation, H.M.S. Queen Mary, April 30, 2003, Long Beach, CA), Earthquake Engineering Research Center, University of California, Berkeley, June.

Seed, H.B. (1979) "Soil liquefaction and cyclic mobility evaluation for level ground during earthquakes," Journal of the Geotechnical Engineering Division, ASCE, Vol. 105 No. GT2, pp 201-255.

Seed, H.B. and Idriss, I.M., 1970, Soil moduli in damping factors for dynamic response analysis, Report No. EERC 70-10, University of California, Berkeley, December.

Shelmon, R.J. and Begg, E.L. 1975. Holocene evolution of the Sacramento-San Joaquin Delta, California, International Union for Quaternary research sponsored by the Royal Society of New Zealand.

Terzaghi, K., and Peck, R. B. (1967), "Soil Mechanics in Engineering Practice," Wiley, New York

The Mark Group Engineers & Geologists, Inc., 1992. Geological/Geotechnical and Seismic Studies, Old River Facility, Los Vaqueros Project.

The Mark Group Engineers & Geologists, Inc. (1992) "Geological/Geotechnical and Seismic Studies, Old River Facility, Los Vaqueros Project"

Thompson, J. 1957. The settlement geography of the Sacramento-San Joaquin Delta, California [Ph.D. Dissertation], Stanford University

U.S. Army Corp of Engineers (USACE), 1987. Sacramento-San Joaquin Delta Levees - Liquefaction potential, Geotechnical Branch, Sacramento Corps of Engineers, USACE.

USACE (1956) "Investigation of Underseepage, Lower Mississippi River Levees," Technical Memorandum 3-424, US Army Engineer Waterways Experiment Station, Vicksburg, MS"

USACE (Original 1986 / Change 1 April 30, 1993) "Engineering and Design, Seepage Analysis and Control for Dams, US Army Corps of Engineers Engineering Manual, EM 1110-2-1901"

USACE (1987) "Sacramento-San Joaquin Delta Levees - Liquefaction Potential" Report by the Geotechnical Branch, Sacramento District, US Army Corps of Engineers

USACE (1999) "Risk-Based Analysis in Geotechnical Engineering for Support of Planning Studies: US Army Corps of Engineers Engineering Technical Letter, ETL 1110-2-556"

USACE, Sacramento District, 1999, "Sacramento and San Joaquin River Basins, California, Post Flood Assessment", March.

Vucetic, M. and Dobry, R., 1991, Effect of soil plasticity on cyclic response, Journal of Geotechnical Engineering, ASCE, Vol. 117, No.1.

Wehling, T.M. et al.,2001, Nonlinear dynamic properties of a fibrous organic soil, Paper accepted for publication in ASCE Journal of Geotechnical Engineering.

Wright, S.G., (1992) "*UTEXAS3, A Computer Program for Slope Stability Calculations*", Austin,Texas, May, 1990, revised July 1991 and 1992.

Yahoo Maps - http://maps.yahoo.com/#env=F

Personal Communications

Personal Communications – Joel Dudas, GIS, DWR

Personal Communications – Mike Driller, Engineering, DWR

Personal Communications – Gilbert Cosio, MBK